UNIVERSITÀ DI PARMA

UNIVERSITA' DEGLI STUDI DI PARMA

DOTTORATO DI RICERCA IN
SCIENZE MEDICHE

CICLO XXXII

Role of lipotoxicity in vascular and β-cell damage in type 2 diabetes

Coordinatore:

Chiar.mo Prof. Carlo Ferrari

Tutor:

Chiar.ma Prof.ssa Alessandra Dei Cas

Co-tutors:

Dott.ssa Valentina Spigoni

Chiar.ma Prof.ssa Miriam Cnop

Dottorando:

Federica Fantuzzi

Anni 2016/2019

Whatever inspiration is,
it's born from a continuous "I don't know."
W. Szymborska

SUMMARY

Background. Diabetes is a complex disease which currently affects 425 million people worldwide and type 2 diabetes (T2D) accounts for 80-90% of all cases. Development and progression of T2D is caused by insulin resistance (IR) and pancreatic β-cell failure, the latter due to dysfunction or destruction of β-cells. Nevertheless, the most prevalent cause of mortality in T2D patients is represented by cardiovascular (CV) disease which occurs with two-three times higher rate in these subjects than in adults without diabetes. Sodium-glucose cotransporter 2 inhibitors (SGLT2-I) – in particular empagliflozin, dapagliflozin and canagliflozin – belong to a recently introduced class of anti-diabetic drugs capable to improve both hyperglycemia and CV risk. The mechanisms underlying SGLT2-I-mediated CV protection are still unclear but, among other hypotheses, it has been proposed the inhibition of the sodium/H+ exchanger (NHE) as putative non-canonical mediator of SGLT2-I-mediated effects.

A key phenomenon in the pathogenesis of both IR, β-cell dysfunction and CV risk, is represented by lipotoxicity, which consists in the deleterious effects caused by elevated free fatty acid (FFA) levels.

The present study focuses on the possible effects of lipotoxicity on two cell types directly involved in (1) vascular complication, with specific focus on impaired reparatory mechanisms, and (2) progression of β-cell dysfunction. As a cell population with a pivotal role in endothelial repair, lipotoxicity has been studied on myeloid angiogenic cells (MACs), which are a subset of cells with pro-angiogenic function. Importantly, a reduction in MAC number and function is associated with both T2D and increased CV morbidity and mortality.

Aims. (1) to investigate the effects of lipotoxicity – specifically mediated by physiological concentrations of the saturated stearic acid (SA) – on MAC viability and function and the capacity of novel anti-diabetic drugs to curb SA-induced lipotoxicity in MACs and (2) to improve the *in vitro* protocol of differentiation of iPSCs into functional β-cells to create novel cell models to study β-cell lipotoxicity.

Results. (1) SA induces lipo-apoptosis in MACs in a dose- and time-dependent manner. Moreover, SA triggers pro-inflammatory cytokines and chemokines and endoplasmic reticulum (ER) and oxidative stress marker gene expression at physiological concentration (100 μM) in MACs. Interestingly, JNK activation has been found to mediate pro-inflammatory response, whilst pro-apoptotic response seems to be mediated by PERK signaling in ER stress response. Of note, SA exposure affects angiogenic function in MACs (*Spigoni V, Fantuzzi F, et al, Atherosclerosis, 2017*).

At the maximum concentration tested (100 μM), both empagliflozin and dapagliflozin curb SA-induced expression of pro-inflammatory and oxidative stress markers, restoring baseline values. NHE isoform 1-6 and 9, but not SGLT2, have been detected in MACs. Amiloride (an aspecific NHE inhibitor), and only partially cariporide (NHE1 specific inhibitor), mimic SGLT2-I mediated anti-inflammatory effects on SA-treated MAC, supporting the hypothesis of an involvement of NHE blocking, independent of SGLT2 inhibition, in SGLT2-I-mediated anti-lipotoxic action (*Spigoni V, Fantuzzi F, et al, unpublished data*).

(2) To date, findings on lipotoxicity in β-cells have been hampered by the difficulty to study the disease tissue, i.e. limited availability and high variability of islet preparations. An alternative solution to human pancreatic islets is represented by the human β-cell line EndoC-βH1. In our experience, pilot experiments show that EndoC-βH1 cells are only moderately susceptible to lipoapoptosis induced by physiological concentration of SA and palmitic acid (PA), although higher concentration

(500 μM) succeeds to be pro-apoptotic. However, in other experiments - led by our collaborator Prof Scharfamann (Paris) - EndoC-βH1 cells are rather resistant to similar concentration of SA and PA and such protection seems to be mediated by the high expression of stearoyl-CoA desaturase (SCD), a key enzyme involved in the synthesis of unsaturated from saturated FFAs (*Oshima M. …, Fantuzzi, F. et al, Diabetologia, accepted for publication*).

Given our contrasting data and considering that EndoC-βH1 are transformed pseudodiploid cells in continuous expansion and, as a consequence, they should not be considered as a direct equivalent of primary β-cells, we can conclude that EndoC-βH1 cells might not represent the best model to study β-cell lipotoxicity.

In the present project, β-cells differentiated from human induced pluripotent stem cells (iPSCs) have been identified as the optimal tool to study β-cell lipotoxicity. Using a 7-stage protocol which mimics the embryonic development of the endocrine pancreas, iPSCs have been differentiated into β-cells. At the end of the process, the yield of insulin-positive β-cells is comparable to that of human islets. In iPSC-derived β-cells at stage 7, high glucose stimulation slight increases insulin release, which is further augmented in response to high glucose plus forskolin (that acts by raising intracellular cAMP levels). Next, iPSC-derived β-cell transplantation, under the kidney capsule of NOD-SCID mice, further boosts their functional maturation. Mice transplanted with iPSC-derived β-cells show an increase in human C-peptide in response to glucose injection and succeed in maintain normoglycaemia after streptozotocin injection, compensating the rodent β-cells ablation. Their dynamic responsiveness has also been confirmed by *in situ* kidney perfusion assay (*Toivonen S. and Fantuzzi F. et al, unpublished data)*.

Among the advantages of iPSC-derived β-cells, it should be recognized that iPSCs are a patient-relevant cell model, as they are directly

reprogrammed from patient's cells. In this regard, iPSCs derived from fibroblasts of a patient affected by Friedreich ataxia – which is an autosomal recessive neurodegenerative disease caused by an intronic repeat expansions in *FXN* gene, characterized by reduced expression of the frataxin protein and with a high prevalence of diabetes – have been differentiated in β-cell by using the protocol described above. The differentiation has been highly efficient, resulting in 58% insulin-positive β-cells and slight glucose-responsive cells. Frataxin levels in these iPSC-derived β-cells result lower than those of healthy control cell lines. Then, this patient-relevant model of β-cells has been exploited to evaluate the effect of an incretin analog, which was found to mildly increase frataxin expression (*Igoillo-Esteve M., …. Fantuzzi F. et al, unpublished data*).

This study demonstrates the feasibility and the advantages of differentiate iPSCs into functional iPSCs and suggests their exploitation for investigating β-cell dysfunction.

Conclusion. This project points to a critical role of lipotoxicity, specifically induced by SA, in driving the development of T2D and of its major complication, i.e. CVD.

Table of contents

ABBREVIATIONS

ACC	Acetyl-CoA Carboxylase
ADA	American Diabetes Association
ADP	Adenosine Diphosphate
AIP	Anterior Intestinal Portal
AMPK	5'-Adenosine Monophosphate-activated Protein Kinase
ATF	Activating Transcription Factor
ATP	Adenosine Triphosphate
BiP	Binding immunoglobulin Protein
BMI	Body Mass Index
BMP	Bone Morphogenetic Proteins
BSA	Bovine Serum Albumin
CAP	Cbl-Associated Protein
Cbl	Casitas B-lineage Lymphoma
CD	Cluster of Differentiation
CHOP	C/EBP Homologous Protein
CPA1	Carboxypeptidase A1
CRISPR	Clustered Regularly Interspaced Short Palindromic Repeats
CS	Carnegie Stages
CV	Cardiovascular
CVD	Cardiovascular Disease
DALYs	Disability-Adjusted Life Years
DAPA	Dapagliflozin
DM	Diabetes Mellitus
DMEM	Dulbecco's Modified Eagle Medium
DNMT	DNA methyltransferase
DPP4-I	Dipeptidyl-Peptidase 4 Inhibitors
EASD	European Association for the Study of Diabetes
EDTA	Ethylenediamine-tetraacetic Acid
EGF	Epidermal Growth Factor
EGM-2	Endothelial cell Growth Medium-2
eIF2α	eukaryotic Initiation Factor 2α
EMPA	Empagliflozin
eNOS	endothelial Nitric Oxide Synthase

EPC	Endothelial Progenitor Cells
EPIC	European Prospective Investigation into Cancer and Nutrition Study
ER	Endoplasmic Reticulum
ERAD	Endoplasmic-Reticulum-Associated Protein Degradation
ERK	Extracellular signal-Regulated Kinases
ESC	Embryonic Stem Cell
ELOVL	Elongation of Very Long chain fatty acids protein
Ex4	Exenatide
FAS	Fatty Acids Synthase
FCCP	Carbonyl Cyanide-4 (trifluoromethoxy) Phenylhydrazone
FDA	Food and Drug Administration
FFA	Free Fatty Acid
FGF	Fibroblast Growth Factor
FOXA	Forkhead Transcription Factor box A
FOX	Forkhead box protein
FPG	Fasting Plasma Glucose
FRDA	Friedreich Ataxia
FXN	Frataxin
G6Pase	Glucose-6-Phosphatase
GAPDH	Glyceraldehyde 3-Phosphate Dehydrogenase
GIP	Glucose-dependent Insulinotropic Polypeptide
GLP	Glucagon-Like Peptide
GLP1RA	GLP1 Receptor Agonist
Grb2	Growth factor Receptor-Bound protein 2
GRP78	78-kDa Glucose-Regulated Protein
GSiXX	γ-Secretase inhibitor XX
GSK3	Glycogen Synthase Kinase 3
GWAS	Genome-Wide Association Study
HbA1c	Glycated Haemoglobin
HI	Human Islets
HO	Heme Oxygenase
HUVECs	Human Umbilical Vein Endothelial Cells
IGT	Impaired Glucose Tolerance
IL	Interleukin
INSR	Insulin Receptor
iPSC	induced Pluripotent Stem Cells

iPSCs-β-cells	iPSCs-derived β-cells
IR	Insulin Resistance
IRE	Inositol-Requiring Enzyme
IRS	Insulin Receptor Substrate
JNK	c-Jun N-terminal Kinase
K_{ATP}	ATP-sensitive Potassium channel
KDR	Kinase insert Domain Receptor
KGF	Keratinocyte Growth Factor
KLF	Krüppel-Like Factor
LDL	Low-Density Lipoprotein
MAC	Myeloid Angiogenic Cells
MCP-1	Monocyte Chemoattractant Protein-1
miRNAs	microRNAs
MODY	Maturity Onset Diabetes of the Young
mRNA	RNA messenger
mTORC	mammalian Target Of Rapamycin Complex
NAC	N-Acetyl-Cysteine
NADPH	Nicotinamide Adenine Dinucleotide Phosphate
NEFA	Non-Esterified Fatty Acids
NEUROD	Neurogenic Differentiation
NF	Nuclear Factor
NGN3	Neurogenin 3
NHE	Na+/H+ Exchanger
NNT	Number Needed to Treat
NO	Nitric Oxide
OCT	Optimum Cutting Temperature
OCT4	Octamer-Binding Transcription Factor 4
P-MACE	Points Major Adverse CV Event
PA	Palmitic Acid
PAX	Paired box Protein
PBS	Phosphate-Buffered Saline
PCSK9-I	Proprotein Convertase Subtilisin/Kexin type-9 Inhibitor
PDK1	Phosphoinositide-Dependent Kinase 1
PDX	Pancreatic and Duodenal homeobox
PEPCK	Phosphoenolpyruvate Carboxykinase
PERK	Protein kinase R (PKR)-like ER Kinase
PI	Phosphatidylinositol
PIP2	Phosphatidyl-Inositol-3,4-bisphosphate
PIP3	Phosphatidyl-Inositol-3,4,5-trisphosphate

PKB	Protein Kinase B
PKC	Protein Kinase C
PPAR	Peroxisome Proliferator-Activated Receptor
PSC	Pluripotent Stem Cell
PTP	Protein Tyrosine Phosphatase
qPCR	quantitative Polymerase Chain Reaction
RIDD	Regulated IRE-1-Dependent Decay of mRNA
RNase	Ribonuclease
RNS	Reactive Nitrogen Species
ROS	Reactive Oxygen Species
S	Stage
SA	Stearic Acid
SCD	Stearoyl CoA Desaturase
SDF	Stromal cell-Derived Factor
SeV	Sendai Viruses
SFA	Saturated FFA
SGLT2-I	Sodium/Glucose co-Transporter-2 Inhibitors
SH	Src homology
SHH	Sonic Hedgehog
SOD	Superoxide Dismutase
SOS	Son of Sevenless
SOX	Sex-determining region-box
SSEA	Stage Specific Embryonic Antigen
STZ	Streptozotocin
sXBP-1	spliced XBP-1
T1D	Type 1 Diabetes
T2D	Type 2 Diabetes
TBP	α-amyloid precursor protein modulator
TGF-β	Transforming Growth Factor β
TLR	Toll-Like Receptor
TNF	Tumor Necrosis Factor
TXN	Thioredoxin
UPR	Unfolded Protein Response
VEGF	Vascular Endothelial Growth Factor
XBP	X-box Binding Protein

FIGURES and TABLES

INTRODUCTION

Diabetes mellitus (DM) is a complex metabolic chronic disease – characterized by hyperglycemia – which involves disorders in carbohydrate, protein and fat metabolism, occurring when blood glucose concentration raises because of an inadequate secretion and/or action of the hormone insulin [1].

There are three major types of diabetes, type 1 diabetes (T1D), type 2 diabetes (T2D) and gestational diabetes [2]. T1D, whose onset is common during childhood or adolescence, results from β-cell destruction, mostly immune-mediated, and characterized by broad insulin deficiency. T2D shows various degrees of β-cells dysfunction and of insulin resistance and a significant higher prevalence of obesity than subjects without diabetes. Gestational diabetes is a peculiar condition in which hyperglycemia is first detected during pregnancy.

Several other types of diabetes have been identified, among which monogenic form of diabetes, triggered by specific gene mutations which cause defects in insulin action or β-cell function, and drug- or chemical-induced or infection-related diabetes. Finally, diabetes can occur concomitantly with other genetic syndromes, e.g. Friedrich's ataxia [3], Down syndrome [4] or Turner syndrome [5], or in various conditions that could affect pancreas, e.g pancreatitis or trauma.

According to the European Association for the Study of Diabetes (EASD) and the American Diabetes Association (ADA), updated diagnostic criteria for diabetes include plasma glucose concentration above 1) 7.0 mmol/L (126 mg/dl) in fasting condition or 2) 11.1 mmol/L (200 mg/dl) after 2-hours post-75 g oral glucose load or 3) 11.1 mmol/L (200 mg/ dl) when randomly tested or 4) the index glycated haemoglobin (HbA1c), which reflects the average blood glucose concentration over the previous 3-month period, above 6.5% (48mmol/mol) [6, 7].

1. Epidemiology of type 2 diabetes

DM has been identified as the 7th prominent cause of death in 2016 by The World Health Organization [8]. Moreover, the Global Burden of Disease Study 2017 identified high fasting plasma glucose (FPG) as the 3rd leading risk factor for disability-adjusted life years (DALYs), a measure of disease burden expressed as numbers of years lost due to illness [9]. Globally, the number of adults (age range, 20-79 years) with diabetes worldwide has increased from 108 million in 1980 to 422 million in 2014, mainly due to the rise in prevalence (28.5%) and to population growth and ageing (39.7%) [10]. Interestingly, half of individuals with DM lives in five countries: China, India, US, Brazil and Indonesia. Currently, DM affects 425 million adults worldwide and it is estimated to rise up to 629 million people by 2045, with an increase of the global prevalence from 8.8% to 9.9%, in absence of any change in the present trend [11]. In particular, the largest expansion will occur in regions whose economies are shifting from low-to-middle income levels, whereas a 20% increase in the number of patients with diabetes is predicted in developed countries [12]. For example, the International Diabetes Federation estimates that the number of people with diabetes in India will pass from 114.4 million in 2017 to 134.3 million in 2045. Broadening the age range to 20-99 years, the current number of DM patients increases to 451 million people. T2D accounts for approximately 87-91% of all diabetes cases, whereas 7-12% are estimated to be T1D and the remaining 1-3% other types of diabetes.

2. Pathophysiology of type 2 diabetes and major risk factors

The main drivers of the global epidemic of T2D are identified as obesity, sedentary lifestyle, high dietary energy intake and nutrient overload and population ageing. Genetic predisposition, epigenetics and gene-

environment interaction are other factors that can affect insulin secretion and action [13].

Briefly, in healthy condition, pancreatic β-cells secrete insulin in response to high glucose levels and the hormone exerts its effect on insulin-sensitive organs, i.e. in the liver by reducing glucose production and in adipose tissue and skeletal muscle by inhibiting lipolysis and increasing glucose uptake, respectively. When β-cells fail in secreting insulin or tissues develop insulin-resistance, these processes are impaired and hyperglycaemia occurs, leading to a disproportionate amount of glucose circulating in the blood (figure 1).

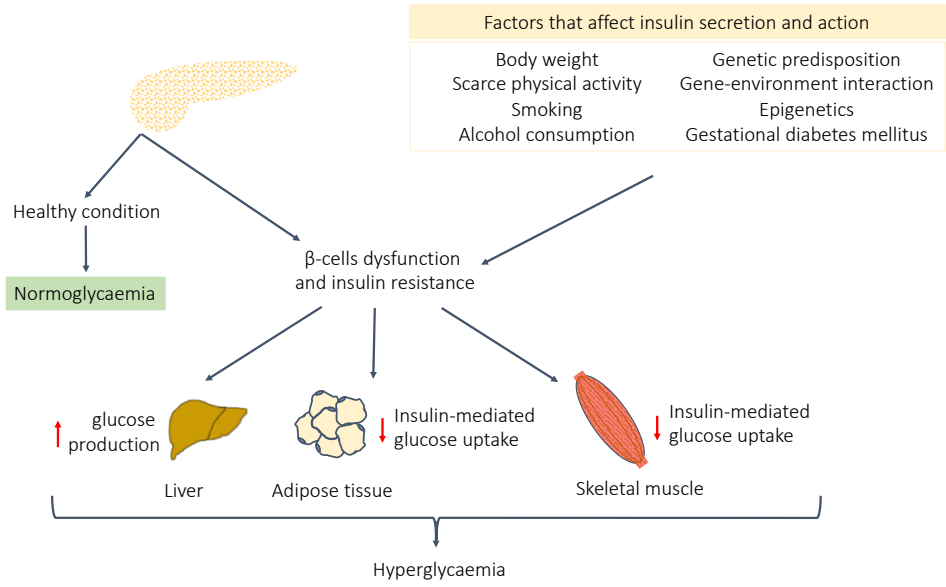

Figure 1. Processes involved in development of hyperglycaemia.

In the pathogenesis of T2D, deficit both in the secretion and action of insulin are involved and, for the disease to become manifest, both events are required. Indeed, initially β-cells are able to adapt and compensate the loss in tissues' insulin-sensitivity (insulin resistance, IR) by increasing the release of insulin. Thus, in this phase, characterized by impaired glucose tolerance (IGT) and metabolism, β-cells succeed in maintaining normoglycaemia. Later, if β-cells undergo to impaired function (β-cell dysfunction and demise), the secretion is impaired and glycemia rises (figure 2) [14].

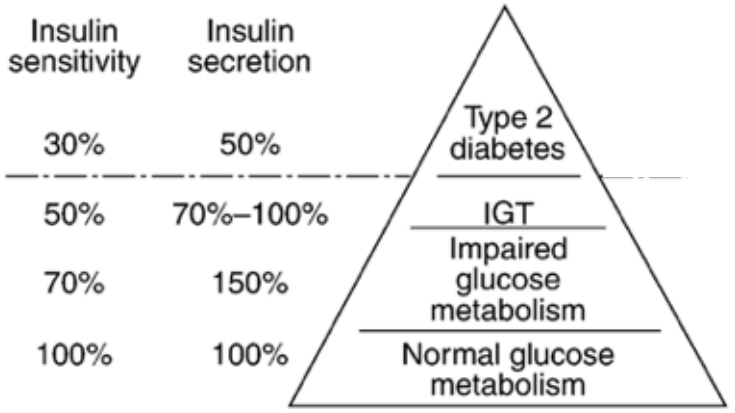

Figure 2. Insulin sensitivity and secretion function (in percentage) in development of type 2 diabetes.

IGT, impaired glucose tolerance. Adapted from "Leslie RDG, ed. Molecular Pathogenesis of Diabetes Mellitus. Karger, 1997, 22: 131-156"

2.1 Insulin resistance

IR is a condition in which cells fail to biologically respond to insulin as they are supposed to. This phenomenon can be discerned as decreased sensitivity to the hormone or as decreased responsiveness, i.e. a reduced action of insulin. Indeed, in a classical dose-response curve, the latter is

represented by a curve with a similar curve design as compared to normal response, but with a decreased maximal response. Otherwise, the amplitude of the response is the same but the curve is shifted to the right (figure 3) [15]. Alterations that may affect insulin interaction with its receptor are more likely to produce a reduced sensitivity, whereas alterations against the intracellular signaling triggered by insulin binding are more likely to produce diminished responsiveness.

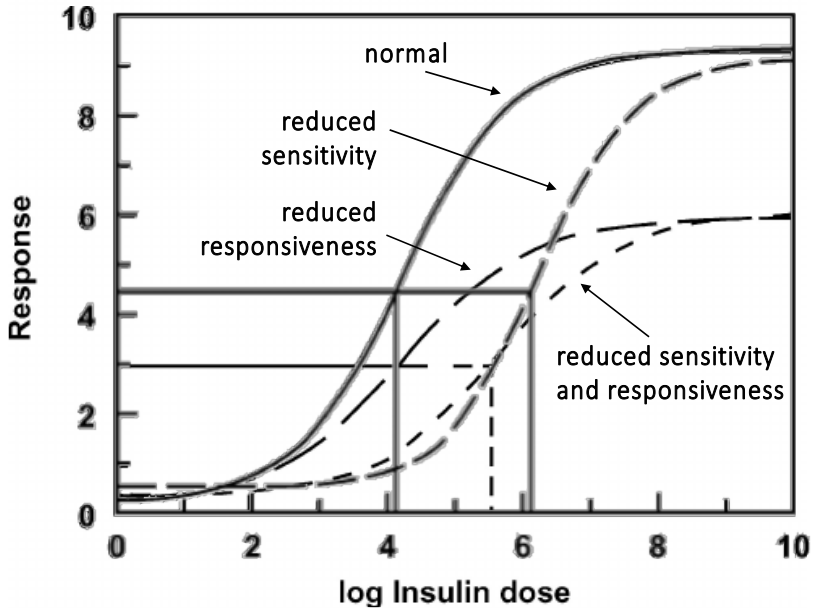

Figure 3. Insulin dose-response curve.

Adapted from "Kahn CR., Insulin resistance, insulin insensitivity, and insulin unresponsiveness: a necessary distinction. Metabolism. 1978 Dec;27".

Insulin receptor (INSR) consists in two domains, an intracellular domain with tyrosine kinase intrinsic activity (two β subunits) and an extracellular ligand binding domain (two α subunits), linked by disulphide bonds [16, 17]. The binding of insulin to the α subunits induces a conformational change which activates the kinase activity of the intracellular portion and causes

the auto-phosphorylation of specific tyrosine aminoacid (Tyr_{1158}, Tyr_{1162}, Tyr_{1163}) [18]. These phosphotyrosine residues are targets for two major scaffold proteins, the insulin receptor substrate (IRS) proteins and the growth factor receptor-bound protein 2 (Grb2), which mediate the activation of the two main branches of the insulin-activated pathway, respectively.

In particular, in the extracellular signal-regulated kinases (ERK) branch, Grb2 binds the IRS phosphorylated residues by its Src homology (SH)-2 domain and, by involving Son of Sevenless (SOS) complex, triggers the activation of the downstream kinase cascade (Ras-Raf-MEK1), leading to the phosphorylation and activation of the MAP kinases ERK1 and ERK2, which translocate into the nucleus and catalyze the phosphorylation of transcription factors that promote cell growth. Otherwise, in the protein kinase B (PKB/Akt) branch, the phosphorylated tyrosine residues of IRS proteins are bound by the SH2 domain of the p85 regulatory subunit of the phosphatidylinositol (PI)-3 kinase [19], which leads the activation of its catalytic subunit p110 and the phosphorylation of phosphatidyl-inositol-4,5-bisphosphate (PIP2) to generate phosphatidyl-inositol-3,4,5-trisphosphate (PIP3) [20]. These 3'-phosphoinositides bind the phosphoinositide-dependent kinase 1 (PDK1), whose substrate is Akt. Once activated, phospho-Akt phosphorylates and inactivates the glycogen synthase kinase 3 (GSK3), promoting glucose storage as glycogen, and the forkhead transcription factor box A (FOXA) proteins [21], which regulate gene expression of key enzymes of gluconeogenesis and glycogenolysis in the liver and kidney, including glucose-6-phosphatase (G6Pase) and phosphoenolpyruvate carboxykinase (PEPCK). A further consequence of the Akt branch is the promotion of the glucose transporter GLUT translocation from intracellular to plasma membrane. A second, INSR-dependent mechanism for GLUT translocation involves a cascade

including Casitas B-lineage lymphoma (Cbl) and the adaptor protein Cbl-associated protein (CAP) (figure 4).

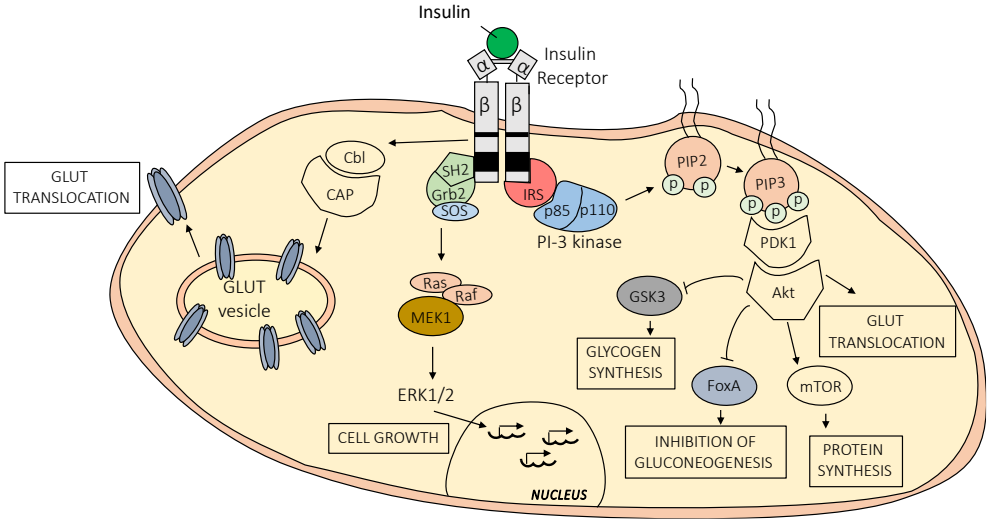

Figure 4. Scheme of the insulin signaling pathway in insulin-sensitive cells. CAP, Cbl-Associated Protein; Cbl, Casitas B-lineage Lymphoma; FOX, Forkhead box protein; Grb2, Growth factor Receptor-Bound protein 2; GSK3, Glycogen Synthase Kinase 3; IRS, Insulin Receptor Substrate; mTORC, mammalian Target Of Rapamycin Complex; PDK1, Phosphoinositide-Dependent Kinase 1; PI, Phosphatidylinositol; PIP2, Phosphatidyl-Inositol-3,4-bisphosphate; PIP3, Phosphatidyl-Inositol-3,4,5-trisphosphate; SH2, Src homology2; SOS, Son of Sevenless.

A few insulin resistant subjects with reduced or absent INSR expression have been reported, mainly because of point mutations in INSR [22], or because of defects in the transcription of INSR RNA messenger (mRNA) [23]. Although structural INSR gene defects, due to mutation in its gene, or in its promoter region, can lead to IR and T2D [24], [25] , [26], they are not a common cause of the disease. In most cases, IR is driven by cellular perturbations, e.g. glucotoxicity and lipotoxicity – conditions characterized

by high glucose and free fatty acid (FFA) levels, respectively –, which are related to inflammation, endoplasmic reticulum (ER) stress and mitochondrial dysfunction [27] and affect insulin signaling by dysregulating and modifying specific genes and proteins. Defects mainly include abnormalities in INSR tyrosine kinase activity [28], in IRS phosphorylation [29] and in the association of the PI-3 kinase subunits, p85 and p110 [30].

2.2 β-cell dysfunction

β-cells failure has a pivotal role in the development/progression of T2D and can be acknowledged both in terms of quantity, because of a progressive loss in β-cell mass (up to 50% reduction in T2D condition compared to healthy individuals [31, 32]), and quality, because of a progressive impairment in secretory function.

Although over 120 gene variants, identified by genome-wide association study (GWAS), have been associated with T2D [33], these findings explain only a minor proportion of total genetic risk and heritability of T2D [34].

In addition, epigenetic mechanisms, which lead to genomic changes without a direct alteration in nucleotide sequence, or microRNAs (miRNAs), which are a class of small noncoding RNA molecules that target specific mRNAs to prevent their translation or promote their degradation, can alter gene expression and contribute to T2D onset.

Global epigenomic analysis of primary human islets from non-diabetic and T2D patients have been performed to identify specific alterations which may affect β-cell function and provide susceptibility to T2D [35, 36]. Histone modifications have also been found to contribute to β-to-α cell trans-differentiation in human islets [37] and histone deacetylases inhibition protects from cytokine-mediated β-cell demise in murine models[38, 39]. On the other hand, it is known that specific miRNAs are critical to β-cell development and function. Indeed, specific miRNAs influence pathways

of β-cell differentiation [40] and insulin synthesis and secretion [41]. Thus, an alteration at this level, mediated by environmental stressors, may considerably affect β-cell function.

Glucose enters the β-cell via the GLUT2 transporter localized at the cell surface, and it is subsequently rapidly metabolized leading to a net increase in adenosine triphosphate (ATP)/ adenosine diphosphate (ADP) ratio which results in the closure of ATP-sensitive potassium channel (K_{ATP}) and in consequent membrane depolarization. This event induces the opening of the voltage-dependent calcium channels. Intracellular Ca^{2+} levels augment and trigger the fusion of the secretory granules and insulin release. A schematic summary of events involved in glucose-stimulated insulin secretion is represented in figure 5.

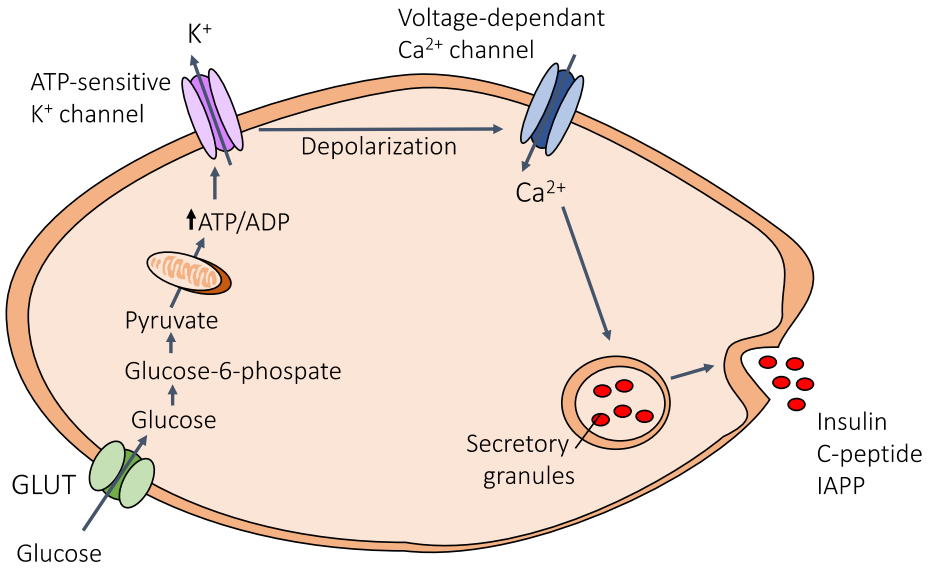

Figure 5. Events involved in glucose-stimulated insulin secretion.

As mentioned above, whereas β-cells initially improve the insulin secretion to compensate the decrease in tissues' insulin sensitivity, eventually they undergo to β-cell dysfunction and, ultimately, to β-cell death.

Among the mechanisms leading to pancreatic dysfunction, β-cells are particularly susceptible to ER stress because of their high rate of protein synthesis.

Moreover, about 20% of proinsulin – the prohormone precursor to insulin – is misfolded already in a healthy β-cell and, under pathological conditions, the total amount of misfolded proinsulin increases [42]. ER stress response, named unfolded protein response (UPR), is triggered by the accumulation of unfolded proteins as a cellular attempt to restore ER function. However, in case of prolonged ER stress condition, apoptotic processes are induced, mainly by C/EBP homologous protein (CHOP) activation. At T2D onset, β-cells show high ER stress markers expression [43] and samples from T2D patients show an increase in both ER volume and β-cell apoptosis compared to those from healthy donors [44].

Another fundamental type of stress affecting β-cells during diabetes onset, is oxidative stress, which results from an imbalanced condition between excessive reactive oxygen species (ROS) or reactive nitrogen species (RNS) production and inadequate antioxidant defense system. Persistent nutrient overload, including FFA and glucose [45, 46] enhances oxidative stress in β-cells, disturbing both the secretory function and cell viability [47]. Indeed, a major source of ROS derives from the mitochondrial respiratory chain, whose activity increases to induce β-cell insulin release [48, 49]. Thereby, it is likely that the chronic stimulation of insulin secretion, as in IR, ultimately may lead to β-cells failure.

Chronic inflammation also has a key role in β-cell dysfunction and in the pathogenesis of T2D. Pancreatic islets from T2D patients show islets-associated pro-inflammatory macrophage infiltration [50, 51] and elevated expression of interleukin (IL)-1β [52], whose levels augment after chronic

exposure to high glucose [53] or FFA [54] or leptin [55]– a hormone mainly produced by adipose cells.

Finally, loss of β-cell identity i.e. the loss of the expression of mature β-cell markers, is another described mechanism which contribute to β-cell failure without involving cell death. Indeed, nutrient overload may induce β-cell de-differentiation, by reversing the phenotype to a fetal state, or reprogramming the cells to express hormones typical of other islet cell type, as glucagon-expressing α-cells or somatostatin-expressing δ-cells [56]. In fact, inactivation of key transcription factors in β-cells, as pancreatic and duodenal homeobox (Pdx)1, Nkx6.1, MafA, paired box protein (Pax)6 and forkhead box protein O (Foxo)1, has been reported in hyperglycemic conditions [57, 58, 59, 60].

A schematic summary of stressors involved in T2D diabetes pathogenesis is represented in figure 6.

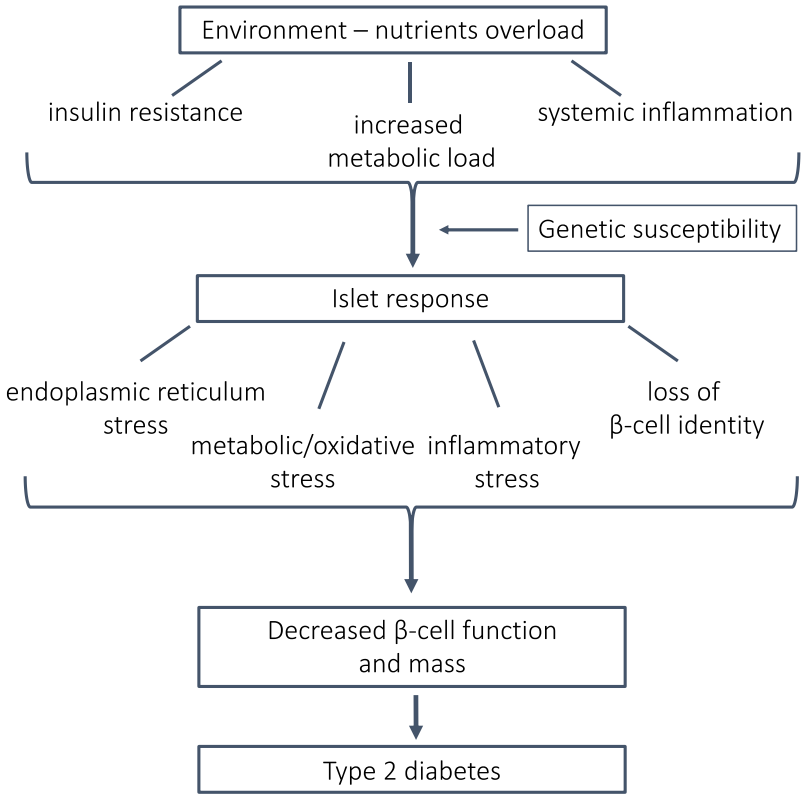

Figure 6. β-cells stressors in type 2 diabetes pathogenesis.
Adapted from "Halban PA, et al., β-cell failure in type 2 diabetes: postulated mechanisms and prospects for prevention and treatment. J Clin Endocrinol Metab. 2014 Jun;99(6):1983-92".

3. Human pancreatic islets

To further unravel the biology of pancreas and to increase knowledge in preventing and treating diabetes, research on human pancreatic islets is crucial.

Human pancreas consists of endocrine and exocrine tissues. The latter includes acinar cells that secrete digestive fluid and the ductal cells which drain this fluid reach the intestine. On the other side, the endocrine portion is made of islets of Langerhans (human islets, HI), which embrace five subtypes of endocrine cells: glucagon-secreting α-cells, insulin-secreting β cells, somatostatin-secreting δ-cells, ghrelin-secreting ε-cells and pancreatic polypeptide-secreting γ-cells. About 1 million islets are present in healthy adult pancreas, representing the 1-2% of the total organ mass. β-cells are the most represented cells in islets, up to 70%, whilst α-cells and δ-cells account for 20 and 10%, respectively.

3.1 Human pancreas morphogenesis

Human embryogenesis lasts approximately 8 weeks, from the fertilization to the moment in which the embryo is indicated as fetus, and it is classified into 23 sequential Carnegie Stages (CS) [61].

The site for pancreas specification occurs at the border between foregut and midgut (which along with the hindgut form the primitive gut tube) and it is shaped when the anterior endoderm invaginates to form the anterior intestinal portal (AIP) at CS10 [62,63]. The notochord, which is the structure defining the chordates, is placed next to the foregut endoderm and

induces the progression of the foregut into the dorsal pancreatic bud, by secreting the sonic hedgehog (SHH) protein, and allowing the expression of PDX1, a key pancreatic transcription factor, at CS12 [64]. At CS13, dorsal and ventral pancreatic buds are clearly evident and show high expression of PDX1, the transcription factors SRY (sex-determining region Y)-box 9 (SOX9) and GATA4, all of which have a fundamental role in pancreas development [65,66,67].

Within CS14 and CS18, pancreatic progenitor cells proliferate and, by CS19, they differentiate in "tip" progenitor cells – which are $SOX9^{+}/GATA4^{+}/NKX6.1^{+}$ cells – and "trunk" progenitor cells, which gradually lose GATA4 expression. Subsequently, pro-acinar "tip" cells will stop to express NKX6.1 and will became mature acinar cells, characterized by the expression of GATA2, carboxypeptidase A1 (CPA1) and amylase. "Trunk" progenitor cells develop in duct cells – expressing SOX9, FOXA2 and, weakly, also PDX1 – or endocrine cells, in which SOX9 expression is absent [68].

For endocrine commitment, neurogenin 3 (NGN3) transient expression plays a key role [69]. Indeed, it increases quickly soon after embryonic period, at the end of the first pregnancy trimester and it is not detected anymore after 26-28 weeks post-conception [70]. SOX9 expression is undetected in $NGN3^{+}$ cells and it is not expressed neither later in maturing endocrine cells. Fetal β-cells are the first cell-type shown during development and the most predominant one.

Figure 7 shows the network of transcription factors involved in human pancreas development.

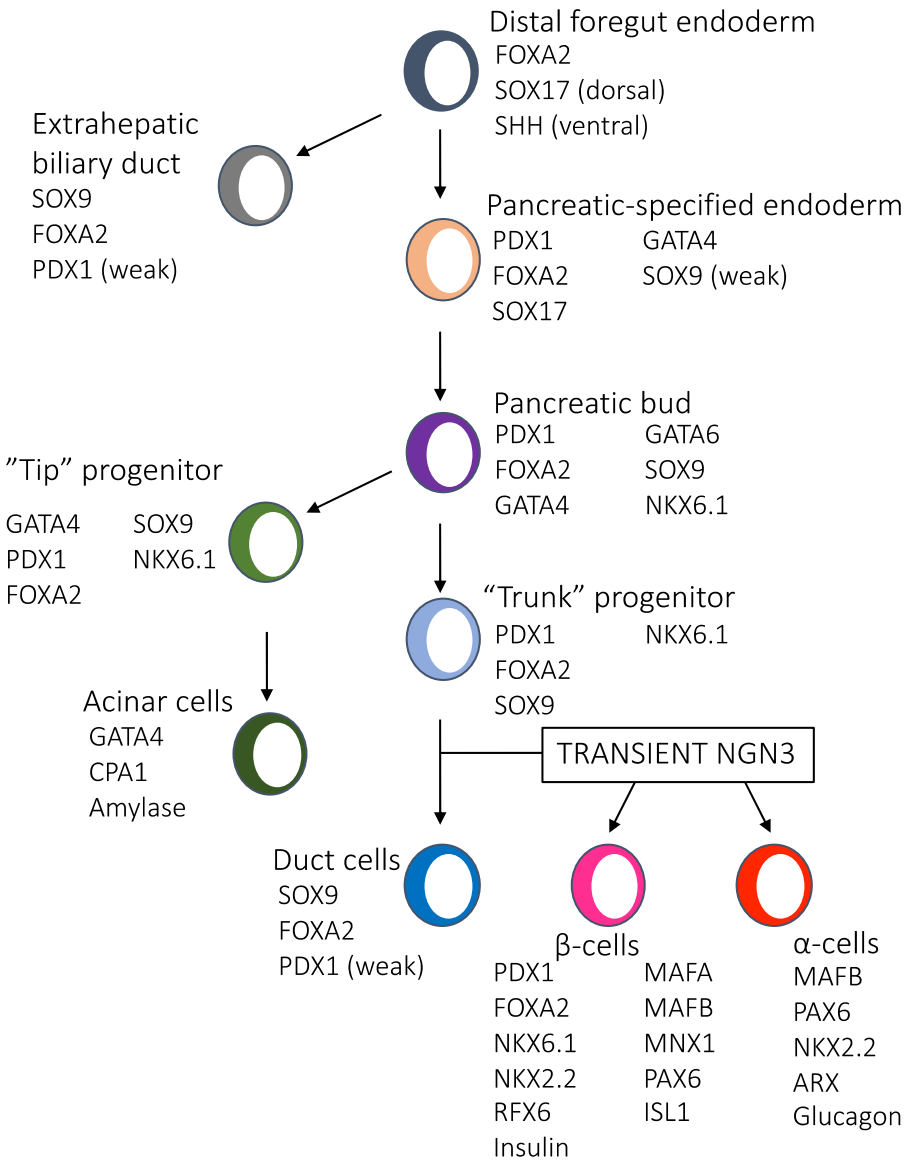

Figure 7. Human pancreas development and involved transcription markers network.

Adapted from “Jennings RE, Berry AA, Strutt JP, Gerrard DT, Hanley NA. Human pancreas development. Development. 2015 Sep 15;142(18):3126-37”.

3.2 Human pluripotent stem cells

Stem cells have the defining characteristics of self-renewal and a differentiation potential and their classification is based on the degree of potency. Indeed, totipotency, which is peculiar of zygotes and blastomeres, refers to the potential ability of initiate all body's tissues, both embryonic and extra-embryonic. Pluripotency is the characteristic of specific stem cell types to progress into cells of the three embryonic germ layer, mesoderm, endoderm and ectoderm. Multipotency and oligopotency - typical of progenitor cells - are two sequential degrees of potency that refer to the capacity of generating just the cell types of their original tissue. Finally, unipotent stem cells still retain the ability of self-renewal, but show a very limited differentiation potential since they give rise to only one cell type [71].

Human pluripotent stem cell (PSCs) can be isolated from the inner cell mass of blastocysts (embryonic stem cells, ESCs) [72] or generated as induced pluripotent stem cells (iPSCs) by the reprogramming of mature cells [73]. The latter have been obtained for the first time in 2006, when the researchers Yamanaka and Takahashi identified four master transcription factors – octamer-binding transcription factor 4 (Oct4), SRY (sex determining region Y)-box 2 (Sox2), Krüppel-like factor 4 (Klf4) and C-Myc – whose forced expression was sufficient to reprogram fibroblasts into ESCs-like cells. Since then, several methods for reprogramming mature cells into iPSCs have been developed based on the vector type. The first developed method was based on retroviral [74, 75] and lentiviral [76, 77] systems, which were highly efficient but requiring an additional step of reprogramming factor silencing because of the integration in the host genome. However, this system could escape the silencing and lead to following issues. Excisable lentivirus [78] represents an alternative to genome permanent integration but it requires extensive subcloning

procedures and intensive screening to confirm the removal of the transgenes. Non-integrating vectors include episomal DNA plasmids [79] – which have a lower efficiency than retroviral or lentiviral systems and occasionally can integrate in the host DNA –, adenoviral system [80] and negative sense RNA virus, as Sendai Viruses (SeV) [81]. This last method has higher reprogramming efficiency compared to DNA plasmids and does not integrate in host genome since it is lost during clonal expansion. Finally, others DNA free vectors which have been utilized are proteins [82], modified mRNA [83] and miRNA [84].

The reprogramming process starts with the binding of key reprogramming factors to regulatory elements of many target genes to affect their expression.

It has been shown that during fibroblast reprogramming, the ectopic expression of OCT4, SOX2, c-MYC and KLF4 is required for about ten days, after which cells undergo to a self-sustaining pluripotent state. Upregulation of stage specific embryonic antigen (SSEA)-1 is an early event, whilst reactivation of endogenous OCT4 and SOX2, telomerase and the silenced X chromosome occur later in the process [85].

Initially, the epigenetic landscape is resistant to the changing of the cell state to pluripotency, but, eventually, it is slowly modified by the prolonged expression of the reprogramming factors to resemble those of ESCs and allows the transcription of those genes that sustain pluripotency [86]. However, a broaden investigation about epigenetic state of iPSCs is still ongoing.

Routine quality controls of the reprogramming process include assessment of a correct iPSCs colonies' morphology – which show clear borders and cells with large nucleus and scarce cytoplasm – and absence of chromosome mutations, by karyotype analysis. Moreover, to identify properly-reprogrammed iPSCs, pluripotency markers gene expression and interrupted exogenous reprogramming factors expression have to be

assessed. Indeed, fully reprogrammed cells are independent from reprogramming factors and express several endogenous pluripotency genes, as OCT4, SOX2 and NANOG, similarly to ESCs. Ohers embryonic antigens, whose expression is good practice to test in order to confirm iPSCs reprogramming efficiency are: SSEA3, TRA-1-81, TRA-1-60, DNA methyltransferase (DNMT)-3β and REX1 [87].

Finally, the differentiation potential is a key feature for pluripotent state and, thus, iPSCs' ability to form the three germ layers is assessed. These tests can be performed both *in vitro* – by allowing the spontaneous formation of embryoid bodies, 3D aggregates structures which include cells positive for markers of mesoderm, endoderm or ectoderm – or *in vivo*, e.g, through teratoma formation assay, which verifies the spontaneous generation of tissue from the three gem layers after injection of PSCs in immune-compromised mice.

iPSCs broad developmental potential offers the opportunity to study different cell types at different developmental stages otherwise often unavailable or inaccessible. In addition, iPSCs technology provides an experimental system which allows the study of specific disease pathogenesis and related therapeutic strategies, when iPSCs come from a patient carrying a genetic mutation responsible for the disease. Otherwise, specific gene mutations can be introduced (or corrected) by genome editing tools – e.g. clustered regularly interspaced short palindromic repeats (CRISPR)/Cas9 technology which operate a double strand break in the target DNA sequence in order to introduce the desire mutation during the repair phase – generating isogenic cell lines which differ only for the mutation of concern. Genome editing in iPSCs offers a solution to the variability due to the donor's specific genetic background or to efficiency in reprogramming.

3.3 PSC-derived β-cells

PSC differentiation into β-cells resembles the sequential developmental stages observed in animal models. To allow the activation or inhibition of the involved signaling pathway, several cocktails of key growth factors and small molecules have to be provided during the entire process, until the achievement of PSC-derived β cells.

In order to reach the stage of definitive endoderm, Activin A – component of the transforming growth factor beta (TGF-β) family – and Wnt3a are required [88, 89].

The following step, which provides for PDX1 expression in order to achieve the primitive foregut stage, requires activation of retinoic acid and fibroblast growth factor (FGF) signaling along with inhibition of SHH signaling [90]. Specific domains of the gut tube give rise to all endoderm-derived organs: lungs, liver, thymus, small and large intestine and pancreas. A boost towards pancreatic specification and blockade of hepatic differentiation is provided by the inhibition of BMP signaling and, to further increase this effect, inhibition of TGFβ signaling [91]. Following, downregulation of Notch signaling by γ-secretase inhibitors in a precise timeframe of the differentiation process allows a transient induction of NGN3 expression, which, as mention above, is fundamental for endocrine commitment.

Following these major guidelines and optimizing the growth factor cocktails across the differentiation process, it is possible to achieve insulin-expressing cells *in vitro* [92]. Nevertheless, often these cells display polyhormonal expression and do not show insulin release in response to glucose stimulus. Rezania and Melton's research groups were the first two groups which independently reached a better degree of maturation in 2014 [93, 94].

Reziana and collegues described a seven-stage protocol which gives rise to *in vitro* differentiated cells displaying key characteristic of more mature β-cells, a modest glucose-stimulated insulin secretion *in vitro* and *in vivo* [93]. They introduced ascorbic acid at early stage of differentiation to increase production of pancreatic progenitor cells co-expressing PDX1+/NKX6.1+. To upregulate NGN3 and stimulate the co-expression of PDX1, NKX6.1, neurogenic differentiation (NEUROD)1 and NKX2.2, they utilized a combination of molecules, including ALK5 and bone morphogenetic proteins (BMP) receptor inhibitors and thyroid hormone (T3) at stage 5. At stage 6 inhibition of Notch signaling was added in order to obtain a population PDX1+/NKX6.1+/NEUROD1+ but glucagon- or somatostatin-negative. Importantly, after transplantation in mice, such differentiated cells displayed the capacity to reverse diabetes induced by treatment with streptozotocin, a drug that ablate selectively murine β-cells [93].

Analogously, Melton's research group reported similar results using a 3D culture system, a stepwise protocol of 4-5 weeks length and cocktails of factors affecting sequentially numerous pathways [94]. They extended the supply of FGF7, SANT1 (inhibitor of SHH) and low concentration of retinoic acid in order to obtain pancreatic progenitor cells PDX1+/NKX6.1+. Similar to Rezania's research group, they found to be crucial the modulation of WNT3, activin, SHH, EGF, TGFβ, thyroid hormone, retinoic acid and Notch signaling pathways to obtain cells displaying β-cells markers, ultrastructure and function both *in vitro* and in *in vivo* [94].

Even if these progresses have been more than remarkable, such β-cell still lack complete mature phenotype (e.g. proper MafA expression) and *in vitro* glucose-stimulated insulin secretion is modest in comparison with isolated human islets, stressing their functional immaturity.

Recently, Velazco-Cruz and collogues reported an interesting study regarding the importance of timing for TGFβ signaling modulation by ALK5

inhibitor II. Indeed, its inhibition is necessary during stage 5 of differentiation to achieve β-cell phenotype, but subsequent interruption of ALK5 inhibitor II exposure results in glucose-responsive differentiated cells [95].

Moreover, *in vivo* environment seems to boost their functional maturation, but which signals are involved is still unknown. Interestingly, it has been shown that both direct interaction with endothelial cells [96] or estrogen receptor signaling [97] may play an important role in maturation.

In 2014, ViaCyte, a private regenerative medicine company, initiated a clinical trial (phase I/II) to test safety and efficiency of their VC-01™, an Encaptra® immunoprotected device including ESCs-derived pancreatic progenitor cells [98]. This study is aimed at assessing whether this device can be safely implanted in T1D patients for two years and at measuring changing in C-peptide levels. The estimated study completion will be January 2021.

Recently, studies of single-cell RNA sequencing have been performed to increase our knowledge about β-cell differentiation [99]. Such kind of studies have been accomplished in human islets too, revealing different subpopulations within α- and β-cell population and highlighting heterogeneity in the regulation of genes related to functional maturation [100, 101].

PSC-derived β-cells represent the optimum option for studying β-cell biology. Indeed, so far, studies on primary β-cells are limited by scarce availability - few donor organ transplantation centers worldwide provide human islets –, high islet preparation variability and difficulties in *in vitro* islets maintenance and in genome editing. As an additional alternative, human β-cell lines have been developed [102, 103, 104, 105]. Nevertheless, these are pseudodiploid, immortalized proliferative cells, and even if they represent a useful tool, they cannot be considered equivalent of primary β-cells and they cannot be used to study developmental intermediates.

iPSC-derived β-cell system allows us to broaden our knowledge about pathogenic mechanisms underlying β-cell dysfunction, to explore islets function directly on patient-derived cells, as well as to screen and develop more efficient and specific drugs for the treatment of the different form of diabetes. Once optimized, this technology would also allow efficient β-cell replacement as clinical therapeutic application.

Finally, specific mutations of interest (e.g. a mutation responsible for monogenic forms of diabetes) may be corrected in patient-derived iPSCs prior to differentiation in β-cells [106]. Otherwise, the same mutation may be introduced in a control (healthy) cell lines, resulting in the generation of isogenic cell lines by CRISPR/Cas9 [107]. This specific application permits to further investigate the mutation-induced effects, excluding confounding factors, i.e the different genetic background in cell lines from different individuals. Otherwise, this tool for genome editing can be used to create novel human β-cell models that have been knocked out for a gene of interested, e.g. related to β-cell dysfunction, or to analyse many risk alleles associated with common form of diabetes [108].

A schematic summary of PSC-derived β cell application is showed in figure 8.

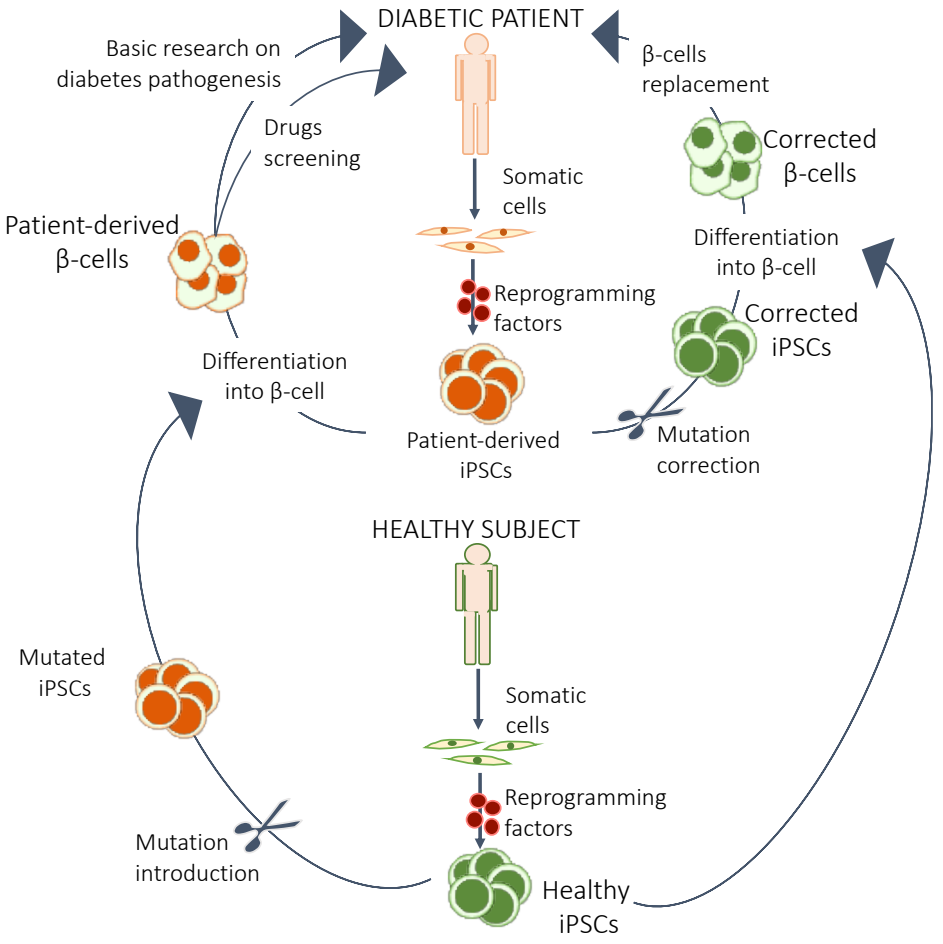

Figure 8. iPSCs-derived β-cell potential applications for disease modeling, drug discovery and β-cell replacement.

4. Cardiovascular complications of type 2 diabetes

The complications of DM are traditionally classified in microvascular – diabetic nephropathy, neuropathy and retinopathy – and macrovascular complications. The latter includes cardiovascular disease (CVD), a class of disease involving, among others, coronary artery disease, peripheral vascular disease and cerebrovascular disease.

T2D patients have been estimated to develop more severe CVD 14.6 years younger than non-diabetic subjects [109]. Moreover, they are more prone to develop CVD (2-3 times higher) than individuals without T2D, independently of classical risk factors as body mass index (BMI), age, smoking, and blood pressure [110, 111].

Globally, CVD represents a major cause of mortality in T2D condition, accounting for about 50% of all deaths [112].

4.1 Cardiovascular disease risk factors

CVD risks factors are identified as behaviors or condition that increase the risk of developing CVD and they can be divided in non-modifiable or modifiable. The first include those factors that cannot be changed, as age, gender, ethnicity and family history. For instance, both older people and south Asiatic, sub-Saharan African or Caribbean subjects have a greater risk than youngers and other ethnic descendants respectively. Women tend to develop CVD later in age than man, indeed their risk is delayed by about 10 years. Finally, a family episode of premature CVD in first-degree relatives (younger than 55 and 65 years of age in men and women, respectively) increases the risk of CVD [113].

Instead, modifiable CVD risks factors may be reduced or controlled by a focused intervention. They include high cholesterol, hypertension, smoking, diabetes, obesity, physical inactivity and diet enriched in fat, salt and sugars.

4.2 Atherogenesis and endothelial dysfunction

The pivotal mechanism leading to macrovascular disease is the atherosclerotic process, namely atherogenesis, which leads to narrowing of vessel walls because of the growth/complication of the atheromatous plaque.

Atherogenesis is the result of a chronic inflammatory condition and involves the adhesion of lymphomonocytes to the surface of endothelial cells and the differentiation of monocytes into macrophages in the subendothelial space [114], [115]. Here, macrophages include low-density lipoprotein (LDL) or oxidated-LDL, leading to the formation of foam cells. These cells, along with T lymphocytes generate the fatty streaks, the first evident atherosclerotic lesion, precursor of the plaque, but still reversible. Anatomically, vessels are composed by three layers: the tunica externa, which is the outmost and which is composed mainly by collagen fibers and elastic tissues, the tunica media, which is characterized by the presence of vascular smooth muscle cells, and the tunica intima, which is composed by one layer of endothelial cells and the one in direct contact with the blood flow. Migration (from the media to the intima) and proliferation (mediated by the platelet-derived growth factor) of vascular smooth muscle cells cooperate to the establishment of the atherosclerotic plaques by promoting the formation of the fibrous cap, a layer of fibrous connective tissue around the atherosclerotic lesion, in case of persistent pro-inflammatory environment.

A healthy endothelium exerts a strict control on vascular tone by releasing several vasodilators – e.g nitric oxide (NO) – and vasoconstrictors, such as endothelin and angiotensin II. On the other hand, endothelial dysfunction is characterised by decreased NO bioavailability, increased production of endothelin and activation of the signaling pathway of nuclear

factor (NF)-kB, which is highly involved in pro-inflammatory responses. This unbalanced condition, which describes a functional alteration, represents a very early step in atherosclerotic process. In case the pro-inflammatory stimuli persist, it evolves in a morphological alteration, due to a stable presence of the atherosclerotic plaque. This scenario is described as “the response to injury” hypothesis by Russel Ross [116].
When the plaque is well established, the major complication is represented by its disruption, which is cause of myocardial infarction and strokes.

4.3 Cardiovascular outcome trials in type 2 diabetes

Since 2008, dedicated cardiovascular (CV) outcome trials have been conducted to test CV safety for every new antidiabetic drug, because of a “Guidance for industry” released by the U.S Food and Drug Administration (FDA) [117]. Considered the high CVD prevalence in T2D patients, the guidance aimed at preventing a further increase in CV risk.
In these clinical trials, enrolled subjects with high risk for CV events are randomized to receive the under-investigation drug – in addition to the standard care – or the placebo (or a comparative drug) in addition to standard of care in order to evaluate the CV safety of the new treatment. These trials are usually conducted at glucose equipoise. The primary outcome is a combined CV endpoint, including CV death, non-fatal myocardial infarction and non-fatal stroke (3-points major adverse CV event, 3P-MACE). Some trials also include an additional primary outcome, as the hospitalization rate for unstable angina pectoris (4P-MACE). Secondary CV outcomes often include all-cause mortality, heart failure, death from CV causes. According to the guidance, the antidiabetic drug must result non-inferior to the standard of care with hazard ratio < 1.8.

So far, every completed trial demonstrated the non-inferiority of the tested drug and, surprisingly, some more recent therapeutic agents show beneficial effects on CVD beyond glucose control.

In particular, three main class of molecules have been tested:

1. dipeptidyl-peptidase 4 inhibitors (DPP4-I, SAVOR-TIMI 53, testing saxagliptin [118]; EXAMINE, testing alogliptin [119]; TECOS, testing sitagliptin [120]);
2. glucagon-like peptide 1 (GLP1) receptor agonists (GLP1RA, ELIXA, testing lixisenatide [121]; LEADER, testing liraglutide [122]; SUSTAIN-6, testing semaglutide [123]; EXSCEL, testing exenatide [124]; Harmony Outcomes, testing albiglutide [125]; REWIND, testing dulaglutide [126]; PIONEER-6, testing oral semaglutide [127]);
3. sodium/glucose co-transporter-2 inhibitors (SGLT2-I, EMPA-REG OUTCOME, testing empagliflozin [128]; CANVAS Program, testing canagliflozin [129]; DECLARE-TIMI 58, testing dapagliflozin [130]).

Whilst CV outcome trials on DPP4-I demonstrated CV safety (3P-MACE), but not CV benefit, members of GLPR1 receptor agonists and SGLT2-I demonstrate to reduce risk of CV outcome.

In addition, two CV outcome trials on insulin (ORIGIN, testing insulin Glargine [131]; DEVOTE, testing insulin Degludec [132]) and two CV safety study on a proprotein convertase subtilisin/kexin type-9 inhibitor (PCSK9-I, FOURIER, testing evolocumab, in which diabetes was established in 37% of the study population [133]; ODYSSEY OUTCOME, testing alirocumab in which diabetes was established in 29% of the study population [134]) have been published. Both the CV outcome trials testing PCSK9-I showed a significant decreased CV outcome (4P-MACE).

4.3.1 GLP1 receptor agonists

Incretins are a group of hormones secreted by enteroendocrine cells following nutrients intake which stimulate insulin secretion in response to variation in glucose levels. The two main incretins are represented by glucose-dependent insulinotropic polypeptide (GIP) and GLP-1. The latter is produced by enteroendocrine L-cells from the ileum and colon, whilst GIP is secreted by duodenal K-cells. Both hormones are processed and undergo to post-translational modification before their release. GLP1 and GIP have a very short half-life in circulation – 1.5 and 7 minutes, respectively [135, 136] – because of the peptidase DPP4 which is responsible of their early degradation. GLP-1 and GIP receptors are expressed on pancreatic β-cells, as well as in brown fat, heart, kidney, brain and endothelium and the binding of their ligand trigger the downstream beneficial effect. GLP1RAs, such as exenatide and liraglutide, are able to bind the GLP1R receptor but they show resistance to the DPP4 action (resulting in a prolonged half-life), thereby they have been developed and proposed for T2D patients' treatment. As GLP1, GLP1RA decrease glycaemia by stimulating glucose-induced insulin synthesis and release (by stimulating cAMP generation) and by reducing glucagon secretion [137]. Effects on pancreatic β-cells also include apoptosis prevention [138, 139]. In addition, GLP1RA-mediated effects include slowing of gastric emptying and of appetite onset [140, 141]. GLP1RA treatment in T2D patients also results in modest decrease in lipids level measurements, blood pressure and body weight. The risk of hypoglycaemic events following GLP1RA administration is very low because of their glucose-dependent action.

T2D patients show a strongly decreased incretin effect mediated by GLP1, although GIP responses were just slightly reduced [142].

In six CV outcome trials (LEADER, SUSTAIN-6, EXSCEL, Harmony outcomes, REWIND, PIONEER-6) the primary outcome is the 3P-MACE,

whilst in ELIXA the primary outcome includes hospital admission for unstable angina (4P-MACE). Except for the ELIXA (lixisenatide) and EXCSCEL (exenatide), all the CV outcome trials show superiority to placebo for CV protection. Of note, in the EXSCEL, a higher proportion of patients without established CVD has been enrolled and this criterium may have affected the results, driving the lack of a clear reduction in the primary outcome. In addition, lixisenatide and exenatide are structurally based on Exendin-4 (a hormone, sequentially similar to human GLP1, derived from the lizard *Gila monster*'s saliva), whilst albiglutide, dulaglutide, liraglutide and semaglutide are structurally closer to native GLP1 [143].

In the pooled analysis, treatment of T2D patients with one of the GLP1RA reduces both the relative risk of 3-P MACE (HR 0.88, 95% CI 0.82–0.94; p<0.0001) and all-cause mortality (HR 0.88, 95% CI 0.83–0.95; p=0.001), as well as the hospitalization for heart failure. The number needed to treat (NNT) is 75 (50-150) to prevent 1 MACE event and 108 (77-260) to prevent 1 death for any cause, over an estimated median follow-up of 3.2 years [144].

Generally, GLP1RAs show cardioprotective outcomes, probably mediated by mainly anti-atherothrombotic effects. There are numerous studies which point out GLP1RA actions on endothelial function, by promoting vasodilation [145], on curbing inflammation in endothelial cells [146] and on plaque stability [147].

However, underlying mechanisms on GLP1RA beneficial effects on heart failure are not well clarified yet.

4.3.2 SGLT2 inhibitors

SGLT2-I, including empagliflozin, canagliflozin and dapagliflozin, are a recently introduced class of glucose-lowering drugs for the treatment of T2D. These molecules aim at reducing the glucose burden by promoting glucose excretion into urine and preventing renal reabsorption. Thus, SGLT2-I treatment lead to glycosuria, improvement in glucose control, weight reduction and decrease in blood pressure.

The original molecular target of SGLT2-I is the Na/glucose co-transporter 2, which is expressed in the early proximal tubule and is responsible for above 95% of the total amount of renal glucose reabsorption. As a consequence of their mechanisms of action, the risk of hypoglycaemic events associated with treatment with SGLT2-I is very low.

CV outcome trials have been conducted with empagliflozin (EMPA-REG OUTCOME), dapagliflozin (DECLARE-TIMI 58) and canagliflozin (CANVAS Program). The first results have been shown from the EMPA-REG OUTCOME study and this has been the first CV outcome trial to point out not only CV safety, but even CV protection for an antidiabetic treatment.

Overall, SGLT2-I treatments have a beneficial CV effect, which happens earlier than CV protection mediated by GLP1RA, and they reduce the risk of major adverse CV events, in patients with multiple risk factors with a class effect.

Indeed, in pooled analysis, treatment of T2D patients with SGLT2-I reduces the risk of a major adverse cardiac event by 11% (HR 0.89 [95% CI 0.83–0.96], p=0·0014) [148], In addition, SGLT2-I reduce the risk of myocardial infarction by 11%, of CV mortality by 16% and of hospitalisation for heart failure by 31% – which represents the highest and most consistent SGLT2-I-mediated effect –, whilst no significant effects on stroke have been shown. Finally, pooling the result from trials with

SGLT2-I shows that SGLT2-I significantly reduce the risk for all-cause mortality by 15% (HR 0.85 [95% CI 0.78–0.93) and the NNT to prevent 1 death for any cause is 101 (69-216).

Although these findings provide striking evidence of SGLT2i-mediated CV protection beyond glucose control, the exact underlying mechanisms are still unclear and several hypotheses have been proposed.

As consequence of SGLT2-I-induced natriuresis and glycosuria, and following osmotic diuresis, and reduction in blood pressure and as wells as in vascular function [149, 150, 151] may results in an overall improvement in ventricular loading conditions.

Another hypothesis is the improvement in cardiac metabolism and bioenergetics as the driving force for overall beneficial CV effects, although a definitive evidence linking myocardial energetics to SGLT2-I-mediated positive effect is still lacking. However, as a support to this theory, also known as “Thrifty Substrate Hypothesis” [152], SGLT2-I slightly increases the production of β-hydroxybutyrate, a ketone body, which can be more efficiently oxidized by the heart in spite of fatty acids or glucose [153, 154]. Moreover, SGLT2-I-mediated increase in β-hydroxybutyrate levels may inhibit histone deacetylases and prevent the activation of pro-hypertrophic signaling pathway [155]. SGLT2-I may also promote branched-chain amino acid degradation, which represents an impaired mechanism in heart failure [156].

It has also been proposed that SGLT2-I may have an effect directly on cardiac fibroblast phenotype and function [157, 158]or alter adipokines and cytokines production [159, 160].

Finally, SGLT2-I-mediated effects may be driven by alternative still un-recognized targets. In this regard, recently Baartscheer and colleagues reported that SGLT2-I may act by inhibiting the Na^+/H^+ exchanger (NHE) in cardiomyocytes. Docking studies have shown that the hydrophilic glucosyl portion of SGLT2-I molecules may fit the hydrophilic Na^+-binding

site of NHE, after which the precise binding affinity is specified by the SGLT2-I aglycone part [161]. SGLT2-I-mediated (empagliflozin) NHE inhibition leads to reduced intracellular Na^{+} and Ca^{++} levels and augmented mitochondrial Ca^{++} levels in cardiomyocytes [162], thereby restoring an altered scenario characteristic of heart failure.

Nevertheless, the question regarding the mechanisms underlying SGLT2-I-mediated beneficial effects on MACE in T2D patients with atherosclerotic CVD remain still open.

5. Myeloid angiogenic cells

Vascular endothelium shows a variety of key function, such as the active regulation of macromolecules, nutrients and hormones passage into the surrounding tissues and the maintenance of vessel health by sustaining a dynamic equilibrium between damage and repair. This delicate equilibrium is influenced by a number of cues and *noxae*.

Endothelium self-repair feature is critical for vascular health and it is mediated by a specific subset of cells, firstly isolated by Asahara and colleagues in 1997 [163]. Indeed, they found a circulating cell population, namely “putative” endothelial progenitor cells (EPC), able to differentiate in mature endothelial cells and to cooperate to the formation of new blood vessels. Recruitment of EPCs into ischemic tissue requires a step-wise process, including mobilization – which is promoted by vascular endothelial growth factor (VEGF), stromal cell-derived factor (SDF)1α, erythropoietin and granulocyte-colony stimulating factor, but also by statins, estrogen, exercise and peroxisome proliferator-activated receptor (PPAR)γ –, chemotaxis – mediated by the binding of SDF1α to the receptor C-X-C chemokine receptor type (CXCR)4 and of VEGF to kinase insert domain receptor (KDR) –, adhesion – mainly mediated by integrins –, tissue invasion and finally differentiation [164, 165, 166, 167].

EPCs arise from bone marrow myeloid stem cells and express stem markers cluster of differentiation (CD)34 and CD133. Across differentiation they acquire endothelial markers, such as vascular endothelial growth factor receptor-2 (VEGFR-2, or KDR), platelet cell adhesion molecule-1 (CD31), vascular endothelial (VE)-cadherin and von Willebrand factor (vWF), after which they start to express endothelial nitric oxide synthase (eNOS), CD146 and E-selectin [167].

Two different approaches can be used to study EPCs [168]. The first involves the use of flow cytometry which allows the assessment of EPCs number based on their antigen expression profile ($CD34^+/CD133^+/KDR^+$).

The other approach, used to study EPC function *ex vivo*, allows the discrimination of two different population, based on their time of appearance in culture, starting from peripheral blood lymphomonocytes [169]. These two cell subtypes, previously named “early” and “late” EPCs, have different phenotypes, hematopoietic and endothelial, respectively [170]. Early EPCs have been defined as circulating angiogenic cells and, lately, as myeloid angiogenic cells (MAC), whilst late EPCs have also been referred as endothelial outgrowth cells or as endothelial colony forming cells [168].

The latter cell population shows specific angiogenic capacity, by contributing to vascular repair of injured endothelium and new blood vessel formation [171].

Morphologically, late outgrowth EPCs form colonies of cells with a cobblestone-like shape [172] and structurally, they display endothelial markers together with CD34, whereas markers of monocyte antigen CD14, CD45 and CD68 are not expressed. They also show both Ac-LDL uptake and lectin binding capacities and express eNOS enzyme [173].

On the other hand, MACs are cultured cells derived from peripheral blood myeloid cells displaying a molecular phenotype similar to that of monocytes. They display a spindle-like morphology and a range of

endothelial markers – as KDR, CD31 – as wells as leukocyte cell-surface markers – such as CD45 and CD14 – [173]. MACs are negative for CD34 and do not differentiate into endothelial cells, but they have a role in endothelial repair, mainly by paracrine secretion of pro-angiogenic factors [174]. The technical-feasibility of MAC culture procedure and their relatively large number in the circulation point to MACs as the ideal cell population to be exploited for the study of the biology of cells with intrinsic pro-angiogenic functions in both healthy or diseased subjects.

5.1 Myeloid angiogenic cells and diabetes

MACs are negatively influenced in number and function by IR, CV risk factors and CVD, thus providing clinical information on the atherosclerotic burden and CV risk. Indeed, MAC number not only is inversely associated to CV events, but it predicts such events [175], [176], [177], [178]. Among CV risk factors, smoking [179], [180], hypertension [181], hypercholesterolemia [182], obesity [183] and T1D and T2D [184], [185] have all been correlated to a reduced number/function in MACs/EPCs. Affected mechanisms may occur at different steps, such as a decrease in survival during mobilization in the bone marrow, trafficking, homing or differentiation [186], [187].

Recently, Chambers and colleagues demonstrated that high glucose environment affects MAC proangiogenic function which is associated to a significant augment in IL1β expression, both at mRNA and protein level. IL1β has also been found upregulated in MACs isolated from T1D patient with microvascular complication in comparison with IL1β expression in MACs isolated from T1D patients without microvascular complication or non-diabetic subjects [188].

Nevertheless, MAC/EPC bioavailability and function can be improved by focused intervention on lifestyle or pharmaceutical therapies. Changes in

lifestyle include both physical exercise, polyunsaturated fatty acids and vegetables-enriched diet and smoking cessation.

Treatment with statins [189], angiotensin converting enzyme inhibitors [190], estrogens [191], PPARγ agonists [173], insulin [192] and DPP4-I [193] in T2D patients have all been associated with an improvement in MAC/EPC biology.

A single trial has been conducted to test SGLT2-I-mediated (dapagliflozin) effect on EPC number in T2D patients and it claims to exclude a significantly increase of EPCs, suggesting that CV protection exerted by SGLT2-I may not directly involve this particular mechanism [194]. Nevertheless, another clinical trial (NCT02964585) aimed at exploring the role of SGLT2-I canagliflozin $CD34^+$ EPC levels in T2D patients, is ongoing.

These data suggest that both availability and function of MACs are fundamental in modulating CVD in diabetic condition, thus representing a potential therapeutic target.

6. Lipotoxicity

Lipotoxicity describes the deleterious effects caused by elevated FFA levels. If initially, these detrimental effects referred specifically to impairment in glucose metabolism, later the term gained a broaden meaning. Indeed, lipotoxicity is a condition characterized by elevated non-esterified fatty acids (NEFA), lipid accumulation in non-adipose tissues, altered fat topography and adiposopathy, globally leading to cellular dysfunction and cell death, mainly by the activation of pro-inflammatory, ER and oxidative stress responses [195].

When energy intake exceeds the expenditure, the balance is positive and adipocytes store the surplus lipids as triglycerides, leading to adipocytes hypertrophy and hyperplasia and resulting in expansion of subcutaneous

adipose tissue. According to the “expandability hypothesis”, in case of prolonged energy positive balance, this capacity of growing in size reaches its limit and additional lipids cannot be safely stored, contributing to elevation in circulating FFA which are collected from non-adipocyte cells and stored in non-adipose tissues “ectopic fat” [196].

In the presence of insulin resistance, because of the altered anti-lipolytic action of insulin, higher levels of FFA can leave the adipocytes to enter the circulation and they might be uptaken by other organs. Moreover, the increased inflammatory state further increases IR and lipolysis.

Dysfunctional adipose tissue leads to adiposopathy (adipose tissue conversion from healthy to “sick” resulting in altered adipokines release profile). Moreover, it is characterized by macrophage infiltration and chronic inflammatory state [197].

Both infiltrated macrophages and adipocytes secrete pro-inflammatory and pro-thrombotic (adipo/cyto)kines, such as tumor necrosis factor (TNF)α, resistin, IL-6, plasminogen activator inhibitor 1 and angiotensinogen, overall contributing to atherogenesis and IR onset [198], [199], [200], [201], [202]. In this context, there is also a significant decrease in adiponectin levels – an insulin-sensitizing and anti-atherogenic adipokine [203].

This chronic metabolic inflammation, namely metaflammation, is typical of metabolic diseases, such as obesity and diabetes, and it occurs in several tissues, including adipose tissue, liver, muscle, brain and vascular system [204].

In particular, saturated FFA (SFA) are recognized to cause greater deleterious effects than the counterparty unsaturated FFA, which are instead considered “healthy fats”. High concentration of SFA directly exerts detrimental effects in several organs, e.g. SFA lead to IR in skeletal muscle [205], promote β-cell dysfunction and death in endocrine pancreas and lipid accumulation in liver [206] and myocytes [207]. Along with

glucotoxicity, lipotoxicity has a pivotal role in T2D pathogenesis. Moreover, in addition to their initial role in atherogenesis [208], high concentration of SFA induce apoptosis in endothelial cells, thereby contributing to plaque instability [209].

Palmitic (PA) and stearic (SA) acids are the most predominant circulating long-chain SFA. In the European Prospective Investigation into Cancer and Nutrition Study (EPIC)-InterAct case-cohort study, including 27296 participants, researchers investigate the association between SFA and incidence of T2D. In this study, SFA account for 46% of total plasma phospholipid fatty acids fraction and PA represents the major contributor (30.1%), followed by SA, which account for the 14.1% [210].

In EPIC-InterAct case-cohort study, even-chain SFA and odd-chain SFA (pentadecanoic acid, 15:0; heptadecanoic acid, 17:0) levels resulted positively and inversely associated with incident T2D, respectively. Similar to odd-chain SFA, longer-chain SFA also are inversely associated with incident T2D [210].

Even-chain SFA are positively associated with dietary consumption of alcohol, soft drinks and butter-like products, such as margarine, whilst they are negatively correlated with fruit, vegetables and vegetable oils. In the other hand, odd-chain SFA generally show positive associations with dairy products, nuts and seeds and baked food products, but negative associations with red meat, soft drinks, alcohol, and margarine. Pentadecanoic and heptadecanoic acids are mainly derived from dietary consumption, while intracellular SA and PA pools may not only be sustained by circulating (e.g. triglycerides, FFA) and intracellular lipids, but may also derive from *de novo* lipogenesis (from carbohydrates or alcohol) processes in the liver or adipose tissue [211, 212] (figure 9). In particular, PA can directly origin from *de novo* synthesis, driven by acetyl-CoA carboxylase (ACC), which is a key enzyme responsible for the reaction rate-limiting step – i.e. the production of malonyl-CoA from acetyl-

CoA–, and by fatty acids synthase (FAS). On the other hand, SA *de novo* synthesis origins from PA elongation, specifically mediated by the enzyme elongation of very long chain fatty acids protein (ELOVL)6, which catalyzes the generation of a SA precursor, 3-Oxostearoyl-CoA, from palmitoyl-CoA and malonyl-CoA. PA may also be processed by stearoyl CoA desaturase (SCD), into the monounsaturated palmitoleate (16:1) with the introduction of a single double bond between the carbons 9 and 10. Similarly, SA may be desaturated by SCD, which converts SA into oleate (18:1). The role of SCD in the conversion of SFA into the non-deleterious unsaturated counterpart suggests a protective role of this enzyme in lipotoxicity, which, in turn, may result from an impaired balance between SFA production (dietary intake and PA *de-novo* lipogenesis or elongation in SA) and SFA desaturation.

Figure 9 shows the sources that feed the intracellular FFA pools.

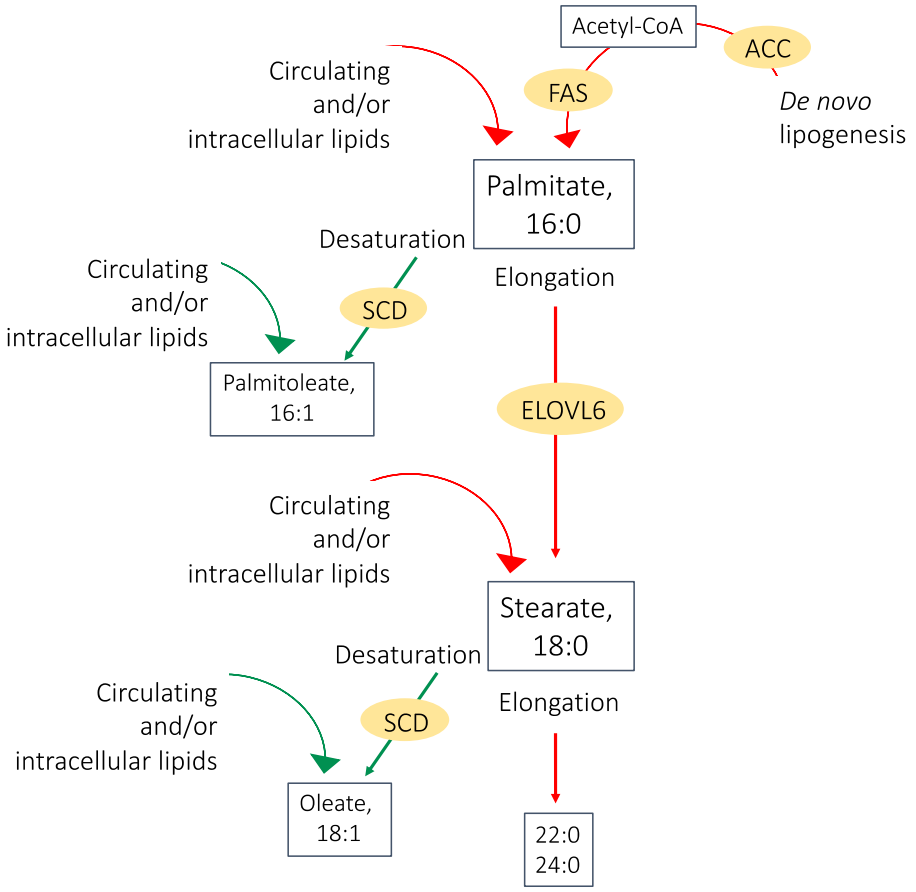

Figure 9. Sources and fates of PA and SA intracellular pools.

Intracellular sources and fates of SFA (red arrows) and unsaturated fatty acids (green arrows) pools. ACC, acetyl-CoA carboxylase; ELOVL6, elongation of very long chain fatty acids protein 6; FAS, fatty acid synthase; SCD, stearoyl CoA desaturase.

6.1 Lipotoxicity and insulin resistance

Obesity is strongly associated with IR and T2D and it is mainly driven by chronic tissue inflammation [213].

Pro-inflammatory mechanisms triggered by SFA are usually mediated by the activation of toll-like receptor (TLR)-4, and/or TLR-2, which results in

stimulation of the pro-inflammatory key mediators NF-kB and c-Jun N-terminal kinase (JNK) [214]. Nevertheless, pro-inflammatory pathways may be also activated through TLR-independent circuits. Indeed, SFAs lead to increase in ROS levels which may result in IL1β maturation and release mediated the activation of the inflammasome machinery [215]. IL1β is known to affect insulin signaling in insulin-sensitive cells, supporting IR establishment [216, 217].

In addition, SFAs are precursors of other lipid products, such as diacylglycerol – whose levels are increased in IR condition and which interfere with IRS1 signaling by protein kinase C (PKC) activation – or ceramides, leading to Akt de-phosphorilation by phosphatase 2A [218,219, 220, 221, 222]. Thereby, both products result in decreased insulin signaling.

SFA-induced ER stress is also involved in progression of IR and T2D.

Three transmembrane proteins, inositol-requiring enzyme (IRE)1, protein kinase R (PKR)-like ER kinase (PERK) and Activating transcription factor (ATF)6, drive the three pathways in UPR. In normal conditions, these three proteins are associated and maintained inactive by the heat shock chaperone protein, binding immunoglobulin protein (BiP) – also known as 78-kDa glucose-regulated protein (GRP78). As misfolded proteins in ER increase, they recruit BiP and lead to the release of the three UPR-mediators. IRE1α has both kinase and ribonuclease (RNase) activity. Under stress conditions, it cuts the X-box binding protein 1 (XBP-1) mRNA, generating the transcription factor spliced XBP-1 (sXBP-1), whose activity supports the transcription of genes involved in the UPR, adipogenesis, lipid metabolism and inflammation. In addition, IRE1α can promote either adaptive or pro-apoptotic responses via regulated IRE-1-dependent decay of mRNA (RIDD). The second pathway involves ATF6 which, after being processed in the Golgi, regulates the transcription of XBP-1 and of genes involved in endoplasmic-reticulum-associated protein degradation (ERAD) process and in protein folding, maturation and

secretion. One of ATF6 downstream chaperones target is BiP expression. Ultimately, activated PERK phosphorylates eukaryotic initiation factor (eIF2α) leads to reduced translation initiation. A downstream protein in PERK signaling is ATF4, which triggers apoptosis by increasing C/EBP homologous protein (CHOP) transcription. CHOP recruitment is engaged also in ATF6 pathway.

Circulating FFAs may trigger ER stress via a PERK-dependent mechanism, which leads to increase in the expression of cytokines, such as TNFα and IL-6 [223], [224]. In addition, it has been shown that PA may induce IR in myotubes by altered IRS phosphorylation via IRE1/JNK pathway. Moreover, protein tyrosine phosphatase (PTP)1B – which acts as a negative regulator of the insulin pathway by targeting the phosphorylated INSR and IRS1 and whose levels are increased by high fat diet – is activated by ER stress and promote ER stress-mediated IR in skeletal muscle [225].

Finally, excessive FFA oxidation generates mitochondrial ROS overproduction [226]. It is known that chronic oxidative stress, due to impaired balance in production/clearance of ROS and RNS, as in obese condition [227], leads to chronic inflammation and IR [228]. Ultimately, excessive FFA oxidation triggers the activation of several downstream signaling pathway, such as JNK and NF-kB, resulting in altered IRS phosphorylation and consequent onset of IR. In addition, diacylglycerol-activated PKC triggers nicotinamide adenine dinucleotide phosphate (NADPH) oxidase activity, which is involved in FFA-mediated ROS generation [229]. In the endothelium, SFA-mediated increase in ROS reduces NO availability, promoting vascular IR and endothelial dysfunction [230].

6.2 Lipotoxicity and β-cell dysfunction

Although representing an important source of energy, chronic high FFA levels are associated with impaired function in β-cells, i.e reduced glucose-stimulated insulin secretion and cell death [231], [232], [233].

Several mechanisms mediating the deleterious FFA effects in β-cells, such as ER and oxidative stress, inflammation, increased intracellular triglycerides and synthesis of ceramides [234], [235], [236], [237] have been investigated.

In particular, FFA-mediated impairment in ER functions and in the consequent ER stress response, contribute to β-cell toxicity.

UPR signaling molecules, such as BiP, sXBP-1, ATF6, eIF2α, ATF4 (downstream of PERK pathway) and CHOP, are all induced by FFA exposure in β-cells leading to β-cell dysfunction and death [238], [239]. SFA can also disrupt protein trafficking from ER to Golgi, overloading ER and contributing to UPR activation [240].

Nutrients overload, including FFA and glucose, results in enhanced oxidative stress and ROS levels, which lead to β-cell injury. In addition, as mention above, β-cells work to maintain euglycaemia in the setting of IR, but intracellular Ca^{2+} concentration oscillations, which are included in the glucose-stimulated insulin secretion machinery, can fuel mitochondrial generation of ROS [241]. Ca^{2+} can also activate PKC and enhance the resulting NADPH oxidase-dependent production of ROS [242], [243]. The following generation of H_2O_2 can culminate in inhibition in insulin secretion [244]. Increased oxidative insult in β-cells cooperates to further immune cell infiltration and cytokine production, worsening the inflammatory burden and damage [245].

Another above-mentioned mechanism of β-cell failure is the loss of β-cell identity. A recent study identifies some pro-inflammatory cytokines, in

particular IL-1β, IL-6 and TNFα, as responsible for β-cell dedifferentiation and pinpoints IL1-β as the most effective in this process [246].

Finally, PA metabolism can generate ceramides, whose signaling pathway leads to apoptosis, both by inhibiting PI-3 kinase/Akt-pro-survival pathway and by promoting ROS-induced cell death [247, 248].

The recent introduction of human β-cell lines and of iPSCs-derived β-cell technology represents an important step ahead in the modeling of pancreatic β-cell pathophysiology. So far, findings on lipotoxicity in human β-cells were hampered by the difficulty to study the disease tissue. Indeed, the majority of findings on FFA-mediated deleterious effects on β-cells come from rodent models, primary islets or β-cell lines [249, 250, 251, 252].

AIMS

Lipotoxicity represents a key phenomenon in the pathogenesis of both T2D and related CVD.

1. We hypothesize that free fatty acids may not only induce a direct damage on the vessel wall, but also alter endogenous repair processes through a direct effect on MACs. Moreover, we hypothesized that also the observed beneficial effects of SGLT2-I on CV outcomes – whose underlying mechanisms have not yet fully clarified – might be mediated by a direct effect on MACs;

2. Given the need to confirm in humans the findings so far obtained about FFA-mediated lipotoxic effects on animal β-cells, we plan to study lipotoxicity in induced pluripotent stem cells (iPSCs) from human subjects

Thereby, the aims of this study are:

1. To investigate the effects of lipotoxicity - specifically mediated by physiological concentrations of stearic acid - on cell viability and function in MACs and the capacity of the novel anti-diabetic drugs, SGLT2 inhibitors to curb stearic acid-induced lipotoxicity in MACs

2. To improve the protocol of iPSCs differentiation into β-cells in order to create novel *in vitro* model of β-cell lipotoxicity

MATERIALS AND METHODS

1. Ethics Statement

The local Institutional Review Board - *Comitato Etico Unico della Provincia di Parma* - approved the study protocol, which was conducted in accordance with the Declaration of Helsinki. Blood donor material was fully anonymized and no informed consent was required.

Skin fibroblasts for human iPSC studies were collected after informed consent obtainment. The study protocol was approved by the Ethics Committees of the Helsinki, Finland, and the Ethical committee of the Erasmus Hospital, Brussels, Belgium.

2. Cell culture

2.1 Myeloid angiogenic cells

Isolation and culture of myeloid angiogenic cells (MAC) have been performed accordingly to literature, in the laboratories of the Department of Medicine and Surgery, Endocrinology and Metabolic Diseases Unit at the University of Parma, Italy [173]. Specifically, peripheral blood mononuclear cells (PBMCs) have been isolated from healthy donor buffy-coats by Lymphoprep™ (Euroclone) density gradient centrifugation. PBMC have been collected, seeded into six-well culture plates coated with fibronectin (10 μg/ml) at a density of $1x10^7$ cells/well and cultured in endothelial cell growth medium-2 (EGM-2) (Lonza) at 37°C and 5% CO_2. EGM-2 was enriched with supplements and growth factors (hydrocortisone, human fibroblast growth factor β, VEGF, R3 insulin like growth factor-1, human epidermal growth factor, ascorbic acid, gentamycin A/amphotericin A, heparin) required for culturing endothelial cells and 2% fetal bovine serum. Medium has been refreshed at days 4

and 7. On day 7, adherent cells have been considered MACs ($CD45^+/CD14^+/CD64^+/CD31^+/KDR^+/CD34^-$ phenotype [173] and showed an elongated spindle-shaped morphology. All the experiments have been performed at day 7.

2.2 EndoC-βH1 cells

Human clonal EndoC-βH1 cells have been kindly provided by Prof. Raphael Scharfmann, from the Université Paris-Descartes, France [102], and cultured as described in literature [253] in the laboratories of the ULB Center for diabetes research at the Universitè Libre de Bruxelles, Belgium. Specifically, cells have been seeded into ninety-six- or twenty-four-well culture plates coated with fibronectin (2 μg/ml) and extracellular matrix (ECM, 2%) at a density of $1.2x10^5$-$1.5x10^5$ cells/ml. EndoC-βH1 have been cultured in Dulbecco's Modified Eagle Medium (DMEM, ThermoScientific) containing 5.6 mM glucose, 2% bovine serum albumin fraction V, 50 μM 2-mercaptoethanol (Sigma-Aldrich, Poole, UK), 10 mM nicotinamide (Calbiochem), 5.5 μg/ml human transferrin (Sigma-Aldrich), 6.7 ng/ml soudium selenite (Sigma-Aldrich), 50 units/ml penicillin and 50 μg/ml streptomicin (Lonza). Cells have been passaged once per week.
For FFA treatment EndoC-βH1 have been cultured in DMEM-F12 (ThermoScientific) supplemented with 5.5 μg/ml human transferrin (Sigma-Aldrich), 6.7 ng/ml sodium selenite (Sigma-Aldrich), 10mM nicotinamide (Calbiochem), 50 μM 2-mercaptoethanol and 100 U/ml penicillin/streptomycin (Lonza).

2.3 Human islets

Human islets from non-diabetic organ donors have been isolated in the laboratories of the Department of Clinical and Experimental Medicine, at the University of Pisa, Italy [254]. Islets have been sent to Brussels, Belgium,

within 1–5 days from isolation and they have been cultured in Ham's F-10 medium containing 6.1 mM glucose, 2 mM GlutaMAX-I, 0.75% bovine serum albumin fraction V, 50 U/ml penicillin and 50 μg/ml streptomycin. Donors have an average age of 66±10 years and an average body mass index of 27.4±3 kg/m2. β-cell purity of the human islet preparations, determined by insulin immunofluorescence, was 53±23%.

2.4 Human induced pluripotent stem cells

iPSC lines HEL115.6 and HEL135.2 have been derived from the reprogramming of fibroblasts by Cytotune iPSC (Life technologies), which uses vectors based on a modified, non-transmissible form of Sendai virus, in the laboratories of Molecular Neurology and Biomedicum Stem Cell Centre at the University of Helsinki, as described in literature [255].

Specifically, iPSC cell line HEL115.6 has been derived from umbilical cord fibroblasts obtained from a 31-weeks-old unborn male fetus, whilst iPSC cell line HEL135.2 has been derived from skin fibroblast obtained from a 26-years-old male affected by Friedreich Ataxia disease.

HEL115.6 pluripotency quality controls have been validated as described in literature [256].

iPSCs have been cultured in Matrigel (Corning BV, Life Sciences)-coated plates in Essential 8 (E8) medium (Life Technologies) as colonies. Cells have been passaged with 0.5 mM ethylenediaminetetraacetic acid (EDTA, Life Technologies) twice per week in the laboratories of the ULB Center for diabetes research at the Universitè Libre de Bruxelles, Belgium.

2.5 Human induced pluripotent stem cells differentiation into β-cells

A stepwise protocol based on previous published protocols, which mimic the embryonic development of the endocrine pancreas [93, 94, 106], has been used for β-cell differentiation in the laboratories of the ULB Center for diabetes research at the Universitè Libre de Bruxelles, Belgium [256]. When cells reached 80% confluency, iPSC have been rinsed with 0.5 mM EDTA, detached by Accutase (Capricorn Scientific) treatment, seeded into six-well Matrigel-coated culture plates at a density of $1x10^6$ cells/ml and cultured in E8 medium containing 5 μM ROCK inhibitor (StemCell technologies).

24 hours after plating, E8 medium has been refreshed without ROCK inhibitor supplement. The 7-stages differentiation protocol has been initiated when the cells reached full confluency. Cells have been differentiated in Matrigel-coated six-wells plates and medium refreshed daily until the end of Stage 4 (S4), after which cells were detached by using Accutase (Capricorn Scientific) to transfer them in 3D culture. Cells have been resuspended in culture stage 5 (S5) medium supplemented with 10 μM ROCK inhibitor and 2 μg/ml Heparin (StemCell technologies) and plated either into rotating (100 rpm) suspension culture in ultra-low attachment 6-well plate (Sigma-Aldrich) or in static culture in microwells (AggreWell™400, StemCell technologies) at a density of $1\text{-}2x10^6$ or $0.45x10^6$ cells/ml, respectively and unless otherwise indicated. Before seeding, microwells plates have been washed with anti-adherence rising solution (StemCell technologies), according to manufacturer's instructions.

Next, cells have been cultured in S5 medium without ROCK inhibitor and heparin for further 4 days and medium refreshed daily. From day 16

(beginning of stage 6, S6) until the end of the differentiation, medium has been refreshed every second day.

MCDB131 (Thermo Scientific) has been used as basal medium and it has been differently supplemented during the differentiation as described in the table 1 and 2.

	BASAL 1	BASAL 2	BASAL 3
Glutmax (mM)	2	2	2
NaHCO3 (g/L)	1.5	2.5	1.5
BSA fV (%)	0.5	2	2
Glucose (mM)	10	10	20
Insulin-Transferrin-Selenium-Ethanolamine (ITS -X; dilution)	/	1:200	1:200
Heparin (μg/ml)	/	/	10
Zinc Sulfate (μM)	/	/	10

Table 1. Basal media composition

	d1	d2	S2	S3	S4	S5	S6	S7
BASAL (n)	1	1	1	2	2	3	3	3
Activin A (ng/ml)	100	100	100	/	10	/	/	/
CHIR-99021 (μM)	5	0.5	/	/	/	/	/	/
Ascorbic acid (mM)	/	/	0.25	0.25	0.25	/	/	/
KGF (FGF-7, ng/ml)	/	/	50	50	50	/	/	/
SANT-1 (μM)	/	/	/	0.25	0.25	0.25	/	/

Retinoic acid (μM)	/	/	/	1	0.1	0.05	/	/
LDN-193189 (nM)	/	/	/	100	200	100	100	/
α-amyloid precursor protein modulator (nM)	/	/	/	200	/	/	/	/
EGF (ng/ml)	/	/	/	/	100	/	/	/
Nicotinamide (mM)	/	/	/	/	10	/	/	/
GC1 (μM)	/	/	/	/	/	1	1	1
γ-secretase inhibitor XX (nM)	/	/	/	/	/	100	100	/
ALK5 inhibitor II (μM)	/	/	/	/	/	10	10	10
Betacellulin (ng/ml)	/	/	/	/	/	20	/	/
Trolox (μM)	/	/	/	/	/	/	/	10
SP600125 (μM)	/	/	/	/	/	/	/	20
Rasveratrol (μM)	/	/	/	/	/	/	/	75
R428 (μM)	/	/	/	/	/	/	/	2
N-acetyl-cysteine (mM)	/	/	/	/	/	/	/	1
Penicillin/ Streptomycin (U/ml)	/	/	/	/	/	50	50	50

Table 2. Supplemented media composition across the differentiation protocol.

All the compounds were dissolved following the manufacturer's instructions. Specifically, retinoic acid (Sigma-Aldrich), R428 (BGB324, Selleckchem), α-amyloid precursor protein modulator (TBP, Santa Cruz Biotechnology), SANT-1 (Sigma-Aldrich), Trolox (Sigma-Aldrich), CHIR-99021 (Axon Medchem), Alk5 inhibitor II (Enzo), GC-1 (Tocris Bioscience), LDN-193189 (Selleckchem), Rasveratrol (Sigma-Aldrich), γ-secretase inhibitor XX (GSiXX, Merck-Millipore) and SP600125 (JNK inhibitor, Selleckchem) were dissolved in DMSO. Y27632 dihydrochloride (ROCK inhibitor, StemCell Technologies), L-ascorbic acid (Sigma-Aldrich), N-acetyl-cysteine (NAC, Sigma-Aldrich), Activin A (PreproTech), recombinant human betacellulin (PreproTech), recombinant human epidermal growth factor (EGF, StemCell Technologies), Keratinocyte Growth Factor (KGF, or FGF-7, PreproTech) and Nicotinamide (Sigma-Aldrich) were dissolved in H_20.

3. Free fatty acid preparation

Free fatty acid (FFA) stock solutions have been prepared by dissolving Palmitic (PA) and stearic acid (SA) (Sigma-Aldrich) at 72°C and 64°C, respectively until the solutions were clear.

3.1 Myeloid angiogenic cells

FFA used for experiments in MACs have been dissolved in 0.1 M NaOH and then 5 mM FFA has been complexed to 10% bovine serum albumin (BSA) (BSA/FFA molar ratio:1/3.3) as previously reported [257].

3.2 EndoC β-H1 cells

Free fatty acid stock solutions used for experiments in β-cells have been dissolved in pure Ethanol (Sigma-Aldrich) and then dried under N_2 gas flux. 5 mM FFA has been complexed to 7.5% bovine serum albumin (BSA)

(BSA/FFA molar ratio:1/4.5), sonicated and warmed at 55°C until the solution was limpid again. 5 mM FFA working stock solutions have been conserved at -20°C and pre-wormed at 55°C prior diluting in treatment medium.

4. Culture conditions

4.1 Myeloid angiogenic cells

At day +7, MACs have been incubated with FFA or vehicle (NaOH/BSA) as treated and control condition, respectively. In the pilot study, 1 and 2 mM PA and 100 and 250 µM SA were incubated to assess their effects on caspase 3/7 activation after 16h and 24h from the stimuli.

Subsequently, to evaluate the lipotoxic effects of SA, dose-response (40-625 µM) and time-course (from 8 to 24 hours) experiments have been performed.

A concentration of 100 µM SA has been used in all the following experiments in MACs.

To investigate the role of JNK in pro-apoptotic and pro-inflammatory responses or the role of PERK in pro-apoptotic response, cells were pre-treated with 20 µM SP600125 (Sigma Aldrich) –specific JNK inhibitor– or with 0.5 µM GSK2606414 (Sigma Aldrich) – specific PERK inhibitor – for 60 minutes followed by stimulation with SA (from 3 to 16h). To assess the effect of SA on the endoplasmic reticulum (ER) stress-activated pathways, cells have been treated with 1 µM Thapsigargin (Sigma-Aldrich), a non-competitive inhibitor of the sarco/endoplasmic reticulum Ca^{2+} ATPase, as a positive control. Thapsigargin, GSK2606414 and SP600125 stock solutions have all been dissolved in DMSO.

To evaluate the potential beneficial effects of the sodium-glucose co-transporter 2 inhibitors (SGLT2-i) in curbing SA-induced lipotoxicity, MACs have been incubated 16 hours with empagliflozin (EMPA,

Selleckchem) and dapagliflozin (DAPA, Selleckchem) over a wide concentration range (1 μM to 100 μM) prior to SA treatment.
To study the effects of EMPA and DAPA in the reduction of SA-induced expression of oxidative stress markers, MACs have been pre-treated with the anti-oxidant molecule N-acetyl-cysteine (NAC, Sigma-Aldrich), used at the final concentration 4 mM, as positive control.
Finally, to evaluate the potential involvement of the sodium-hydrogen exchanger (NHE), MACs have been treated with 100 μM amiloride and 10 μM cariporide, which are an unselective and an isoform 1-specific inhibitor of NHE, respectively (both from Cayman Chemical).
EMPA, DAPA, amiloride and cariporide have been dissolved in DMSO, NAC was dissolved in H_2O.

4.2 EndoC β-H1 cells

Similarly, EndoC β-H1 have been incubated with FFA or vehicle (NaOH/BSA) as treated and control condition, respectively. To evaluate the lipotoxic effects of FFA on human β-cells, dose-response (100 to 500 μM) experiments have been performed using PA and SA.

4.3 hiPSCs-derived β-cells

hiPSC-derived β-cells at stage 7 (S7), differentiated from the Friedreich Ataxia patient's hiPSCs cell line HEL135.2, have been treated with 50 nM Exendin-4 in order to evaluate a possible drug-induced effect on frataxin expression and function in human β-cells.

5. Viability assay

5.1 Myeloid angiogenic cells

Effects of SA on cell viability have been assessed by VisionBlue fluorescence cell viability assay kit (BioVision), following manufacturer's

instructions, as reported in literature [173]. This kit measures metabolically active cells which transform the dye resazurin into a highly fluorescent product upon reduction.

Specifically, MACs ($2.5x10^5$ cells/well) have been transferred in 96-well culture plates and exposed to vehicle condition or to increasing concentrations (40-100-250-625 μM) of SA for 8-12-16 and 24 hours. Cells have been then incubated 2 hours at 37°C - 5% CO_2 supplemented with VisionBlue reagent (10% of medium volume), after which fluorescent signal has been measured (excitation, 540 nm) using Cary Eclipse spectrophotometer (Varian/Agilent). Data are expressed as fold decrease in viability compared to vehicle.

6. Apoptosis assessment

6.1 Myeloid angiogenic cells

Pro-apoptotic effects of SA have been assessed by using Caspase-Glo 3/7 assay (Promega Corporation) according to manufacturer's instructions. Specifically, the assay contains a caspase-3/7 substrate, which, after cleavage, generates a luminescent signal proportional to the amount of caspase activity. MACs ($2.5x10^5$ cells/well) have been cultured in 96-well culture plates and exposed to vehicle condition or to increasing working concentrations (40-100-250-625 μM) of SA for 8-12-16 and 24 h. Cells have been then incubated 30 minutes at 37°C and 5% CO_2 with 100 μl of Caspase-Glo 3/7 reagent, after which luminescence has been measured by Cary Eclipse fluorescence spectrophotometer (Varian/Agilent). Data are expressed as fold increase in apoptosis compared to vehicle.

Cell death induced by 100 μM SA in MACs has also been assessed by Multi-parameter Apoptosis Assay Kit (Cayman Chemical), according to manufacturer's instructions.

This kit uses FITC-conjugated Annexin V which binds to the membrane of early apoptotic cells, TMRE as a probe for measuring the mitochondrial membrane potential and Hoechst Dye for nuclei detection.
Specifically, MACs have been incubated with 100 μM SA or vehicle for 8h, then washed with Phosphate-Buffered Saline (PBS) (Euroclone) and detached by Trypsin-EDTA (Sigma-Aldrich). A total of $5x10_5$ cells have been incubated 20 minutes at 37°C and 5% CO_2 with TMRE/Hoechst dye solution, after which cells have been collected through centrifuge at 400 *g* for 5 minutes, stained with FITC-conjugated Annexin V solution and incubated in the dark at room temperature for 10 minutes. After washing, samples have been processed in a FACS CantoII cytometer (BD Biosciences) and analysed using FACSDiva software (BD Biosciences).
Potential effects of SGLT2- and NHE-inhibitors on apoptosis have been assessed by using Caspase-Glo 3/7 assay, as described above. MACs have been pre-treated 16 hours with/without EMPA or DAPA or amiloride or cariporide before adding vehicle or 100 μM SA. After 24h of incubation, caspase 3/7 activity has been assessed. Data are expressed as fold increase in apoptosis compared to vehicle.

6.2 EndoC β-H1 cells and hiPSCs-derived β-cells

Apoptosis in EndoC β-H1 cells and hiPSCs-derived β-cells has been assessed by staining with the DNA binding dyes Hoechst-33342 (5 μg/ml, Sigma-Aldrich) and propidium iodide (5 μg/ml, Sigma-Aldrich) for 15 min at 37°C prior inverted fluorescence microscopy. Cell death has been determined in at least 600 cells by two independent trained operators, one of them uniformed of the experimental conditions. Data are expressed as percentage of apoptosis.

7. Tube formation assay

7.1 Myeloid angiogenic cells

The capacity to cooperate in in vasculogenesis represents one the one of the most important function of MACs. To evaluate the SA-mediated effects on MACs pro-angiogenic function, the tube formation assay has been performed, as previously reported in literature [173].

Human umbilical vein endothelial cells (HUVECs) (BD Biosciences), which grow and form extensive tube networks, have been seeded $2x10^4$ cells/well and cultured in Matrigel (BD Bioscince)-coated 96-well plates in EGM-2.

MACs have been incubated with or without 100 μM SA for 16 hours, then washed with PBS (Euroclone) and detached by Trypsin-EDTA (Sigma-Aldrich). $3x10^3$ cells/well were transferred in co-colture with HUVECs for 16 hours, after which the number of closed circles and total tube length have been measured per field of view, in each well.

The capacity of MACs to participate at formation of tube networks has been expressed as ratio of total tube length formed by HUVECs with treated or untreated MACs and the total tube length formed by HUVECs alone. The ratio of the total number of closed circles formed by HUVECs with treated or untreated MACs and the total number of closed circles formed by HUVECs alone has also been evaluated.

8. Quantitative PCR (qPCR) for gene expression analysis

8.1 Myeloid angiogenic cells - pro-inflammatory, ER stress and oxidative stress markers

Pro-inflammatory, ER stress and oxidative stress marker gene expression has been assessed by quantitative PCR (qPCR) in time-course experiments (1.5-3-6-16 hours) in 100 μM SA-treated or vehicle-treated

MACs. To evaluate the potential beneficial action of drugs (EMPA or DAPA or amiloride or cariporide, as indicated above) in curbing SA-mediated effects, pro-inflammatory and oxidative stress marker gene expression has also been assessed in SA-stimulated MACs (16 hours drug pre-incubation plus 3-6 hours of SA stimulus versus vehicle). Specifically, cells have been lysed with QIAzol lysis reagent (Qiagen) and, subsequently, total RNA extracted using miRNeasy Mini Kit (Qiagen) and quantified by NanoDrop (NanoDrop Technologies).

cDNA has been obtained by the reverse transcription of 250 ng of total RNA, using the iScript Reverse Transcription Kit (Bio-Rad Laboratories). The pro-inflammatory profile has been assessed by the measurement of *IL-1β, IL-6, IL-8*, *TNF-α*, and monocyte chemoattractant protein-1 (*MCP-1*) gene expression. The qPCR assay has been performed using the SsoAdvanced Universal Probes Supermix (Bio-Rad) with TaqMan primers and probes (Applied Biosystems) on a CFX Connect Real-Time (Bio-Rad). Optimized thermal cycling conditions have been used: 98°C for 30 sec, followed by 40 amplification cycles (95°C for 3 s; 60°C for 20 sec). The same protocol has been used to assess *CHOP, ATF4, BiP, XBP-1,* and *sXBP-1* gene expression as a measure of ER stress and to assess superoxide dismutase (*SOD*)-2, thioredoxin (*TXN*) and heme oxygenase (*HO*)-1 gene expression as measure of oxidative stress. Glyceraldehyde 3-phosphate dehydrogenase (*GAPDH*) has been selected as reference gene to be used in all the experiments.

8.2 Myeloid angiogenic cells - SGLTs and NHEs

The gene expression of the different isoforms of SGLTs and NHEs were assessed by qPCR in untreated MACs as indicated above. *SGLT-1*, *SGLT-2*, *NHE-1*, *NHE-2*, *NHE-3*, *NHE-4*, *NHE-5*, *NHE-6*, *NHE-7*, *NHE-8*, *NHE-9* gene expression was assessed using SsoAdvanced Universal Probes Supermix (Bio-Rad) with TaqMan primers and probes (Applied

Biosystems) on a CFX Connect Real-Time (Bio-Rad). The above-mentioned conditions of thermal cycling have been used. Gene expression values have been calculated based on the ΔΔCt method and *GAPDH* and/or *RPS18* have been selected as reference genes.

8.3 hiPSCs-derived β-cells

To evaluate the efficiency of the differentiation process of hiPSCs into mature β-cells, the progressive gene expression of β-cell markers has been evaluated.

Cells have been lysed and RNA extracted with RNeasy Plus Micro Kit (Qiagen) following manufacturer's instructions. Subsequently, RNA has been quantified by nanodrop (BioDrop) and 250 ng of total RNA reverse transcribed using the Reverse Transcriptase Core Kit (Eurogenetec). Real-time PCR has been performed using SSO Advanced Universal SYBR green supermix (BioRad) on a CFX Connect Real-Time (Bio-Rad). Standards have been prepared by conventional PCR and he standard curve approach have been used to calculate gene expression (as copies/µl) [258]. Expression values have been corrected for the geometric mean of reference genes GAPDH and β-actin. Specific thermal cycling conditions have been used: 95°C for 3 minutes sec, followed by 40 amplification cycles (95°C for 15 s; 58°C for 20 sec). The sequences of human primers used for real time PCR and in conventional PCR to generate standards are listed in tables 3 and 4, respectively.

Gene	Forward sequence (5'→3')	Reverse sequence (5'→3')
ACTB	CTGTACGCCAACACAGTGCT	GCTCAGGAGGAGCAATGATC
GAPDH	CAGCCTCAAGATCATCAGCA	CAGCCTCAAGATCATCAGCA
GGC	GCTAAACAGAGCTGGAGAGTAT	AAGCCCTCTTTGGGAACTT

GLP1R	AAGGACAACTCCAGCCTGC	ATGATGTAGAGGAACAGGAG
INS	CCAGCCGCAGCCTTTGTGA	CCAGCTCCACCTGCCCCA
MAFA	GCCAGGTGGAGCAGCTGAA	CTTCTCGTATTTCTCCTTGTAC
NEUROD1	CTATCACTGCTCAGGACCTACT	CCACTCTCGCTGTACGATTT
NGN3	GACGACGCGAAGCTCACCAA	TACAAGCTGTGGTCCGCTAT
NKX2.2	GAACCCCTTCTACGACAGCA	ACCGTGCAGGGAGTACTGAA
NKX6.1	GGGCTCGTTTGGCCTATT	CGTGCTTCTTCCTCCACTT
PDX1	AAAGCTCACGCGTGGAAA	GCCGTGAGATGTACTTGTTGA
SOX9	ATCAAGACGGAGCAGCTGAG	GGCTGTAGTGTGGGAGGTTG

Table 3. List of primers used for real time PCR

Gene	Forward sequence (5'→3')	Reverse sequence (5'→3')
ACTB	AAATCTGGCACCACACCTTC	CCGATCCACACGGAGTACTT
GAPDH	CTGAGAACGGGAAGCTTGTC	AGGTCAGGTCCACCACTGAC
GCG	GGGAGAGGGAAGTCATTTGTAA	GTAGAACAGAGGAGGTGAAGAG
GLP1R	AGAAATGGCGAGAATACCGAC	TGTGCTATACATCCACTTCAG
INS	TGTCCTTCTGCCATGGC	CCATCTCTCTCGGTGCA
MAFA	TCATCCGGCTCAAGCAGAAG	CGCCTAXAGGAAGAAGTCGG
NEUROD1	CTATCACTGCTCAGGACCTACT	GTCATCCTCCTCTTCCTCTTCT
NGN3	AAGAGCGAGTTGGCACTGAG	GGAGACTGGGGAGTAGAGGG
NKX2.2	AAGACGGGGTTTTCGGTCAA	TGTCATTGTCCGGTGACTCG
NKX6.1	AAACACACGAGACCCACTTT	GCTTATTGTAGTCGTCGTCCTC
PDX1	CTGCCTTTCCCATGGATGAA	CTTGATGTGTCTCTCGGTCAAG
SOX9	TGGATGTCCAAGCAGG	GAGCTGGAGTTCTGGTGGTC

Table 4. List of primers used for standard PCR to generate standards

9. Digital PCR for gene expression analysis

9.1 Myeloid angiogenic cells - SGLTs

To confirm qPCR results, the absolute quantification of SGLT1 and SGLT2 gene expression in MACs has been performed by digital PCR (QX200, Bio-Rad) by the laboratories of Department of Surgical, Medical, Molecular and Critical Area Pathology at the University of Pisa, Italy (Prof. Anna Solini). cDNA has been obtained by the reverse transcription of 300 ng of total RNA, using the High Capacity cDNA Reverse Transcription Kit (Applied Biosystems) and has been amplified with TaqMan Gene Expression assay (SGLT1:Hs01573790_m1 and SGLT2: Hs00894642_m1, Life Technologies) following manufacturer's instructions. For each sample, about 20.000 droplets have been generated. PCR steps followed specific thermal cycling conditions: 1 cycle at 95°C for 10 minutes, 44 cycles at 95°C for 30 seconds and 60°C for 1 minute, 1 cycle at 98°C for 10 minutes in a conventional thermal cycler. The number of target molecules in each sample has been estimated according to Poisson distribution using the Bio-Rad QuantaSoft software and, finally, the expression of the target genes normalized to GAPDH reference gene.

10. Pro-inflammatory molecule secretion

10.1 Myeloid angiogenic cells

Cell cultures supernatants have been collected and assayed to quantify MACs pro-inflammatory molecule secretion following SA exposure. Specifically, IL-6, IL-8, MCP-1 and TNF-α levels have been assessed by a magnetic bead multiparameter kit (Merck-Millipore) according to manufacturer's instructions and quantified on a MagPix instrument

(Luminex Corporation). This technology is based on the coupling of the target protein to magnetic beads which are coded with a specific fluorescent signal upon LED excitation. IL-1β concentration in cell supernatants was quantified by IL-1β Ultrasensitive ELISA Kit (Thermo Fisher Scientific) using the microplate reader Multiskan™ FC Microplate Photometer (Thermo Scientific) as indicated by manufacturer's instruction (absorbance, 450 nm). Serial dilutions of reconstituted standards provided with the kit have been used to generate a standard curve.

11. Signaling protein activation

11.1 Myeloid angiogenic cells

To evaluate the activation of key mediators in intracellular signaling pathways, MACs have been cultured with 100 μM SA or vehicle for 2-4-8-16h, after which cells have been collected and protein extracted. Specifically, cells have been washed twice with PBS (Euroclone), detached by Trypsin-EDTA (Sigma-Aldrich) and collected by centrifugation. Cell pellets have been lysed using Mammalian Protein Extraction Reagent (M-PER, Thermo Fisher Scientific) supplemented with Halt™ Protease and Phosphatase Inhibitor (Single-Use Cocktail, Thermo Scientific) after which cell underwent to gentle shacking for 10 minutes and centrifugation at 13000x g for 15 min. Protein quantification has been performed according to the Bio-Rad Protein Assay (Bio-Rad), which is based on the Bradford method, using BSA as standard.

Subsequently, target proteins have been detected by Western blotting. Briefly, cell lysates have been prepared by adding from 15 to 40 μg of total protein, NuPAGE™ LDS Sample Buffer (lithium dodecyl sulfate, pH 8.4, ThermoFisher Scientific) and Bolt™ reducing agent (which contains dithiothreitol, ThermoFisher Scientific).

Samples have been boiled at 70°C for 10 min, separated on 4-12% pre-cast polyacrylamide gel (NuPAGE® Novex® 4-12% Bis-Tris Gels, ThermoFisher Scientific) and transferred to nitrocellulose filters using the iBlot® Dry Blotting System (ThermoFisher Scientific). Membranes have been blocked with 5% skim milk (Membrane Blocking Agent, GE Healthcare) in Tris-buffered saline solution containing 0.1% Tween-20 and incubated overnight at 4°C with primary antibodies. The following day membranes have been incubated with secondary Horseradish peroxidase-labeled goat anti-rabbit antibody (1:3000, Cell Signaling Technology) for 1 hour, after which protein signals have been detected by chemiluminescence using ECL western Blotting Detection Reagent (GE Healthcare). Signal bands have been analysed using NIH ImageJ software. The ratio between the phosphorylated and the total protein, normalized to control culture condition has been used as index of protein activation. β-actin has been used as loading control.
Specific primary rabbit antibodies are described in table 5.

Peptide/protein target	**Antibody name**	**Manufacturer, catalogue #**	**Species raised in; mono- or polyclonal**	**Dilution**
p38	p38 MAPK Antibody	Cell Signaling Technology #9212	Rabbit, monoclonal	1:1000
Phospho-p38	Phospho-p38 MAPK (Thr180/Tyr182) Antibody	Cell Signaling Technology #4511	Rabbit, monoclonal	1:1000

Erk1/2	p44/42 MAPK (Erk1/2) Antibody	Cell Signaling Technology #9102	Rabbit, polyclonal	1:1000
Phospho-Erk1/2	Phospho-p44/42 MAPK (Erk1/2) (Thr202/Tyr204) Antibody	Cell Signaling Technology #4370	Rabbit, monoclonal	1:1000
JNK	SAPK/JNK Antibody	Cell Signaling Technology #9252	Rabbit, monoclonal	1:1000
Phospo-JNK	Phospho-SAPK/JNK (Thr183/Tyr185)	Cell Signaling Technology #4668	Rabbit, monoclonal	1:1000
β-Actin	β-Actin (D6A8) Rabbit mAb	Cell Signaling Technology #4967	Rabbit, polyoclonal	1:10000

Table 5. List of primary rabbit antibodies used for signaling protein activation detection

12. Cell aggregate dispersion

12.1 hiPSCs-derived β-cells

In order to perform subsequent analysis, stage 7 (S7) hiPSCs-derived β-cell aggregates have been dispersed into single cells solution through optimized protocol, as described in literature [259]. Specifically, cell aggregates have been washed twice with 0.5 mM EDTA (Life Technologies) prior proceeding with 8 minutes incubation at 37°C with Accumax (Sigma-Aldrich) or Accutase (Capricorn Scientific). Cell dispersion has been promoted by gently pipetting and the solution quenched by adding an equal volume of Knock-out Serum (Life Technologies) supplemented with 10 μM ROCK inhibitor. Cells have been

collected and seeded in S7 medium supplemented with 10 μM ROCK inhibitor on Matrigel-coated plates.

13. Immunocytochemistry

13.1 hiPSCs-derived β-cells

To evaluate the specific expression of specific β-cell markers during the differentiation, cells, growing as monolayer (day 0 - stage 4) or dispersed (stage 5 – 7), have been washed twice with PBS (Lonza), fixed in 4% paraformaldehyde for 20 minutes, permeabilized with 0.5% triton-X100 (Sigma-Aldrich) and blocked with UltraV block solution (Thermo Scientific) for 8-10 min. In between these passages, fixed cells have been washed once with 0.1% Tween (Sigma-Aldrich) in PBS. Finally, cells have been incubated with primary antibodies diluted in 0.1% PBS-Tween, as indicated in table 6, either for 3 hours at room temperature or overnight at 4°C. Following incubation with secondary antibodies for 60 min at room temperature samples have been washed and prepared for analysis with Vectashield mounting medium with DAPI (Vector Laboratories). After primary and secondary antibody solutions incubation, samples have been washed at least three times to remove the antibodies exceed. Antibodies and dilutions used are provided in the table 6.

Peptide/protein target	**Antibody name**	**Manufacturer, catalogue #**	**Species raised in; mono- or polyclonal**	**Dilution**
Insulin	Polyclonal Guinea Pig Anti-Insulin antibody	DAKO, IR00261-2	Guinea pig; polyclonal	NA

OCT-3/4	Monoclonal Mouse Anti-OCT3/4 antibody	Santa Cruz Biotechnology, sc-5279	Mouse; Monoclonal	1:250
NKX6.1	Purified Mouse Anti-Nkx6.1	BD Biosciences, 563022	Mouse; Monoclonal	1:250
PDX1	Polyclonal Goat anti-PDX1- antibody	R&D System, AF2419	Goat; Polyclonal	1:500
Glucagon	Monoclonal Anti-Glucagon-Antibody	Sigma, Bornem, G2654	Mouse; Monoclonal	1:1000
SOX17	Polyclonal Goat IgG	R&D System, AF1924	Goat; polyclonal	1:500
Vimentin	Anti-vimentin antibody	Abcam, ab137321	Rabbit; Polyclonal	1:100
Beta tubulin III	Anti-beta-Tubulin III antibody	Sigma-Aldrich, T8660	Mouse; Monoclonal	1:100
TRA1-60	TRA-1-60 Monoclonal Antibody, IgM	ThermoFisher Scientific, MA1-023	Mouse; Monoclonal	1:125

SSEA-4	SSEA4 Monoclonal Antibody (MC-813-70)	ThermoFisher Scientific, MA1-021 MC-813-70	Mouse, Monoclonal	1:500
Goat anti-guinea pig IgG	Goat anti-Guinea Pig IgG (H+L) Highly Cross-Adsorbed Secondary Antibody, Alexa Fluor 488	Life technologies, A11073	Goat, polyclonal	1:500
Goat anti-rabbit IgG	Goat anti-Rabbit IgG (H+L) Highly Cross-Adsorbed Secondary Antibody, Alexa Fluor 568	Life technologies, A11036	Goat, polyclonal	1:500
Donkey Anti-Mouse IgG	Donkey anti-Mouse IgG (H+L) Highly Cross-Adsorbed Secondary Antibody, Alexa Fluor 488	Life technologies, A21202	Donkey	1:500
Donkey Anti-Goat IgG	Donkey anti-Goat IgG (H+L) Cross-Adsorbed Secondary Antibody, Alexa Fluor 546	Life technologies, A11056	Donkey	1:500
Donkey Anti-Guinea Pig IgG	Alexa Fluor488-conjugated AffniPure Donkey Anti-Guinea Pig (H+L) antibody	Jackson ImmunoResearch Laboratories, 706-545-148	Donkey	1:500
Rabbit Anti-Mouse IgG	Donkey anti-Goat IgG (H+L) Cross-Adsorbed Secondary Antibody, Alexa Fluor 568	Life technologies, A11061	Rabbit	1:500

Table 6. List of antibodies used for immunocytochemistry analysis.

14. Cell aggregates cryo-section

14.1 hiPSCs-derived β-cells

To confirm their composition, S7 hiPSCs-derived β-cells aggregates have been processed for cryo-section, accordingly to a published protocol [260]. Specifically, at least 100 S7 cell aggregates per sample have been fixed in cool 4% paraformaldehyde (Sigma-Aldrich) for 1.5 hour, after which S7 cell aggregates were washed twice with cold PBS (Lonza), resuspended in warm 2% agar (Life Technologies) in PBS, centrifugated for 4 minutes at 400xg and let the agar solidify on ice for 10 minutes. The retrieved agarose block has been immersed in a solution of 30% sucrose at 4°C overnight and the day after placed on a suitable cryomold, embedded in the Tissue-Tek OCT (optimum cutting temperature) compound for frozen sectioning and let solidify slowly in a liquid nitrogen pool. Once the block was completely solidified, it has been stored in liquid nitrogen until cutting by cryotome. Slides have been stored at -80°C until use.

15. Flow cytometry

15.1 hiPSCs-derived β-cells

Stage 7 (S7) aggregates have been dispersed into a single cell solution, resuspended in in PBS (Lonza) and Zombie Aqua™ Fixable Viability kit (BioLegend, diluition 1:500), and incubated 20 minutes in the dark at room temperature to discern live from dead cells. Then cells have been washed twice in PBS, fixed and permeabilized using Cytofix/Cytoperm™ (BD Biosciences), following manufacturer's instruction. Cells have been incubated with conjugated antibodies for 2 hours in the dark at room temperature in Perm/Wash™ buffer (BD Biosciences) containing 4% fetal bovine serum. After three washes, cells have been analyzed using FACSCalibur cytometer (BD Biosciences) and FlowJo software (Tree Star). At least $2x10^5$ cells per each staining tube were used.

Antibodies and dilutions are provided in the table 7.

Peptide/protein target	Antibody name	Manufacturer, catalogue #	Species raised in; mono- or polyclonal	Dilution
Insulin	Rabbit-anti-insulin Alexa Fluor 647 conjugated	Cell Signaling Technologies, 3014S	Rabbit; monoclonal	1:50
Glucagon	Mouse-anti-glucagon BV421 conjugated	BD Bioscience, 565891	Mouse; monoclonal	1:50

Table 7. Lis of antibodies used for in flow cytometry.

16. Glucose stimulated insulin secretion

16.1 hiPSCs-derived β-cells

The capacity to produce and release insulin quickly in response to an increase in extracellular glucose concentration represents the primary β-cell function. To evaluate the function of S7 hiPSCs-derived β-cells aggregates, the *in vitro* glucose-stimulated insulin secretion assay has been performed as describe below. 40 hiPSCs-derived β-cell aggregates per glucose condition have been washed with glucose-free Krebs buffer (UniverCell Biosolutions) supplemented with 0.1% BSA fraction V (Roche) and incubated in 1.6 mM glucose Krebs buffer supplemented with 0.1% BSA fraction V for 30 minutes at 37°C and 5% CO_2 incubator (adaptation phase). Next, aggregates have been exposed to 1.6 mM (low glucose condition), 16.7 mM (high glucose condition) or 16.7 mM glucose plus 10 μM forskolin (high glucose pus forskolin condition) for 1 hour in a parallel manner (secretion phase). Both supernatant and aggregates have been

collected. Cell pellets have been washed once with PBS, centrifuged (4 minutes at 700xg), resuspended in H_2O and frozen at -20°C. Subsequently frozen samples have been thawed and underwent to 3 cycles of sonication (10 second sonication plus 10 second resting each) in order to lyse the aggregates. After 10 minutes centrifuge at maximum speed at 4°C, cell lysates have been diluted 1:3.5 in acid ethanol (95% Ethanol, 5% 12N HCl) and incubated at 4°C overnight in order to extract the insulin content.

16.2 Human islets

To compare the function of S7 hiPSCs-derived β-cells aggregates, *in vitro* glucose-stimulated insulin secretion assay has been performed in human islets as described above. Differently from S7 hiPSCs-derived β-cells aggregates, 20 human islets per glucose condition have been assayed and the adaptation phase.

17. Insulin measurement

After *in vitro* glucose-stimulated insulin secretion, insulin concentration in supernatants and insulin content, extracted as described above in hiPSCs-derived β-cell aggregates, have been quantified by human insulin ELISA Kit (Mercodia) as indicated by manufacturer's instruction. Supernatants and content samples have been diluted 1:10 1:200, respectively, in Diabetes Sample Buffer (Mercodia). Data have been normalized to total protein content, measured by protein assay dye reagent (Bio-Rad).

18. Transplantation studies

iPSCs-derived β-cells have been transplanted under the kidney capsule of immunocompromised NOD/SCID mice at the end of the differentiation

by a trained equipe of the ULB Center for Diabetes Research at the animal facility at the Universitè Libre de Bruxelles, Brussles (Belgium) following the guideline for animal care.
All transplanted mice are males and surgery occurred between 6-12 weeks of age.

18.1 Intraperitoneal glucose tolerance test, human C-peptide detection, streptozotocin injection and nephrectomy

At 7, 14 and 20 weeks post-transplantation mice transplanted with iPSCs-derived β-cells have undergone to intraperitoneal glucose tolerance test (IPGTT), as described in literature [261]. After 16 hours fasting, 2 mg glucose/g boy weight has been administered via intraperitoneal injection and glycemia has been measured (glucometer Accu-Check Aviva, Roche) at time 0 (before glucose administration), 15, 30, 60, 90 and 120 minutes (after glucose administration). Blood sample have been collected from the tail and human C-peptide measured using the C-peptide ELISA (Mercodia) following manufacturer's instructions.
At 21 weeks post-transplantation mice have been intraperitoneal injected with a single dose of streptozotocin (STZ) at 200 mg/kg body weight freshly prepared and glycaemia measured at the tail end for 1 week. After which (22-weeks post-transplantation) grafts have been recovered via nephrectomy and glycemia monitored. Nephrectomy has been performed by a trained equipe of the ULB Center for Diabetes Research at the animal facility at the Universitè Libre de Bruxelles, Brussles (Belgium).

18.2 *In situ* kidney perfusion

At 22-weekd post-transplantation, 3 mice, instead of nephrectomy, have undergone to *in situ* kidney perfusion assay to test *in vivo* graft function.
The assay has been performed by research group led by Prf. Patrick Gilon at the Institute of Experimental and Clinical Research at Université Catholique de Louvain, Brussels (Belgium).
The iPSCs grafted kidney has been perfused *in situ* at 37°C at a flow rate of 1 mL/min in a single-pass circuit through renal artery and vein. Therefore, a catheter is inserted in the abdominal aorta and the venous effluent is collected by a second catheter, which inserted in renal vein, where the graft is. Following an initial equilibration phase of 20 minutes, the effluent is collected every 4 min, after which insulin measurement is assayed with a home-made radioimmunoassay at the Institute of Experimental and Clinical Research at Université Catholique de Louvain, Brussels (Belgium).

19. Frataxin measurement

19.1 hiPSCs-derived β-cells

Frataxin protein expression has been measured in cell lysates by frataxin ELISA (Abcam) according to the manufacturer's instructions.
Briefly, aggregates have been resuspended in the lysis buffer provided with the kit and undergone to 3 cycles of sonication (10 second sonication plus 10 second resting each) in order to lyse the aggregates. After 10 minutes centrifuge at maximum speed at 4°C, cell lysates have been collected, sample diluted and frataxin levels measured. Data have been normalized to total protein.
After *in vitro* glucose-stimulated insulin secretion, insulin concentration in supernatants and the insulin content, extracted as described above, in hiPSCs-derived β-cell aggregates has been quantified by human insulin

ELISA Kit (Mercodia) as indicated by manufacturer's instruction. Supernatant have been diluted 1:10 and content samples 1:200 in Diabetes Sample Buffer (Mercodia). Data have been normalized to total protein content, measured by protein assay dye reagent (Bio-Rad).

20. NAD(P)H measurement

20.1 hiPSCs-derived β-cells

For NAD(P)H measurements, aggregates were incubated for 2 hours in glucose-free bicarbonate-buffered Krebs solution and then perfused with Krebs containing 0, 2 and 20 mM glucose at a flow rate of about 1ml/min. NAD(P)H autofluorescence was recorded by microspectrofluorometry in 6 perfused aggregates as described in literature [262]. The data were normalized to fluorescence levels measured 15 min after addition of 10 µM Carbonyl cyanide-4 (trifluoromethoxy) phenylhydrazone (FCCP), an uncoupling agent that leads to disruption of the mitochondrial membrane potential.

21. Statistical analysis

Data are shown as means ± SEM, unless otherwise indicated.

Comparisons among groups have been performed by ANOVA followed by Bonferroni or Tukey's post-hoc correction for multiple comparisons. A value of $p<0.05$ was considered statistically significant. Data analysis was performed using SPSS version 25 (for data on MACs), or Prism 8 version 8.2.1 (279) (β-cell results).

RESULTS

1. AIM 1. Effects of stearic acid-mediated lipotoxicity on cell viability and function in myeloid angiogenic cells

Part of the data shown in this section have been published in the following paper:

“Spigoni V, Fantuzzi F, Fontana A, Cito M, Derlindati E, Zavaroni I, Cnop M, Bonadonna RC, Dei Cas A. Stearic acid at physiologic concentrations induces in vitro lipotoxicity in circulating angiogenic cells. Atherosclerosis. 2017 Oct;265:162-171. doi: 10.1016/j.atherosclerosis.2017.09.004. Epub 2017 Sep 4. [PubMed PMID: 28892713].”

1.1 Stearic acid affects viability in myeloid angiogenic cells

Stearic (SA) and palmitic (PA) acids are the most predominant circulating long-chain SFA.

Pilot experiments have showed that MAC apoptosis could be induced by SA at physiological concentration (100 μM), whilst higher PA concentration (1-2 mM) are needed to obtain a comparable apoptosis enhancement in MACs (figure 10).

SA (100 μM) and PA (2 mM) have induced an increase of about 4-fold in activation of executioner caspase 3 and 7 with respect to vehicle at 24h in MACs.

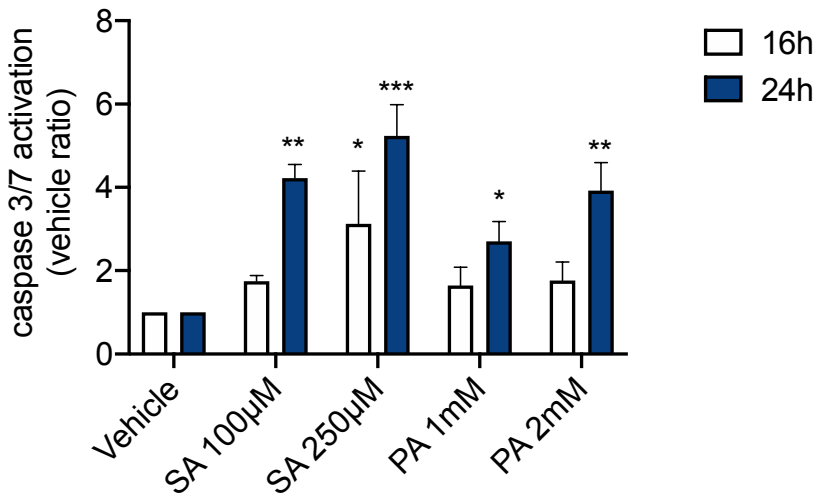

Figure 10. SA and PA induce apoptosis in MACs. Caspase 3/7 activation in MACs treated with SA (100 µM or 250 µM) or PA (1 or 2 mM) at 16 and 24h after stimuli. Data are expressed as mean ± SEM from 3 independent experiments. *p<0.05 vs. vehicle; **p<0.01 vs. vehicle; ***p<0.005 vs vehicle. SA, stearic acid; PA, palmitic acid.

We then have selected SA as the FFA to be used in the following experiments, as more physiological than PA, which was effective at supraphysiological concentrations.

A wide range of SA concentrations has been tested (40 to 625 µM) over time (8-24 hours) and SA has been found to reduce MAC viability in a dose-dependent manner, compared to vehicle treated cells (figure 11A).

Starting from 12 h after stimulus, a coherent increase in caspases 3 and 7 activation has been observed, mirroring the fall in cell viability (figure 11B). In particular, 100 µM SA has induced a 2.2±0.6-fold increase in apoptosis with respect to vehicle at 16 h, without causing dramatic loss of cells, as observed at higher SA concentration (250 and 625 µM).

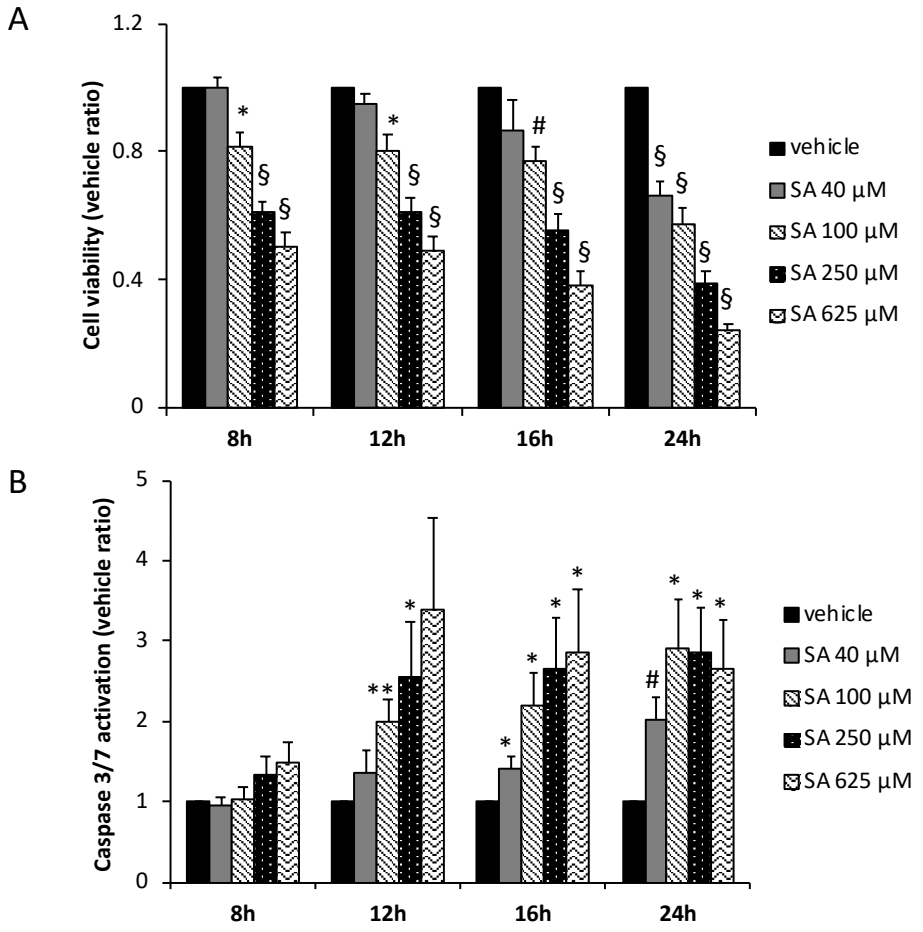

Figure 11. SA affects viability and induce apoptosis in a dose- and time-dependent manner in MACs. (A) Cell viability and (B) caspase 3/7 activation on MACs treated with increasing concentrations (40 to 625 µM) of SA or vehicle over time (8 to 24 h). Data are expressed as mean ± SEM from 6 independent experiments. *p<0.05 vs. vehicle; **p<0.01 vs. vehicle; #p<0.005 vs vehicle; §p<0.001 vs. vehicle. SA, stearic acid.

Annexin V is a probe for phosphatidylserine, which is expressed on the outer membrane of early apoptotic cells, whilst TMRE is a probe for the mitochondrial membrane potential, which is progressively lost during apoptosis.

SA-induced apoptosis has also been confirmed by measurement of both mitochondrial transmembrane potential and annexin V binding at 8 hours in MACs (Fig. 12). TMRE and Annexin V have been found reduced and augmented, respectively, resulting in an increase in early apoptosis from 2.6% to 10%.

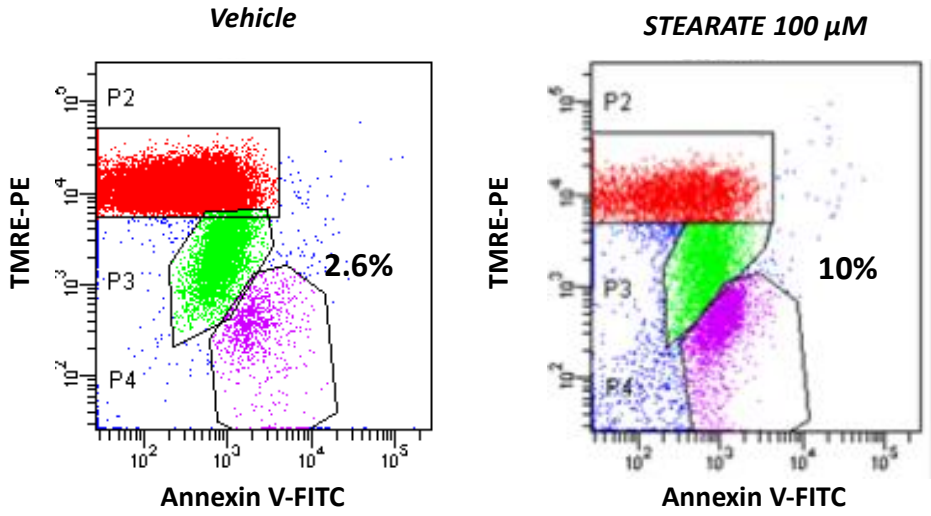

Figure 12. SA induces early apoptosis in MACs.
Representative cytofluorimetric plot of annexin-V (FITC conjugated) and TMRE (PE-conjugated) probe detection in MACs treated with 100 µM SA (right) and vehicle (left) for 8 hours. P2 (red dots) represents healthy mitochondria in live cells, showing intact mitochondrial membrane potential and negative for Annexin V binding; P3 (green dots) represents cell population in an intermediate state, with reduced mitochondrial membrane potential but low annexin-V binding; P4 (purple dots) represents cells positive for annexin binding and with loss of mitochondrial transmembrane potential (apoptotic cells).

Thereby, the 100 µM has been selected to perform all subsequent experiments.

1.2 Stearic acid affects cell function in myeloid angiogenic cells

The capacity to cooperate in vasculogenesis represents one the most important MAC functions. To evaluate SA-mediated effects on MAC pro-angiogenic function, tube formation assay has been performed. As shown in figure 12, 100 μM SA significantly reduces the capacity of MACs to participate in forming tube-like structures along with the endothelial cells HUVEC. This peculiar ability has been calculated as the number of closed structures (average decrease, 16% figure 13A) and as total tube length (average decrease, 10%, figure 13B) per frame, compared to vehicle-treated MACs.

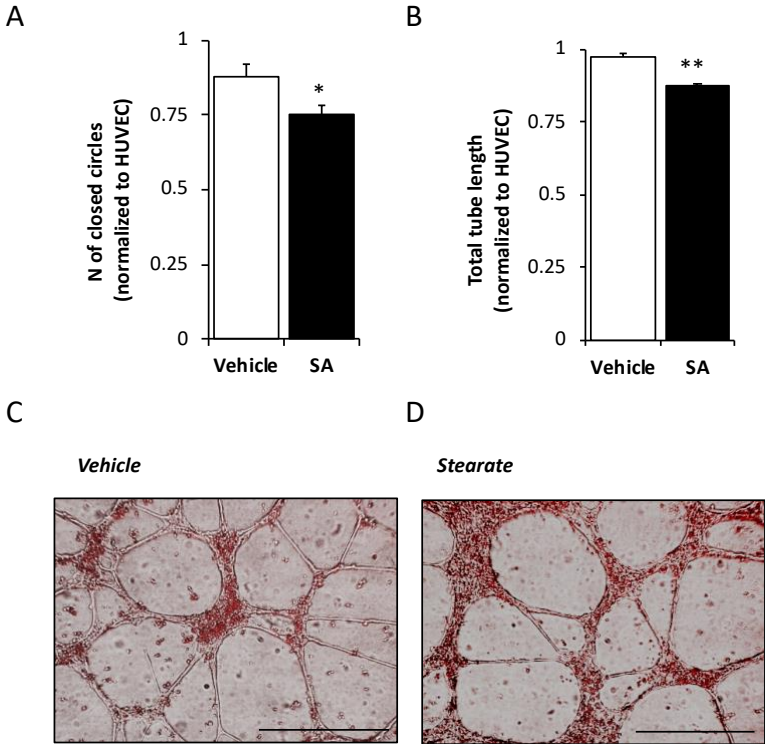

Figure 13. SA reduces MAC function.

Effect of 100 μM SA or vehicle on MAC ability to assist HUVEC tube formation. Tube formation capacity is expressed as total tube length (mm) or as number of

closed circles formed by HUVEC plus MACs pre-incubated with vehicle (white columns) or with SA (black columns). Data are expressed as ratio between (A) number of closed circles formed by HUVEC plus MACs to number of closed circles formed by HUVEC alone and (B) total tube length (mm) formed by HUVEC plus MACs to total tube length (mm) formed by HUVEC alone. (C) Representative pictures of the network formed by HUVEC plus MACs (stained with DiI, red) in presence of vehicle (left) or SA (right). Data are expressed as mean ± SEM from 6 independent experiments. Bar = 500 μm. *p < 0.05 vs. vehicle; **p < 0.01 vs. vehicle. SA, stearic acid.

1.3 Stearic acid triggers inflammation in myeloid angiogenic cells

Prolonged exposure of FFA is known to induce inflammation in several cellular models.

To evaluate whether SA-induced lipotoxicity in MACs involves enhanced inflammation, pro-inflammatory cytokine/chemokine (*IL-1β*, *MCP-1*, *IL-6*, *TNF-α* and *IL-8*) gene expression and secretion have been assessed.

Overall, 100 μM SA causes significant exponential increase in *IL-1β*, *MCP-1*, *IL-6*, *TNF-α* and *IL-8* gene expression from 3 h up to 16 hours (figure 13).

Of note, the strongest stimulatory effect induced by SA exposure has been observed on *IL-8* gene, whose expression reaches a 40-fold increase following 16 h from the stimulus. A 6±2-fold increase in *MCP-1* gene expression has been measured at 16 hours, a later time point than for other cytokines/chemokines expression induction (figure 14).

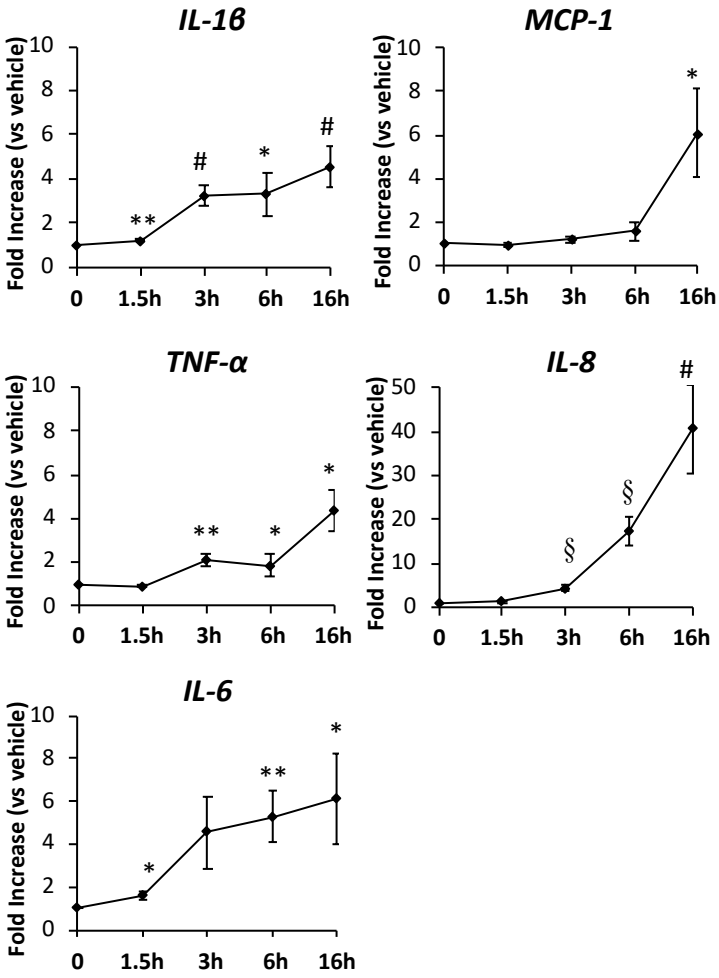

Figure 14. SA triggers pro-inflammatory cytokine/chemokine gene expression in MACs.

Effect of 100 µM SA on *IL-1β*, *MCP-1, IL-6*, *TNF-α* and *IL-8* gene expression in MACs from 1.5 to 16 hours. qPCR data are normalized to GAPDH housekeeping gene and expressed as fold induction of the vehicle. Data are expressed as mean ± SEM from 9 independent experiments. *p<0.05 vs. vehicle; **p<0.01 vs. vehicle; #p<0.005 vs. vehicle; §p<0.001 vs. vehicle.

Pro-inflammatory cytokine/chemokine (*IL-1β*, *MCP-1*, *IL-6*, *TNF-α* and *IL-8*) secretion has also been assessed in cell culture supernatants of MAC treated with SA or vehicle by ELISA assays. A similar, but delayed as expected, trend has been observed in protein secretion (figure 15).

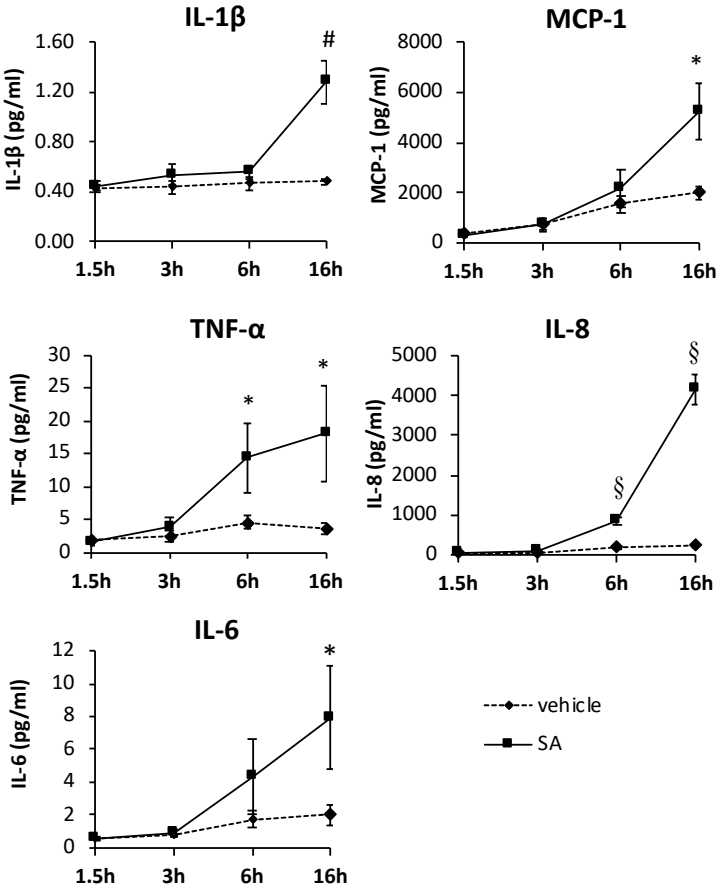

Figure 15. SA triggers pro-inflammatory cytokine/chemokine secretion in MACs.

Effect of 100 µM SA on IL-1β, MCP-1, IL-6, TNF-α and IL-8 secretion in MAC supernatant from 1.5 to 16 hours. Data are expressed as pg/ml. Data are expressed as mean ± SEM from 9 independent experiments. *p<0.05 vs. vehicle; #p<0.005 vs. vehicle; §p<0.001 vs. vehicle. SA, stearic acid.

1.4 Stearic acid leads to JNK activation in myeloid angiogenic cells

A potential involvement of different MAPKs – p38, extracellular signal-regulated kinase (Erk)1/2 and JNK – in SA-induced lipotoxicity has been evaluated over time (2 to 16 hours).

SA treatment does not lead to a statistically significant increase neither in p38 (figure 16A) nor Erk1/2 activation (figure 16B), but it does in JNK – 1.8 to a 3.2-fold increase over time compared to vehicle –, reaching its peak 4 hours following stimulation (figure 16C).

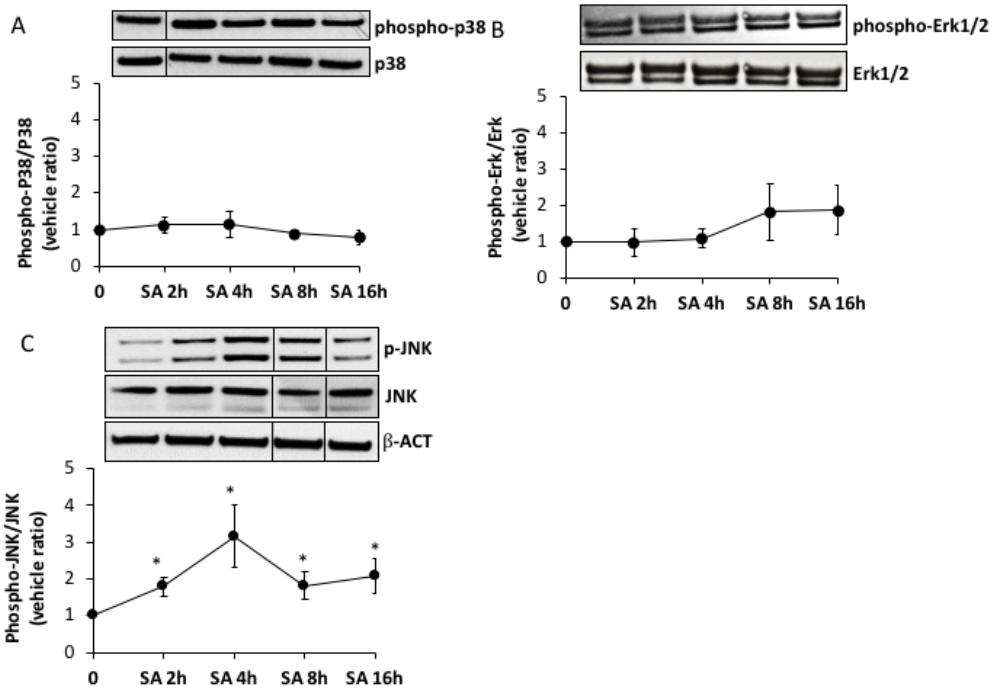

Figure 16. SA activates JNK, but not p38 nor Erk1/2 in MACs. Effects of 100 µM SA or vehicle on (A) p38, (B) Erk1/2, (C) JNK MAPK activation in MACs following 2, 4, 8, and 16 hours of incubation. One representative blot is shown each protein. Data are expressed as the ratio between phosphorylated and total protein and is normalized to vehicle. Data are expressed as mean ± SEM from 9 independent experiments. *p<0.05 vs. vehicle. SA, stearic acid.

1.5 Stearic acid leads to JNK-mediated inflammation but not apoptosis in myeloid angiogenic cells

To examine whether JNK may mediate SA-induced pro-inflammatory and pro-apoptotic responses in MACs, a specific JNK inhibitor (SP600125) has been used in culture.

20 μM SP600125 almost completely abolishes SA-induced *IL- 1β*, *TNF-α* and *MCP-1* gene expression (figure 17A, B, E), with the exception of IL-8 expression, whose induction is not affected by JNK inhibition (figure 17D). SP600125 curbs SA-dependent IL-6 gene expression at 3 hours, but not after 16 hours from SA stimulus (figure 17C).

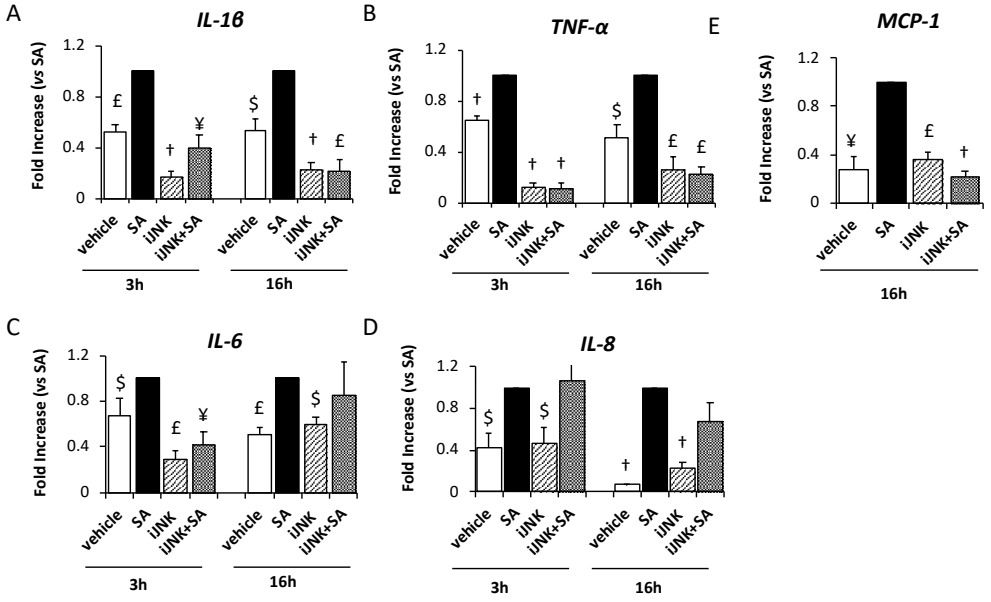

Figure 17. SA-mediated JNK activation leads to pro-inflammatory response. Effects of JNK-inhibition on (A) *IL-1β*, (B) *TNA-α*, (C) *IL-6*, (D) *IL-8* and (D) *MCP-1* gene expression in MACs treated with 100 μM SA or vehicle with or without 20 μM SP600125 for 3 and 16 hours. qPCR data are normalized to GAPDH housekeeping gene and expressed as fold change of SA condition. Data are expressed as mean ± SEM from 9 independent experiments. $p<0.05 vs. SA;

¥p<0.01 vs. SA; £p<0.005 vs. SA; †p<0.001 vs. SA. SA, stearic acid; iJNK, JNK inhibitor.

These data suggest that JNK activity mediates, at least partially, SA-induced pro-inflammatory response.

Surprisingly, no reduction in caspase activation has been observed after JNK inhibition by SP600125 (figure 18), suggesting that its activation is not involved in SA-induced lipo-apoptosis.

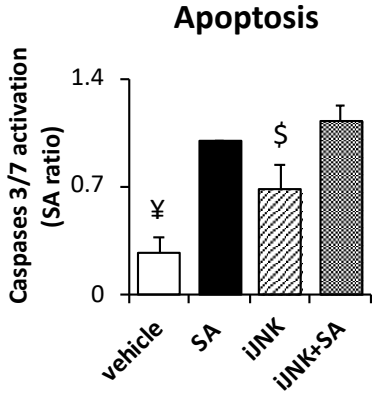

Figure 18. SA-mediated JNK activation is not required for pro-apoptotic response.

Effects of JNK-inhibition on caspase 3/7 activation in MACs treated with 100 µM SA or vehicle with or without 20 µM SP600125 at 16 hours. Data are expressed as mean ± SEM from 5 independent experiments. $ p<0.05 vs. SA; ¥ p<0.01 vs. SA. SA, stearic acid; iJNK, JNK ihnibitor.

1.6 Stearic acid leads to endoplasmic reticulum stress response in myeloid angiogenic cells

Potential involvement of ER stress as a possible transducer of SA-mediated effect on MAC apoptosis has been assessed.

Three transmembrane proteins, PERK, ATF6 and IRE1, drive the three pathways in UPR. In particular, a key downstream effector of PERK signaling is represented by ATF4, which triggers apoptosis by increasing its downstream target CHOP transcription. SA induced a 1.8-fold upregulation of *ATF4* at 6 and 16 hours compared to vehicle (figure 19A) and a 5.1-fold induction of *CHOP* gene expression at 16 h (figure 19B). Downstream mediators of ATF6 activation UPR branch are the chaperone BiP and the transcription factor *XBP-1*, whose expression is induced by SA after 16 hours from the stimulus (7.7 and 1.9-fold increase to vehicle, respectively, figure 19)

Finally, to investigate the involvement of the third UPR pathway, the IRE1-mediate alternative splicing of XBP-1 product, *sXBP1*, has been assessed. Data show a 2-fold increase in sXBP-1 in MACs cultured with SA for 6 and 16 hours (figure 19B-C).

The ER inducer thapsigargin, a non-competitive inhibitor of the sarco/ER Ca^{2+} ATPase, has been used as positive control.

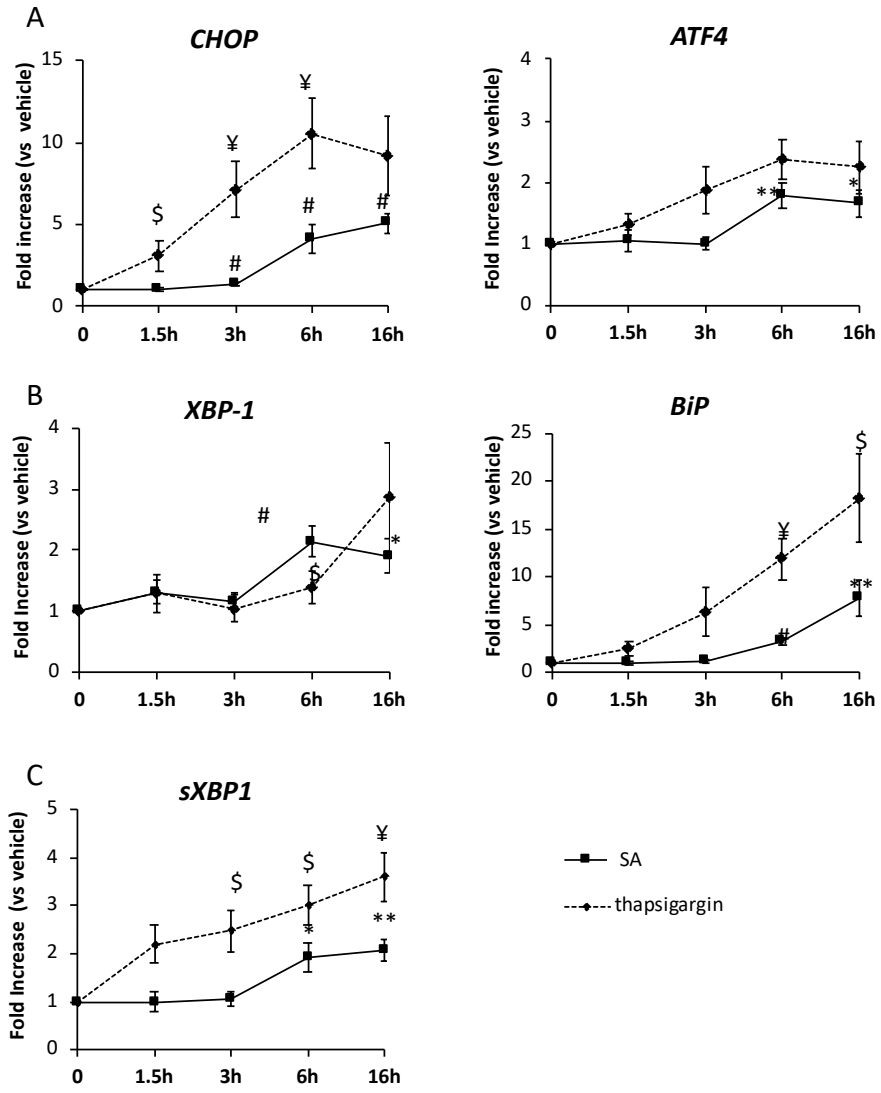

Figure 19. SA induces ER stress markers expression in MACs

Effect of 100 µM SA and 1 µM thapsigargin on ER stress marker, (A) *CHOP*, *ATF4*, (B) *BiP*, *XBP-1* and (C) *sXBP-1*, expression from 1.5 h to 16 h, qPCR data are normalized to *GAPDH* (not for *sXBP-1* which is normalized for the geometric mean of *GAPDH* and *ACTB*) housekeeping gene and expressed as fold induction of the vehicle. Data are expressed as mean ± SEM from at least 5 independent experiments *p<0.05 vs. vehicle; **p<0.01 vs. vehicle; #p<0.005 vs. vehicle; $p<0.05 vs. SA; ¥p<0.01 vs. SA. SA, stearic acid.

Overall, these data indicate ER stress responses activation as in SA-treated MACs.

In addition, to examine whether UPR may mediate SA-induced pro-apoptotic response in MACs, an inhibitor of PERK (GSK2606414) has been added in culture.

A reduction in caspase activation has been observed after PERK inhibition by GSK2606414 (figure 20), suggesting that its activation is involved in SA-induced lipo-apoptosis.

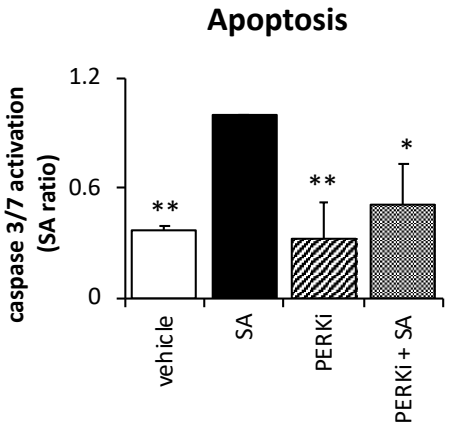

Figure 20. SA-mediated PERK activation is involved in pro-apoptotic response.

Effects of PERK-inhibition on caspase 3/7 activation in MACs treated with 100 µM SA or vehicle with or without 0.5 µM GSK2606414 at 16 hours. Data are expressed as mean ± SEM from 3 independent experiments. *p<0.05 vs. SA; **p<0.01 vs. SA. SA, stearic acid; PERKi, PERK inhibitor.

1.7 Stearic acid leads to oxidative stress response in myeloid angiogenic cells

Finally, to evaluate whether SA-induced lipotoxicity in MACs involves enhanced oxidative stress, oxidative stress markers (*SOD2*, *TXN* e *HO-1*) gene expression over time (1.5 to 16 hours) has been evaluated.

Overall, 100 µM SA causes significant increase in *SOD2* and *HO-1* gene expression at 6 and 16 hours. *HO-1* gene expression peak results at 6h, following which it falls back to basal levels (figure 21).

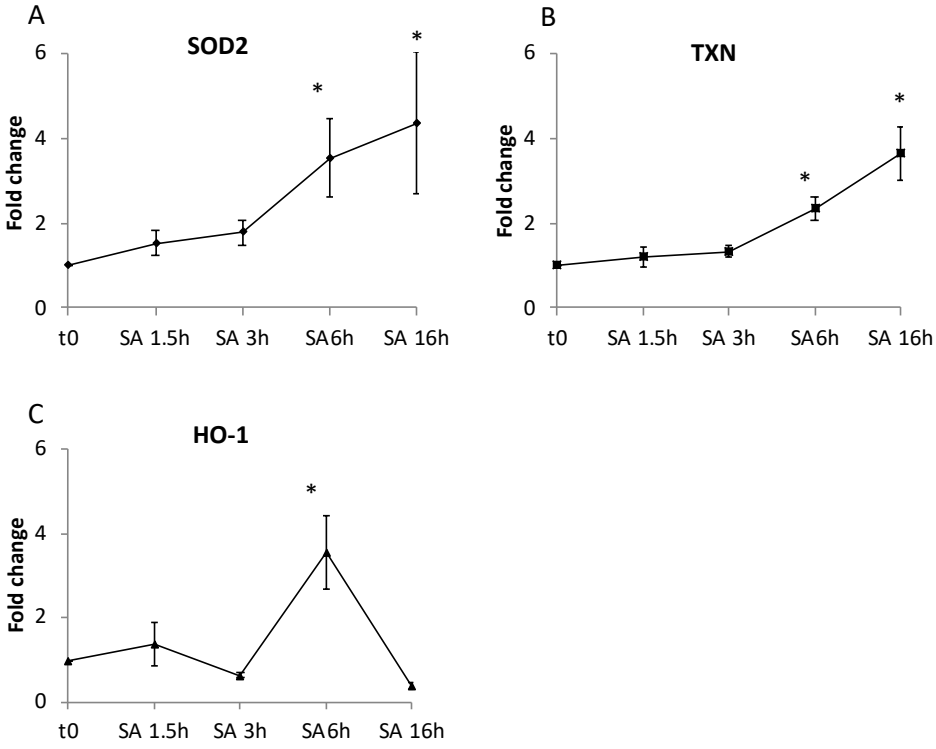

Figure 21. SA triggers oxidative stress markers gene expression in MACs. Effect of 100 µM SA on *SOD2*, *TXN* a[B] *-1* gene expression in MACs from 1.5 to 16 hours. qPCR data are normalized to *GAPDH* housekeeping gene and expressed as fold induction of the vehicle Data are expressed as mean ± SEM from 5 independent experiments. *p<0.05 vs. vehicle. SA, stearic acid.

2. AIM 1. Antagonizing effects of SGLT2 inhibitors on stearic acid-induced lipotoxicity in myeloid angiogenic cells

Data shown in this section have been included in the manuscript submitted for publication:

"Spigoni V, Fantuzzi F, Fontana A, Carubbi C, Pozzi G, Masselli E, Gobbi G, Solini A, Bonadonna RC, Dei Cas A. SGLT2 inhibitors antagonize lipotoxicity in human myeloid angiogenic cells and ADP-dependent activation in human platelets: potential relevance to prevention of cardiovascular events."

2.1 SGLT2 inhibitors curb SA-induced inflammation in myeloid angiogenic cells

To evaluate whether SGLT2-I (EMPA or DAPA) exert beneficial effects on SA-induced inflammation, pro-inflammatory cytokine/chemokine (*IL-1β*, *IL-8*, *TNF-α* and *MCP-1*) gene expression has been assessed on MACs pre-incubated over a wide range of concentration of SGTL2-I (10 to 100 μM) for 16 hours prior 3- and 6-hours treatment with 100 μM SA.

At the highest concentration tested, data show a striking decrease in SA-induced pro-inflammatory markers (*IL-1β*, *IL-8*, *TNF-α* and *MCP-1*) gene expression in both EMPA (figure 22A) and DAPA (Figure 22B) experiments at 3 hours.

Moreover, both EMPA and DAPA (100 μM) pre-treatment also reduces pro-inflammatory cytokine/chemokine (*IL-1β*, *IL-8*, *TNF-α* and *MCP-1*) gene expression induced by 6 hours of SA stimulation (Figure 22C).

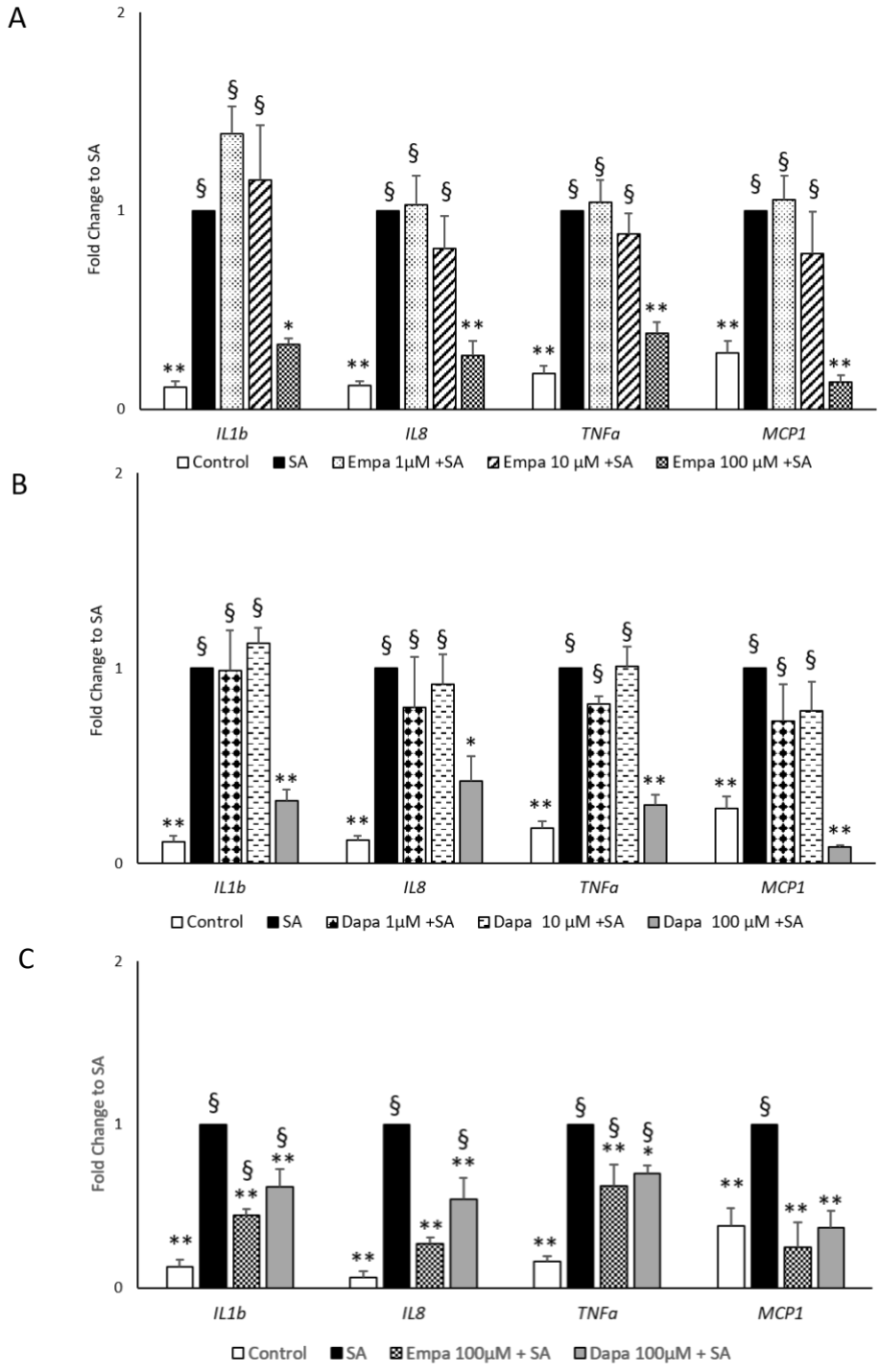
A
Fold Change to SA
IL1b
IL8
TNFa
MCP1
Control
SA
Empa 1µM +SA
Empa 10 µM +SA
Empa 100 µM +SA
B
Fold Change to SA
IL1b
IL8
TNFa
MCP1
Control
SA
Dapa 1µM +SA
Dapa 10 µM +SA
Dapa 100 µM +SA
C
Fold Change to SA
IL1b
IL8
TNFa
MCP1
Control
SA
Empa 100µM + SA
Dapa 100µM + SA

Figure 21. SGLT2 inhibitors curb SA-induced inflammation in MACs.
IL-1β, *IL-8*, *TNF-α* and *MCP-1* gene expression in 1, 10 and 100 μM (A) EMPA or (B) DAPA pre-treated MACs (for 16 hours) followed by 3 hours of SA stimulation or (C) 100 μM EMPA or DAPA pre-treated MACs (16-hours) followed by 6 hours of SA stimulation. qPCR data are normalized to *GAPDH* housekeeping gene and expressed as fold induction of SA. Data are expressed as mean ± SEM from at least 3 independent experiments *p<0.05 vs SA; **p<0.01 vs SA; ¥p<0.05 vs control §p<0.01 vs control. SA, stearic acid; EMPA, empaglifozin; DAPA, dapagliflozin.

2.2 SGLT2 inhibitors curb SA-induced oxidative stress response in myeloid angiogenic cells

To further explore the beneficial effects of SGLT2-I in lipotoxic MACs, their potential role in curbing SA-induced oxidative stress response in MACs has been evaluated.

An increase in oxidative stress marker gene expression has been observed at 6 hours of SA-incubation. Data show that both EMPA and DAPA pre-treatment significantly reduce SA-induced *SOD2* and *HO-1* gene expression, whilst *TXN* expression was significantly lowered only by EMPA. As positive control for anti-oxidant activity, 4 mM NAC has been used. The effects mediated by SGLT2-I and NAC are comparable (figure 23).

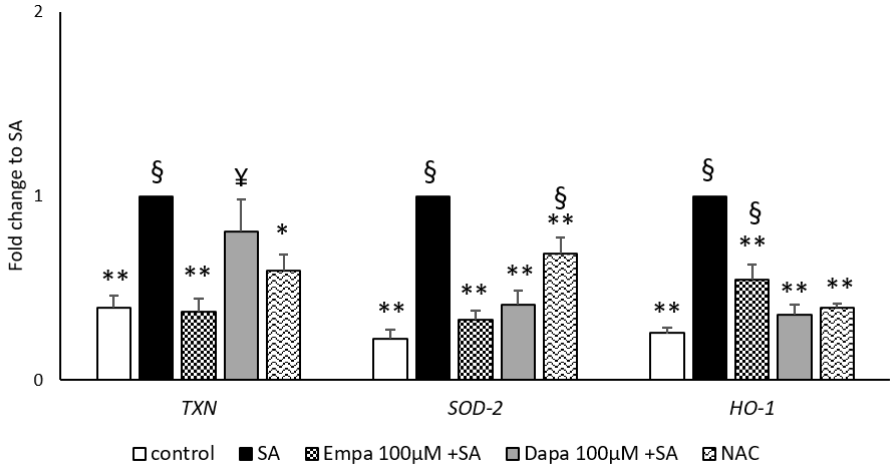

Figure 23. SGLT2 inhibitors curb SA-induced oxidative stress markers in MACs.

TXN, *SOD-2* and *HO-1* gene expression in 100 µM EMPA or DAPA or 4 mM NAC pre-treated MACs (16 hours) followed by 6-hours of SA stimulation. qPCR data are normalized to *GAPDH* housekeeping gene and expressed as fold induction of SA. Data are expressed as mean ± SEM from at least 3 independent experiments *p<0.05 vs SA; **p<0.01 vs SA; §p<0.01 vs control. SA, stearic acid; EMPA, empagliflozin; DAPA, dapagliflozin; NAC, N-acetyl-cysteine.

2.3 SGLT2 inhibitors do not resolve SA-induced lipo-apoptosis in myeloid angiogenic cells

Since SGLT2-I demonstrated to exert beneficial effects on SA-induce pro-inflammatory and oxidative stress marker gene expression, the hypothesis that they could exert a similar protective action on SA-induced lipo-apoptosis has been evaluated.

However, neither EMPA nor DAPA have been able to hamper the activation of caspase 3 and 7 after 24 hours of SA stimulation (figure 24).

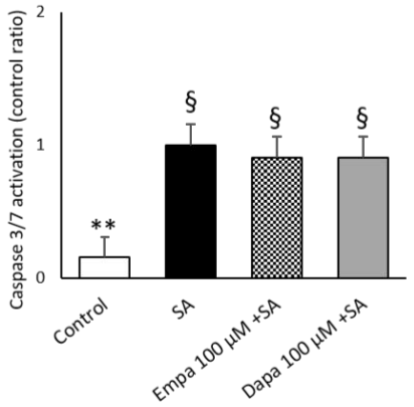

Figure 24. SGLT2 inhibitors do not curb SA-induced apoptosis in MACs.
Caspase 3/7 activation in MACs pre-treated for 16 hours with EMPA or DAPA (both 100 µM) followed by 24 hours of SA stimulation. Data are expressed as mean ± SEM from 3 independent experiments.; **p<0.01 vs SA; §p<0.01 vs control. SA, stearic acid; EMPA, empagliflozin; DAPA, dapagliflozin.

2.4 *SGLT2* is not expressed, but it is *NHE* in myeloid angiogenic cells

qPCR results show lack of expression of SGLT2, whilst SGLT-1 expression is barely detectable in MACs. These results have been confirmed by digital PCR, performed by the laboratories of Department of Surgical, Medical, Molecular and Critical Area Pathology at the University of Pisa, Italy (Prof. Anna Solini).

Since SGLT2-I-mediated effects could be driven by alternative targets, the hypothesis of an involvement of NHE (as reported for cardiomyocytes), has been explored also in MACs.

Firstly, *NHE* isoform (1 to 9) expression has been assessed by qPCR in MACs. NHE isoforms *NHE-1*, *NHE-6*, *NHE-7*, *NHE-8*, *NHE-9* have been found to be expressed in untreated MACs (data not shown).

2.5 Amiloride curbs SA-induced inflammation in myeloid angiogenic cells

To explore the putative involvement of NHE as mediator of SGLT2-I beneficial action, a non-specific inhibitor of NHE (amiloride) has been added in SA-treated MACs, alone or in combination with 100 µM EMPA.

Pre-treatment (for 16 hours) with 100 µM amiloride curbs SA-induced *IL-1β*, *IL-8*, *TNF-α* and *MCP-1* gene expression similar to EMPA, suggesting a shared mechanism of action (i.e. NHE inhibition).

Of note, the culture condition EMPA plus amiloride display an additive effect in restraining SA-induced inflammation (figure 25), suggesting that maybe EMPA and amiloride's mechanisms of action could be just partly shared.

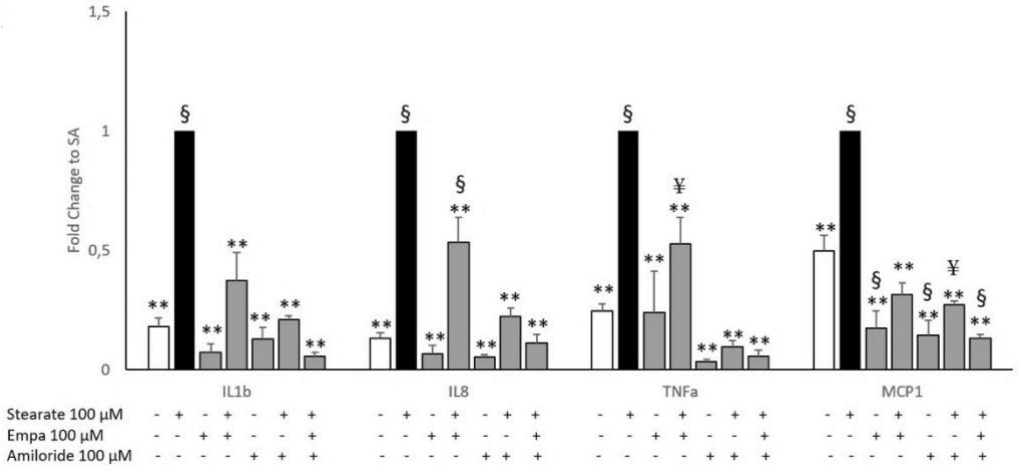

Figure 25. Both amiloride and EMPA curb SA-induced inflammation in MACs.

IL-1β, *IL-8*, *TNF-α* and *MCP-1* gene expression in MACs pre-treated with 100 µM EMPA and/or 100 µM amiloride for 16 hours followed by 3 hours of 100 µM SA incubation. Data are expressed as mean ± SEM from at least 3 independent

experiments. * p<0.05 and **p<0.01 *vs* SA; ¥p<0.05 and §p<0.01 *vs* control. SA, stearic acid; EMPA, empagliflozin.

To identify which NHE isoform is mainly involved in the observed SGT2-I-mediated effects, each isoform should be selectively targeted for inhibition.

So far, only NHE-1 isoform has been investigated by the specific inhibition of cariporide.

Data show that 10 µM cariporide induces a slight decrease in SA-induced *IL-8* and *MCP-1*, but not *IL-1β* and *TNF-α* gene expression (figure 26).

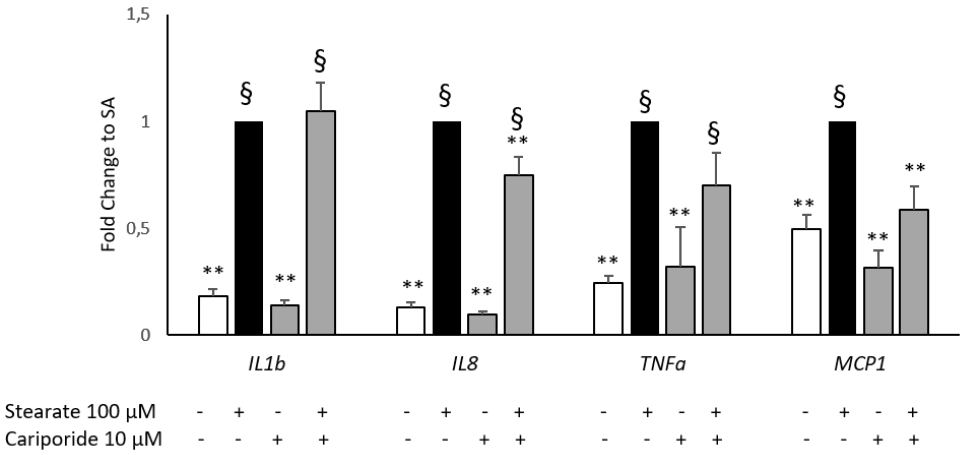

Figure 26. Cariporide partially curbs SA-induced inflammation in MACs.
IL-1β, *IL-8*, *TNF-α* and *MCP-1* gene expression in MACs pre-treated with 10 µM cariporide for 16 hours followed by 3 hours of 100 µM SA incubation. Data are expressed as mean ± SEM from at least 3 independent experiments. **p<0.01 *vs* SA; §p<0.01 *vs* control. SA, stearic acid.

Thus, although NHE inhibition may actually play a role in EMPA/DAPA-mediated SGLT2-independent mechanisms, these latter data suggest an only marginal involvement of the isoform 1 of NHE in the reduction of

inflammation mediated by SGLT2-I. Further studies are needed to fully clarify this issue.

3. AIM 2. Improve the protocol to differentiate *in vitro* induced pluripotent stem cells into β-cells in order to create novel models to study β-cell lipotoxicity

3.1 Stearic and palmitic acid affect viability in EndoC-βH1

Pilot experiments have showed that the human β-cell line EndoC-βH1 is susceptible to apoptosis induced by SA and PA. However, higher concentration than in MACs is requested to observe an effective decrease in cell viability in EndoC-βH1 cells.

SA and PA (both 500 μM) treatment for 24 hours induce 2.3±0.3- and 1.4±0.1-fold increase with respect to vehicle, in number of apoptotic EndoC-βH1 cells, respectively (figure 27).

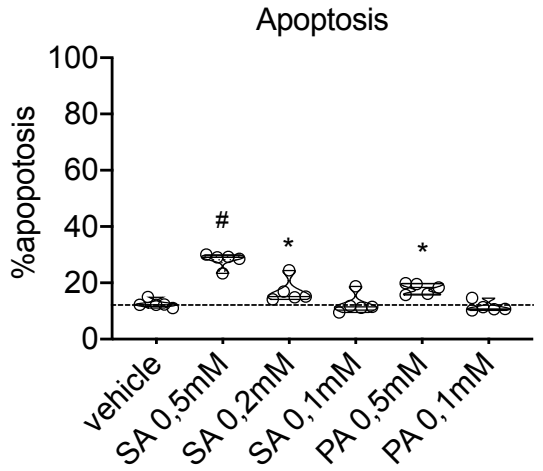

Figure 27. SA and PA induce apoptosis in EndoC-βH1 cells.
Percentage of positive propidium iodide-positive EndoC-βH1 cells treated with with SA (200 µM or 500 µM) or PA (200 µM or 500 µM) or vehicle 24h after stimuli. Dots represent single experiments. Data are expressed as violin plot, with the median represented by the horizontal line, from 5 independent experiments. *p<0.05 vs. vehicle; #p<0.001 vs. vehicle. SA, stearic acid; PA, palmitic acid.

3.2 Stearoyl CoA desaturase is highly expressed in EndoC-βH1

Data shown in this section have been included in the manuscript (accepted for publication, Diabetologia, 2019):
"Oshima M, Pechberty S, Bellini L, Göpel SO, Campana M, Rouch C, Dairou J, Cosentino C, Fantuzzi F, Toivonen S, Marchetti P, Magnan C, Cnop M, Le Stunff H, Scharfmann R. Stearoyl CoA desaturase is a gatekeeper that protects human β-cells against lipotoxicity and maintains their identity."

Stearoyl-CoA desaturase (SCD) is an enzyme involved in the systhesis of unsatured FFA from SFA and, in particular, desaturates PA or SA into palmitoleate (C16:1) or oleate (C18:1), respectively. It has been hypothesized that SCD, given its action in processing SFA, may have a protective role against lipotoxicity in β-cells.
Indeed, qPCR data show a high expression of SCD gene in EndoC-βH1, higher than in human islets (figure 28).

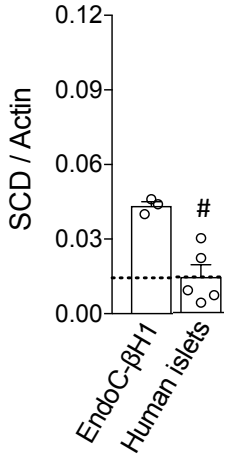

Figure 28. SCD expression is higher in EndoC-βH1 cells than in human islets.

Gene expression of *SCD* in EndoC-βH1 cells and in human islets. qPCR data are normalized to *ACTB* housekeeping gene. Dots represent single experiments. Data are expressed as mean ± SEM from at least 3 independent experiments. #p<0.001 vs. EndoC-βH1. SCD, Stearoyl-CoA desaturase.

Of note, in experiments aimed to explore the protective role of SCD, performed by Prof. Scharfmann's research group at Université Paris Descartes INSERM in Paris (France), EndoC-βH1 cells are resistant to PA- and SA-induced toxicity unless *SCD* gene is silenced.

Although EndoC-βH1 cells show many advantages, as transformed pseudodiploid cells in continuous expansion, they should not be considered as a direct equivalent of non-dividing primary β-cells. Moreover, FFA-treatment in EndoC-βH1 are contrasting.
An alternative (and intriguing) tool to model lipotoxicity in pancreatic β-cell may be represented by iPSCs-derived β-cells technology. However, since current *in vitro* differentiation strategies enable to generate immature β-cells, in the present study, it has been aimed to differentiate *in vitro* induced pluripotent stem cells into β-cells to create novel models to study β-cell lipotoxicity.

3.3 iPSCs-derived β-cells express β-cell markers across the differentiation

Part of the data shown in this section have been included in the manuscript:
"Toivonen S*, Fantuzzi F*, Schiavo AA, Demine D, Sawatani T, Demarez C, Pachera N, Rajaei B, Cosentino C, Cai Y, Marchetti P, Jonas JC, Gilon P, Eizirik DL, Igoillo-Esteve M, Cnop M. 3D microwell platform to generate human induced pluripotent stem cell-derived β-cells *in vitro*. "

Using a step-wise protocol, iPSCs successfully differentiate into definitive endoderm cells (at stage 1, S1), displaying the typical morphology and expressing the definitive endoderm marker, SOX17. At this stage, over 95% of cells has interrupted the expression of the pluripotent marker OCT4 (figure 29A-B). Then, cells progress through primitive gut tube, posterior foregut and form pancreatic progenitors co-expressing PDX1 and NKX6.1 at stage 4, S4 (figure 29C). At this time point, the cells are transferred from monolayer culture to 3D culture in order to sustain the

formation of cell aggregates into pancreatic islet-like structures (figure 29D).

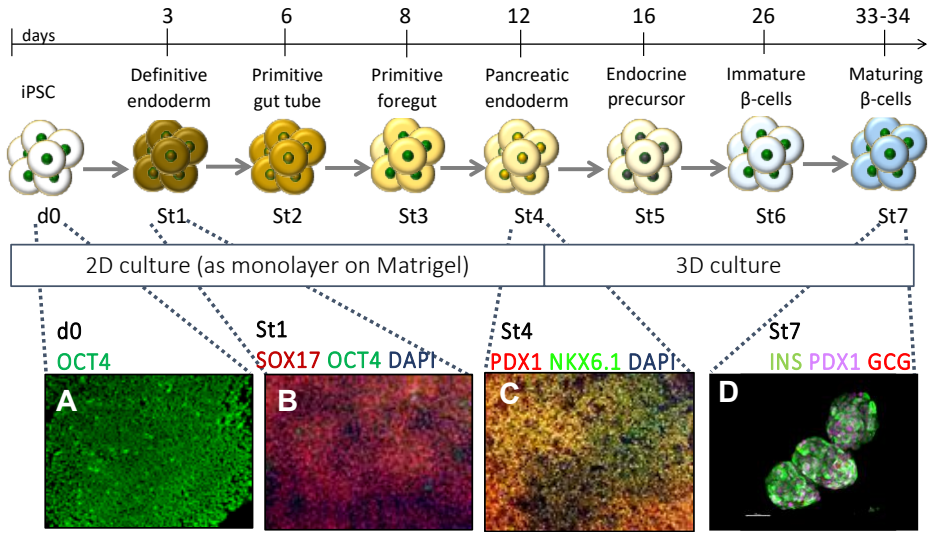

Figure 29. Scheme of the 7-stage differentiation protocol from iPSCs into maturing β-cells.

Representative immunofluorescent staining of (A) iPSCs (d0) for OCT4 (green), (B) S1 cells for SOX17 (red) and OCT4 (green), (C) S4 cells for PDX1 (red) and NKX6.1 (green) and (D) S7 cell aggregates for insulin (green), PDX1 (pink) and glucagon (red). Nuclei are stained with DAPI (blue).

qPCR data across the differentiation show that the cells follow a normal developmental pathway (endocrine commitment, pancreatic and β-cell development) by transiently expressing the pancreatic progenitor marker *SOX9* at S4 (figure 29A) and *NGN3* at S5 (figure 30B) with subsequent upregulation of *NKX2.2* and *NEUROD1* ((figure 30C, D). β-cell specific transcription factors *PDX1* and *NKX6.1* expression started by stages 3-4 and increased in the course of the differentiation (figure 30E, F). INS expression starts to be detected at S5 and increase until the end of the differentiation (figure 30G). At S7 a slight but significant increase in GCG expression has been detected. Mature β-cell marker *MAFA*, although

expressed, remains very low compared to expression in human islets (figure 30I).

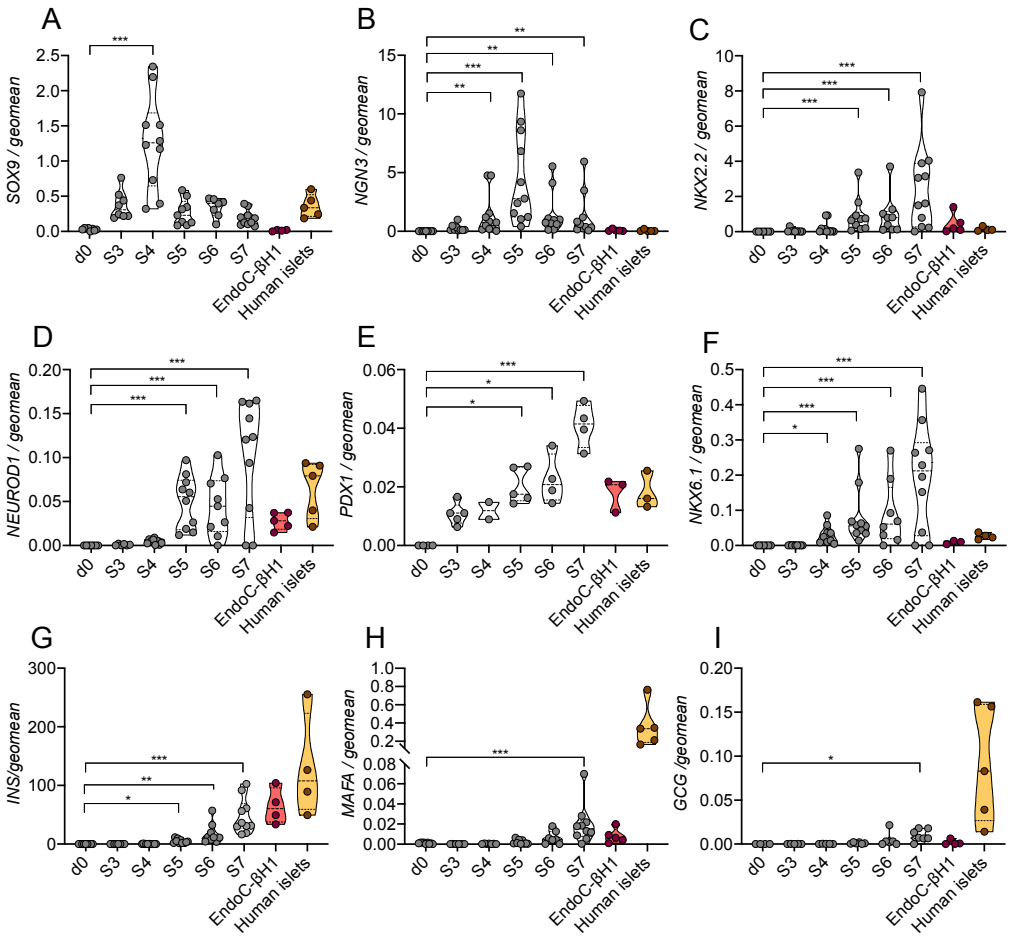

Figure 30. Cells follow a normal developmental pathway across the differentiation into β-cells.

Gene expression of *SOX9*, *NGN3*, *NKX2.2*, *NEUROD1*, *PDX1*, *NKX6.1*, *INS*, *MAFA* and *GCG* across the differentiation. qPCR data are normalized to the geometric mean of *GAPDH* and *ACTB* housekeeping genes and expressed as copies/µl using the standard curve approach. cDNA obtained from EndoC-βH1 and isolated human pancreatic islets have been used as positive control. Dots represent single experiments. Data are expressed as violin plots, with the median

represented by horizontal line, from at least 3 independent experiments. *p<0.05; **p<0.01; ***p<0.005 as indicated. d0, day 0; S1-7, stages 1-7.

At the end of differentiation at stage 7, cell counting from insulin and glucagon immunocytochemistry analysis shows that aggregates are composed by 44.5±2.2% of insulin-positive β-cells, 4.6±0.5% of glucagon-positive α-cells and 3.9±0.7% of insulin- and glucagon-positive bi-hormonal cells (figure 31A-B). Data have been confirmed by FACS analysis (figure 31C). The percentage of β-cells at stage 7 is comparable with that of human islets (49±1%, data not shown).
Almost no Ki67-positive cells have been detected (data not shown).

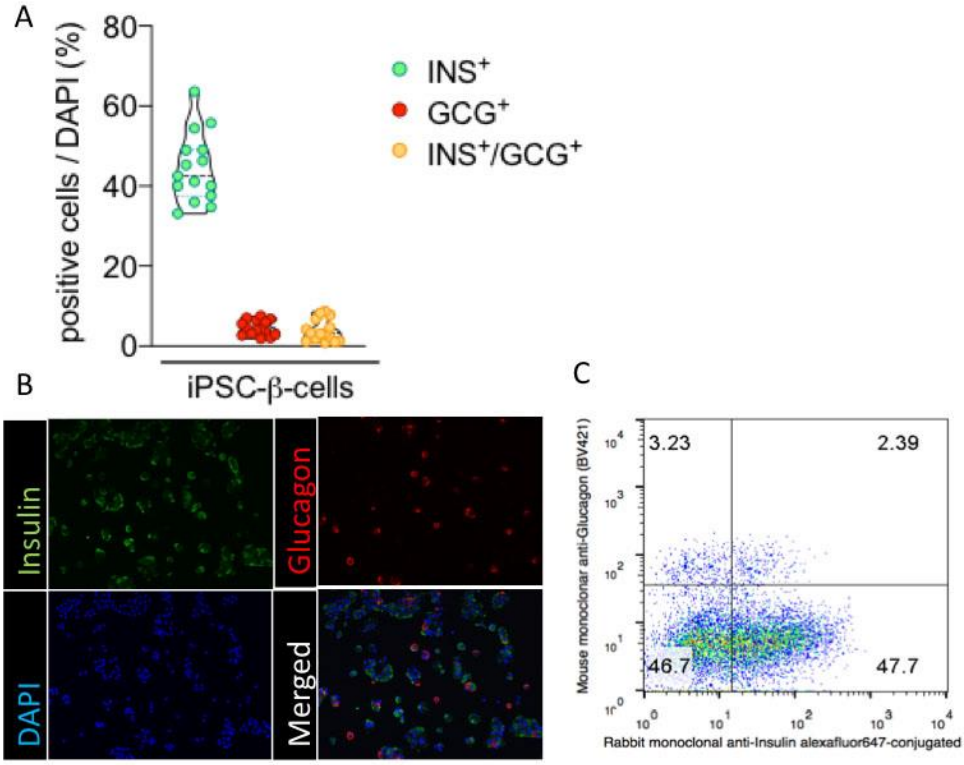

Figure 31. iPSCs-derived β-cells account for about the half of the total cell population at the end of the differentiation.

(A) Yield of insulin-positive (INS^+), glucagon-positive (GCG^+) and bi-hormonal (INS^+/GCG^+) cells at the end of the differentiation (S7) manually counted after immunofluorescence staining. (B) representative immunofluorescent staining S7 cell aggregates for insulin (green) and glucagon (red). Nuclei are stained with DAPI (blue). (C) Representative cytofluorimetric plot of insulin and glucagon in S7 cell aggregates. Data are expressed as violin plot with the median represented by horizontal line from at 15 independent experiments. INS, insulin; GCG, glucagon.

3.4 iPSCs-derived β-cells show limited β-cell function *in vitro*

It is known the glucose enters in the β-cell, via the GLUT transporter, where it is metabolized and leads to increase in the ATP/ADP radio which causes the closure of ATP-sensitive potassium channel, the consequent membrane depolarization and the opening of the voltage-dependent calcium channels. These events trigger the fusion of the secretory granules and the insulin release which is found to be further stimulated in presence of cAMP.

Thereby, to evaluate *in vitro* function of iPSCs-derived β-cells, glucose-stimulated insulin secretion assay has been performed.

A solution of 17.6 mM glucose (high glucose condition) induces a slight, but not significant augment (1.25±0.42, compared to 1.67 basal mM glucose) in insulin release in iPSCs-derived β-cells. However, the insulin secretion is significantly increased in response to high glucose plus 10 μM forskolin, which triggers an increase in intracellular cAMP, in respect to vehicle (3.83±0.85 compared 1.67 mM basal glucose), as shown in figure 32A.

Nevertheless, the *in vitro* glucose-induced insulin secretion is still very low in comparison to human pancreatic islets, which display an augment of 5.6±2.6-fold to basal in response to 17.6 mM glucose and 13.15±5.3-fold to basal in response to 17.6mM glucose plus 10 µM forskolin (figure 32B). Of note, there is no statistical difference in insulin content (following protein normalization) in iPSCs-derived β-cells and human islets (data not shown).

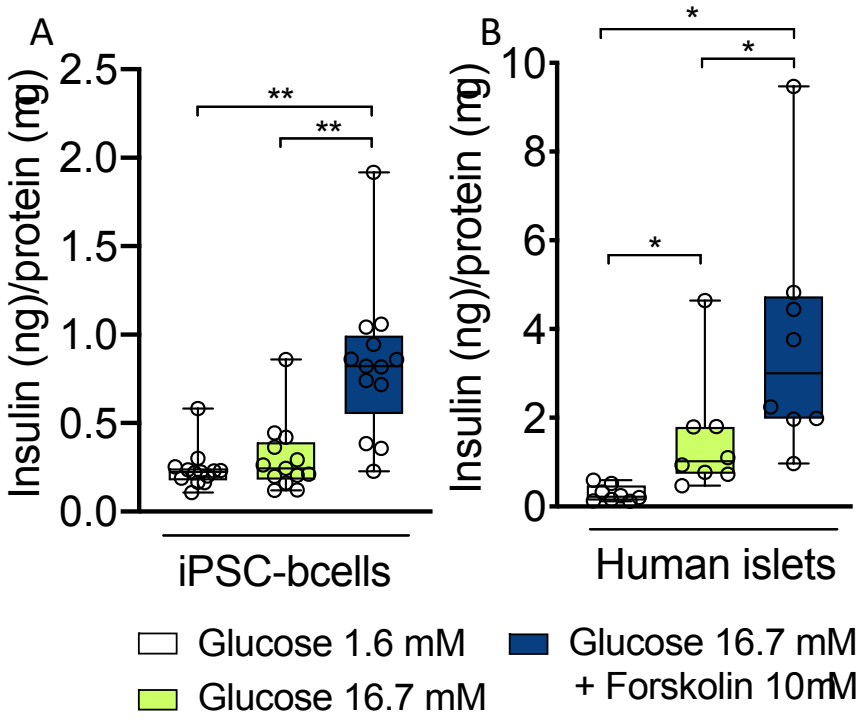

Figure 32. iPSCs-derived β-cells display limited β-cell function *in vitro*.
Glucose-stimulated insulin secretion assay in response to high glucose stimulus alone (17.6 mM) or high glucose plus 10 µM forkolin in (A) iPSCs-derived β-cell and in (B) isolated human pancreatic islets. Basal glucose level is set at 1.6 mM. Data are expressed ad insulin secreted (ng) and normalized by total protein (µg). Dots represent single experiments. Data are expressed using boxplots, with the median represented by horizontal line and the 25th and 75th percentiles at the bottom and top of the box, from least 8 independent experiments. Whiskers

represent the minimum and maximum values *p<0.05 vs glucose 1.67 mM; **p<0.01 vs glucose 1.67 mM.

3.5 iPSCs-derived β-cells become gluco-responsive after *in vivo* transplantation in NOD-SCID mice.

In order to evaluate the in vivo function of stage 7 iPSCs-derived β-cells, 1000-3000 aggregated have been transplanted under the kidney capsule of immunodeficient NOD/SCID mice by a trained *equipe* at the ULB Center for diabetes research.

At 7-, 14- and 20-weeks post-transplantation intraperitoneal glucose tolerance test (IPGTT) has been performed (figure 33A) and human C-peptide has been measured in iPSCs-derived β-cells transplanted mice (figure 33B). Although human C-peptide is detectable at 7-weeks post-transplantation, grafts became glucose-responsive by 14-20 weeks post-transplantation (figure 33B).

At 21-week post-transplantation mice have been injected with STZ (200 mg/kg), that selective ablate rodent β-cells, and glycaemia has been recorded in the following weeks, before proceeding with nephrectomy to recover the graft.

After STZ, untransplanted mice become diabetic (figure 33C), whilst iPSCs-derived β-cells transplanted mice succeed in maintain normoglycaemia. After nephrectomy they develop diabetes (figure 33C).

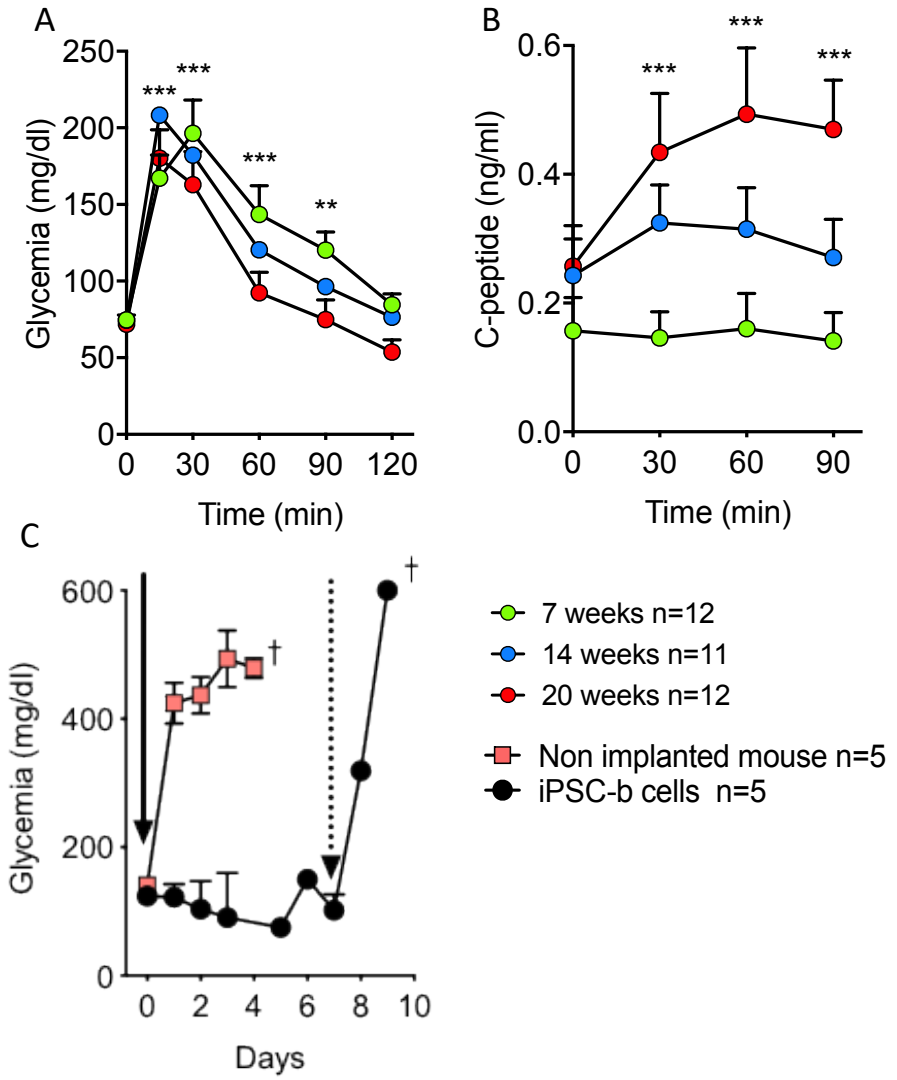

Figure 33. iPSCs-derived β-cells display acquired β-cell function *in vivo*.

At 7-, 14- and 20-weeks post-transplantation, (A) intraperitoneal glucose tolerance test (IPGTT) have been performed and (B) human C-peptide measured in iPSCs-derived β-cells transplanted mice. (C) Glycaemia after STZ injection (black arrow) in iPSCs-derived β-cells transplanted mice and in untransplanted mice at 21 weeks post-transplantation and after nephrectomy (dotted arrow) at 22 weeks post-transplantation. Data are expressed as mean ± SEM from a number of mice as indicate **p<0.01 vs t0; ***p<0.005 vs t0.

The pathway leading to insulin release can be modulated by the action of several external agents. Besides forskolin, which stimulates insulin secretion through increasing cAMP levels as mention above, also gliclazide – a potassium channel blocker – or high potassium can all stimulate the insulin release. On the contrary, diazoxide – a potassium channel opener – inhibits the insulin secretion.

A number of thee iPSCs-derived β-cells-transplanted mice have undergone to *in situ* kidney perfusion.

This technique, performed by the research group headed by Prof. Patrick Gilon at Université Catholique de Louvain, Brussels (Belgium), consists in a single-pass circuit in which the desired solution is injected via abdominal aorta and the effluent is collected via the renal vein.

After an initial stabilization phase in a glucose-free solution (0 mM), the sequential injection of 20 mM glucose alone and in combination with 1 µM forskolin, 250 µM diazoxide, 20 µM gliclazide or 30 mM KCl shows that iPSCs-derived β-cells acquire a functional secretory machinery after *in vivo* transplantation and graft are able to quickly modulate the release of insulin in response to different stimuli (figure 34).

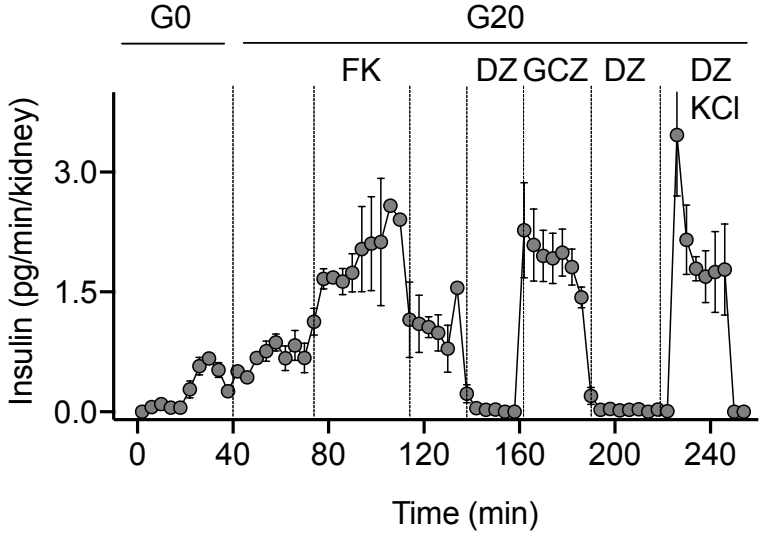

Figure 34. iPSCs-derived β-cells modulate the release of insulin in response to different stimuli *in vivo*.

In situ kidney perfusion in iPSCs-derived β-cells transplanted mice at 22 weeks post-transplantation. Data are expressed as insulin released (pg/min/kidney) in response to 0 mM or 20 mM glucose solution injection as indicated and following subsequent injection of 20 mM glucose solution plus 1 μM forskolin, 250 μM diazoxide, 20 μM gliclazide or 30 mM KCl. Data are expressed as mean ± SEM from 3 mice. G0, 0 mM Glucose, G20, 20 mM glucose; FK forskolin; DZ, diazoxide; GCZ, gliclazide.

Overall those data show that iPSC-derived β-cells display β-cell characteristics but they still lack fully mature β-cell function *in vitro*. However, *in vivo* environment following transplantation boosts iPSC-β-cell maturation.

3.6 Stearoyl CoA desaturase (*SCD*) expression in iPCs-derived β cells

Given the ability to *in vitro* differentiate iPSCs in proper β-cells, this technology does provide a valid alterative tool to explore lipotoxicity in human β-cells.

In regards to iPSCs-derives β-cell susceptibility to SFA-mediated effects, qPCR data show a high expression of SCD gene in this model, higher than in human islets, but lower than in EndoC-βH1 (figure 35)

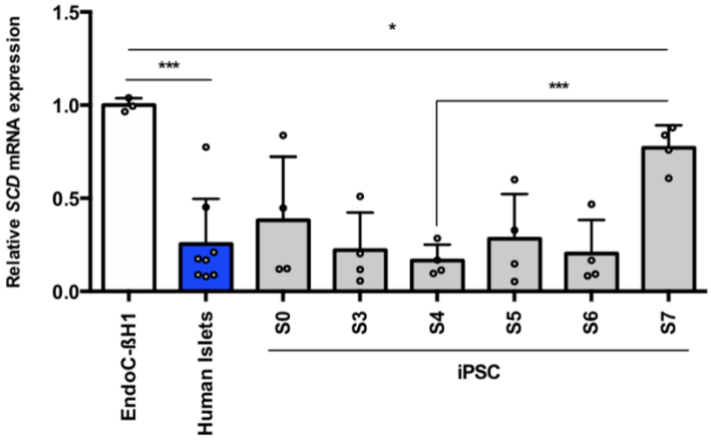

Figure 35. SCD is expressed in iPSCs-derived β-cells.

Gene expression of SCD in EndoC-ßH1, human Islets and iPSCs differentiation into β-cells (stages 0 to 7). qPCR data are normalized to *ACTB* housekeeping gene Dots represent single experiments. Data are expressed as mean ± SEM from at least 3 independent experiments. *p<0.05 and ***p<0.001 relative to EndoC-ßH1 cells.

These data suggest that, as EndoC-βH1, iPSCs-derived β-cells may display a certain level of protection against FFA-exerted detrimental effects. However, further studies will be needed to clarify its role.

4. A further iPSCs-derived β-cell application: iPSCs derived from a patient affected by Friedreich ataxia efficiently differentiate in β-cells

Data shown in this section have been included in the manuscript:
"Igoillo-Esteve M, Oliveira F, Cosentino C, Fantuzzi F, Demarez C, Toivonen S, Hu A, Chintawar S, Lopes M, Pachera N, Cai Y, Abdulkarim B, Rai M, Marselli L, Marchetti P, Tariq M, Jonas JC, Boscolo M, Pandolfo M, Eizirik DL, Cnop M. Exenatide induces frataxin expression and improves mitochondrial function in Friedreich ataxia"

Friedreich ataxia (FRDA) is an autosomal recessive neurodegenerative disease, with a high prevalence of diabetes, for which so far, there is no available treatment. FRDA is caused by a reduction in frataxin (*FXN*) expression – because of an intronic GAA trinucleotide repeat expansions in FXN gene – which results in mitochondrial dysfunction and cell apoptosis.
Hereby, fibroblast from a patient affected by FRDA have been reprogrammed into iPSCs (HEL 135.2) and subsequently differentiated in β-cells.
iPSC line HEL135.2 satisfies the quality control check by expressing the pluripotency markers OCT4, SSEA4 and TRA1-60, by showing exogenous transgenes silenced, by successfully differentiating into endoderm, mesoderm and ectoderm in the embryoid body assay, and displaying a normal 46, XY karyotype (data not shown).
iPSC line HEL135.2 differentiates efficiently into β-cells.

Indeed, at the end of the process stage 7 aggregates are composed by 58% of insulin positive β-cells. Only few glucagon α-cells or insulin- and glucagon-double positive cells have been observed. (Figure 36A-B).

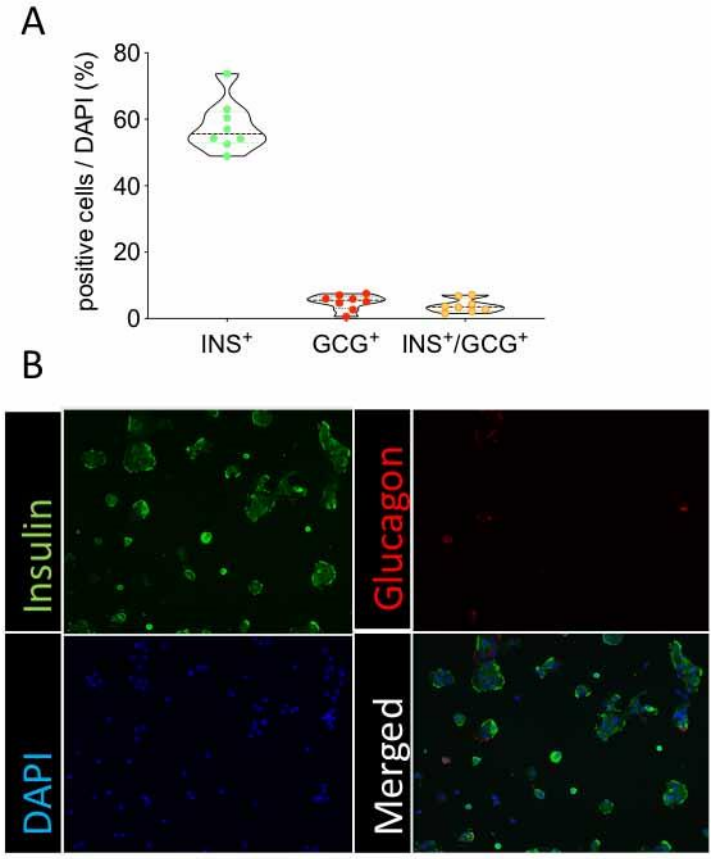

Figure 36. HEL135.2 efficiently differentiate in β-cells.

(A) Yield of insulin-positive, glucagon-positive and bi-hormonal cells at the end of the differentiation (S7) manually counted after immunofluorescence staining. (B) Representative immunofluorescent staining S7 cell aggregates for insulin (green) and glucagon (red). Nuclei are stained with DAPI (blue). INS, insulin; GCG, glucagon.

Similar to qPCR data shown on control iPSCs cell line differentiation into β-cells, gene expression of key markers across the differentiation stages follows a normal developmental pathway, displaying levels of gene

expression that are overall comparable to EndoC-βH1 cells and primary human islets (figure 37).

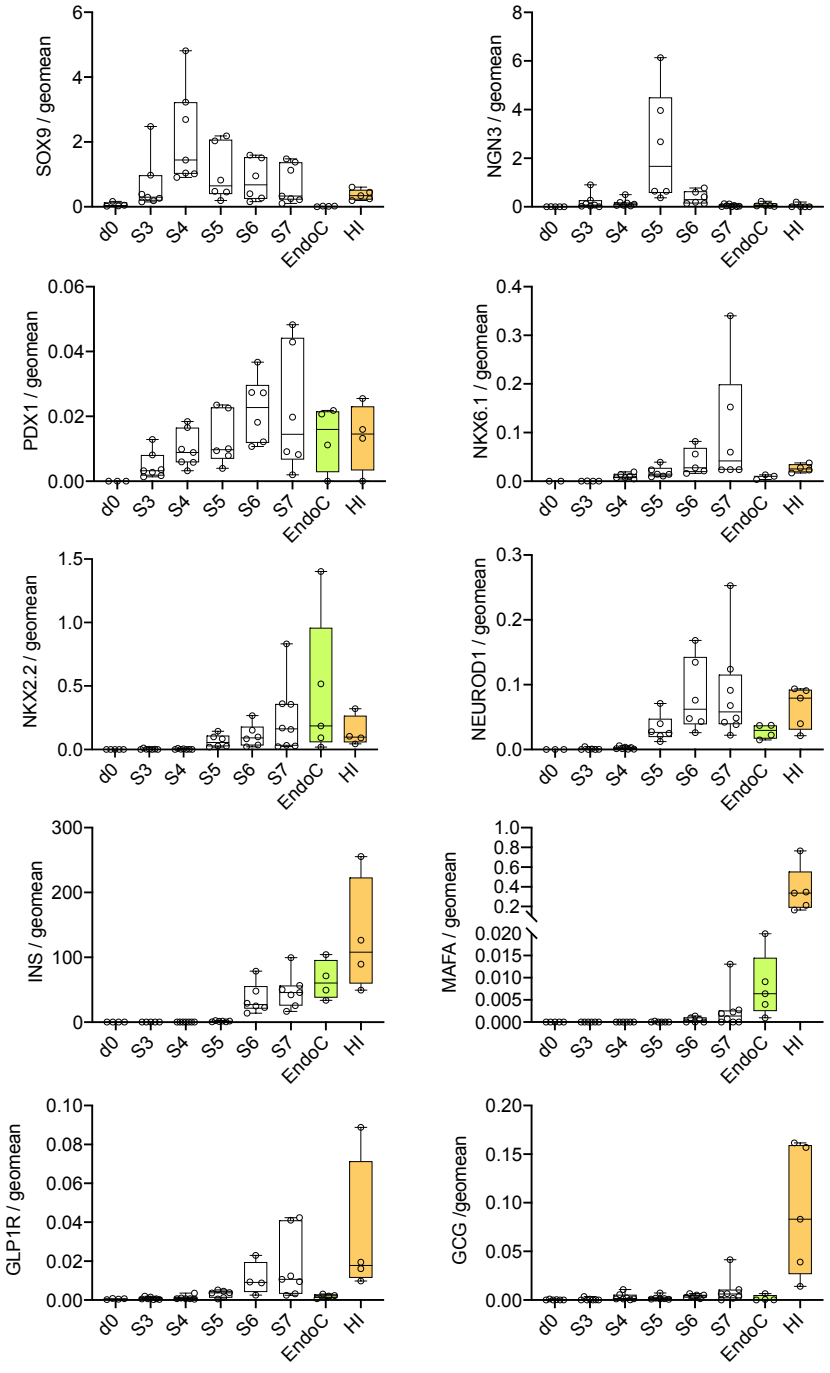

Figure 37. HEL 135.2 follow a normal developmental pathway across the differentiation into β-cells.

Gene expression of *SOX9*, *NGN3*, *PDX1*, *NKX6.1, NKX2.2*, *NEUROD1*, *INS*, *MAFA, GLP1R* and *GCG* across the differentiation. qPCR data are normalized to the geometric mean of *GAPDH* and *ACTB* housekeeping genes and expressed as copies/µl using the standard curve approach. cDNA obtained from EndoC-βH1 and isolated human pancreatic islets have been used as positive control. Dots represent single experiments. Data are expressed using boxplots, with the median represented by horizontal line and the 25th and 75th percentiles at the bottom and top of the box, from at least 4 independent experiments. Whiskers represent the minimum and maximum values. d0, day 0; HI, human islets; S-17, stages 1–7.

FRDA is caused by a reduction in frataxin protein expression.

In iPSCs(HEL 153.2)-derived β-cells, frataxin protein expression levels, measured by frataxin ELISA, are 35% lower than in the control cell line (figure 38A-B). Treatment with 50 nM exenatide (Ex4) slightly increases frataxin after 72 hours (figure 38B). Glucose-induced insulin secretion assay shows a slight but significant increase in insulin release after high glucose (17.6 mM) stimulation and a more potent induction following high glucose (17.6 mM) plus forskolin (10 µM) stimulation in iPSCs(HEL 153.2)-derived β-cells. However, no insulin secretory function improvement has been observed after 50 nM Ex4 treatment (figure 38C). Finally, as an indicator of variation in glucose metabolism, NAD(P)H autofluorescence has been measured in iPSCs(HEL 153.2)-derived β-cells. Data show that NAD(P)H autofluorescence rises with a greater effect when iPSCs-derived β-cells are stimulated with 2 mM glucose solution, after glucose starvation, than when they are later exposed to a 20 mM glucose solution. NAD(P)H autofluorescence signal modestly increases after exenatide treatment (figure 38D).

Finally, treatment with FCCP, which is a mitochondrial uncoupler, rapidly reduce NAD(P)H autofluorescence in the aggregates (Figure 38D), indicating that the iPSC-β-cell mitochondria are metabolically active.

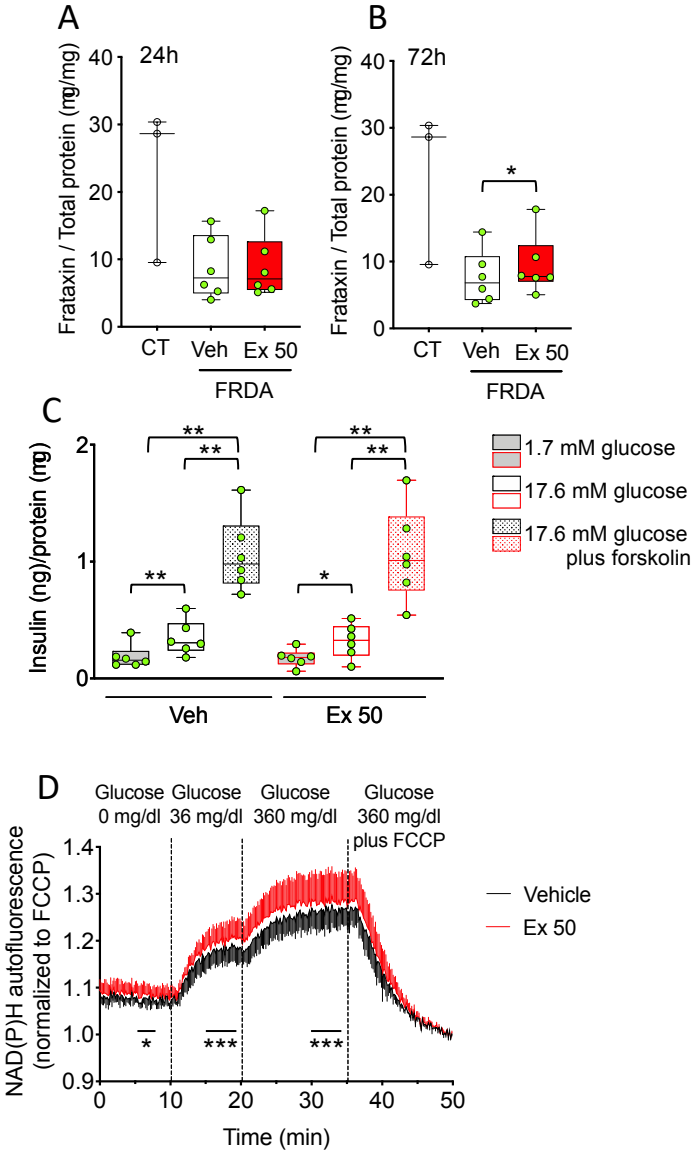

Figure 38. Exendin treatment induces moderate increase in frataxin protein expression in HEL 135.2-derived β-cells

Frataxin protein quantified by ELISA in control-derived and iPSCs(HEL 135.2)-derived β-cells treated with Ex 50 or vehicle for (A) 24 or (B) 72 hours. *p<0.05 Ex vs Veh by paired t-test. (C) Glucose-stimulated insulin secretion assay in response to high glucose stimulus alone (17.6 mM) or high glucose plus 10 µM forkolin in iPSC(HEL 153.2)-derived β-cells treated or not with 50 nM Ex4 for 24 hours. Data are corrected for total protein. *p<0.05, **p<0.01 vs vehicle. Data points correspond to individual experiments. The median is shown by a horizontal line in the box plots; the 25th and the 75th percentiles are at the bottom and top of the boxes, respectively; whiskers represent the minimum and maximum values (C) NAD(P)H autofluorescence of HEL 135.2-derived β-cells untreated (black line) or treated with 50 nM Ex4 (red line) for 24 hours. NAD(P)H data are means ± SEM for 6 aggregates from 3 different preparations. *p<0.05, ***p<0.005 Ex vs Veh by two-way ANOVA for matched data followed by Bonferroni correction for multiple comparisons. CT, control cell line; Veh, vehicle; Ex 50, 50 nM exendin; FCCP, Carbonyl Cyanide-4 (trifluoromethoxy) Phenylhydrazone.

DISCUSSION

Diabetes is a complex disease which currently affects 425 million people worldwide and T2D accounts for 80-90% of all cases. Development and progression of both type 1 and T2D is caused by pancreatic β-cell failure, due to dysfunction or destruction of β-cells. Nevertheless, the most prevalent cause of mortality in T2D patients is represented by CV disease which occurs with two-three times higher rate in subjects with diabetes compared to adults without diabetes [110, 111]. A shared mechanism in the pathogenesis of both T2D and related CVD is represented by lipotoxicity, whose deleterious effects are mediated by elevated FFA levels [195].

In the present study, we hypothesized that FFAs may not only induce a direct damage on the vessel wall, but also may alter endogenous endothelial repair processes through a direct effect on MACs, a subset of cells – isolated from peripheral blood – displaying pro-angiogenic function. Of note, T2D patients show lower MAC levels compared to healthy individuals, and a reduction in MAC bioavailability and function predicts increased CV events.

This study reports that stearic acid (SA) induces a dose- and time-dependent lipo-apoptosis in MACs, which appears to be mediated by PERK signaling in the UPR pathway. SA also induces pro-inflammatory cytokines and chemokines, through JNK activation, and oxidative stress markers gene expression. Importantly, SA exposure affects angiogenic function in MACs.

Given the broad spectrum of conditions in which lipotoxicity is involved (e.g among which, but not limited to, insulin resistance and diabetes) and the key role played by MACs in maintaining vascular homeostasis, this model of lipotoxicity in MACs acquires a major significance.

Although high concentrations of SFA are known to directly exert harmful effects in several tissues, these findings represent the first evidence pointing out the role of lipotoxicity in both bioavailability –- via increasing in MAC apoptosis – and function – via alteration of tube formation capacity – in human MACs.

Of note, these detrimental effects have been induced by physiological concentration of SA (i.e. 100 μM) which is comparable to that of individuals with T2D [263]. On the other hand, palmitic acid (PA), which is the most abundant FFA in circulation, induced apoptosis only at supraphysiologic concentration (1-2 mM) in MACs. In accordance, a previous study showed that SA has the major effect in activating caspase 3/7 compared to other FFA, including PA, in endothelial cells models and late EPCs [264].

In the setting of IR (or IR-associated conditions), several studies highlight the emerging role of SA. High fat diets enriched in SA, are associated with a worse metabolic phenotype in mice – in terms of both liver and peripheral IR and greater gluconeogenesis – than high fat diets based on palm oil [265, 266]. Moreover, IR is characterized by a low-grade chronic systemic inflammation, namely *metaflammation*, which underlies the onset of the atherosclerotic process [267]. In this study, SA triggers pro-inflammatory cytokine/chemokine expression and secretion in MACs. The translation of these results to the *in vivo* settings suggests that SA contributes to the worsening of the inflammatory burden and to *metaflammation*. Among the pro-inflammatory cytokine/chemokine upregulated by SA, IL-8, which is a neutrophil chemoattractant and has a role in atherosclerotic lesion progression, is the highest expressed. Similarly, high levels of IL-8 have been found in other lipotoxicity-associated conditions, such as obesity, diabetes and atherosclerosis [268, 269].

This stimulation of the pro-inflammatory response has been demonstrated to be induced by JNK. The role of JNK in inflammation and lipotoxicity-

associated conditions has been confirmed in several studies [264, 270, 271, 272]. Nevertheless, it cannot be excluded the involvement of additional mediators, e.g. NF-kB. IL-8 and, at least partially, IL-6 up-regulation escape from the action of JNK inhibitor, supporting the hypothesis of other player(s) involved.

SA fuels ER stress response in MACs, leading to the activation of all the three branches of the UPR. Similarly, an increase in the expression of oxidative stress markers have been observed. The correlation among ER stress, oxidative stress and lipotoxicity have been explored in several *in vitro* and *in vivo* models [273, 274]. Of note, in our study the inhibition of PERK reduces SA-induced apoptosis, strongly suggesting that ER stress response is the mechanism through which, at least partly, SA affects MAC bioavailability.

Overall, this study highlights MAC vulnerability to physiologic concentration of SA which negatively affects both MAC viability and function. Thus, SA does exert a direct damage on MACs, resulting in an impairment of endothelial repair capacity. Importantly, dysfunctional lipotoxic MACs may not only result in loss of endothelial repair, but also boost vessel injury, through the release of pro-inflammatory molecules, and promote atherosclerotic plaque instability.

Ameliorating lipotoxicity in MACs may be particularly significant in the setting of altered vessel homeostasis, endothelial dysfunction and increased CV risk, typical of T2D.

Since 2008 dedicated CV outcome trials have been conducted to test the CV safety of each new drug proposed for the treatment of T2D. A recently introduced class of anti-diabetic drugs is SGLT2 inhibitors, also called gliflozins, which demonstrated, not only CV safety, but even CV protection, beyond the improvement of hyperglycemia. SGLT2-I, specifically empagliflozin, dapagliflozin and canagliflozin, show beneficial CV effects in T2D patients reducing the CV risk, but through not yet

clarified mechanisms. Thus, we hypothesized that the observed beneficial effects of SGLT-2-I on CV outcomes might be also mediated by a direct effect on MACs. In particular, because of the detrimental effects exerted by lipotoxicity on MACs and the consequent possible effects on the related CV outcomes, the capacity of the novel anti-diabetic drugs SGLT2-I (EMPA and DAPA) to curb stearic acid-induced lipotoxicity in MACs has been explored.

At the maximum concentration tested (100 μM) both EMPA and DAPA curbed the SA-induced expression of pro-inflammatory and oxidative stress markers, restoring baseline values.

Given the pivotal contribution of inflammation (*metaflammation*) and oxidative stress in lipotoxic-related diseases, and particularly in relation to the atherosclerotic process, SGLT2-I-mediated beneficial effects in lipotoxic MACs may play a remarkable positive role. These beneficial effects may result in vascular damage reduction and in plaque stability and endothelial repair enhancement through the improvement of MACs dysfunction.

Anti-inflammatory or anti-oxidant effects mediated by SGLT2-I have been observed in a number in other studies [275], [276], [277]. As example, in cardiofibroblast form T2D mice, physiological concentration of DAPA reduces IL-1β expression and inflammasome recruitment through a mechanism 5'-adenosine monophosphate- activated protein kinase (AMPK)-dependent but SGLT2-independent [278].

Since no expression of SGLT-2 was detected in MACs, it has been hypothesized that a non-canonical mediator of gliflozin effects is involved. Docking simulation studies, recently applied by Uthman et al, show high binding affinity of SGTL2 inhibitors, empagliflozin, dapaglifozin and canagliflozin, with NHE, an ion exchanger which mediates the transport of Na^+ and H^+ in and out of the cell, respectively. NHE isoform 1-6 and 9 expression is detected in MACs and SGLT2-I effects are mimicked by

amiloride (a broad NHE inhibitor), and only partially by cariporide (NHE1 specific inhibitor), likely suggesting a similar mechanism of action by amiloride and SGLT-2 inhibitors, such as NHE blocking.

It is well known that amiloride exerts an anti-inflammatory action by restraining LPS-induced pro-inflammatory cytokine production and NK-kB production in both endothelial cell and macrophages [279, 280].

Thus, the present study not only suggests a direct action of SGLT2-I in curbing lipotoxicity in a CVD-relevant model, but also highlights SGLT2 independent mechanism(s) of action of SGLT2-I and extends the evidence of NHE inhibition-dependent effects of this class of drugs.

Lipotoxicity has a pivotal role in CVD as well as represents a major cause of IR and T2D [195].

So far, findings on lipotoxicity in β-cells almost exclusively derive from rodent models, namely from primary islets or β-cell lines [251, 252]. A few studies have been performed in human islets [234, 281, 282] , due to limited cell availability - few donor organ transplantation centers worldwide provide human islets – and high islet preparation variability. An alternative solution to human pancreatic islets is represented by the human β-cell line EndoC-βH1, an immortalized human cell line which shows glucose-responsive insulin secretion capacity. In our experience, pilot experiments have shown that EndoC-βH1 cells are susceptible to lipoapoptosis induced by SA and PA. Nevertheless, a higher concentration than in MACs is requested to induce an effective decrease in cell viability. Of note, also in EndoC-βH1 cells, SA seems to have a more toxic outcome compared to PA. In literature, data regarding FFA-mediated effects in human β cell lines are scarce. A very recent study reports that both PA and SA induce caspase 3 activation and peroxisomal H_2O_2 generation, but not mitochondrial H_2O_2 generation and ER stress response [283]. However, in one additional study, led by Prof. Raphael Scharfmann (Paris), authors do not claim EndoC-βH1 cell susceptibility to

lipoapoptosis. On the contrary, they show that this human β-cell line is rather resistant to FFA (PA and SA). In line with these data, it has been observed that stearoyl-CoA desaturase (SCD), a key enzyme involved in processing of saturated FFA in unsaturated FFA, is highly express in EndoC-βH1 cells, suggesting that it may mediate the peculiar resistance to FFA of EndoC-βH1 cells. Indeed, in the study coordinated by Prof. Scharfamm, SCD knockdown sensitizes the cells to saturated FFA-induced lipotoxicity, causing an increase in pro-inflammatory and ER stress markers gene expression and reduced expression of β-cell identity markers. However, contrasting data have been highlighted also in an additional study in which PA induces apoptosis and ROS production when cultured in a mixture of DMEM/Ham's F12 culture medium but not in DMEM alone [284]. Although authors suggest that linoleic acid may have a partial role in DMEM/Ham's F12-driven effects, this issue remains unclarified.

Overall, given the reported contrasting data and considering that EndoC-βH1 cells should not be considered as a direct equivalent of non-dividing primary β-cells as they are transformed pseudodiploid cells in continuous expansion, EndoC-βH1 cells might not represent the best model to study β-cell lipotoxicity.

The recent introduction of iPSCs-derived β-cell technology represents an important step ahead in the modeling of pancreatic β-cell pathophysiology. Nevertheless, current *in vitro* differentiation strategies enable to generate only immature β-cells. Thus, one aim of this project is to optimize a protocol for *in vitro* differentiation of induced pluripotent stem cells into β-cells to create novel models to study β-cell lipotoxicity.

Induced PSC-derived β-cells have been obtained using a 7-stage protocol (4-5 weeks), based on previously published protocols [93, 94, 106, 256], which mimic the embryonic development of the endocrine pancreas. Until the pancreatic progenitor stage (stage 4), cells have been cultured as

monolayer and then transferred to 3D systems to sustain the formation of islets-like structures. At the end of the process, the yield of insulin-positive β-cells at stage 7 is comparable to that of human islets. In our hands, *in vitro* high glucose stimulus leads to a slight increase in iPSC-derived β-cell insulin release, which it is significantly further augmented in response to high glucose plus forskolin stimulation.

These results, although encouraging, remark the lacking of a fully *in vitro* functional maturation.

Of note, β-cell development occurs during the fetal growth, but the capacity to respond to glucose stimulation is acquired after birth.

In vitro differentiation of iPSCs into β-cells gives arise to β-cell which resemble a more fetal phenotype, as indicated by low MAFA expression and scarce *in vitro* function.

Interestingly, a recent study investigating the molecular mechanisms responsible for the β-cell functional maturation, highlights the involvement of the nutrient sensor target of rapamycin (mTORC1) and AMPK. They identify that the master control of β-cellular signaling switches from mTORC-1 to AMPK in adult β-cells [285]. Dysfunctional glucose-stimulated insulin secretion response in T2D patients may be driven by a reversion in mTORC-1/AMPK regulation, as well as the absence of a proper response in *in vitro* iPSCs-derived β-cells may be due to a lack of AMPK in taking the lead.

In addition, Velazco-Cruz and collogues have recently pointed out the importance of TGFβ signaling modulation over time for phenotypical and functional iPSCs-derived β-cell maturation. Indeed, although TGFβ signaling inhibition is necessary at the stage of pancreatic progenitors to achieve a clear β-cell phenotype, continuous exposition to Alk5 inhibitor II (TGFβ inhibitor) results in non-glucose-responsive differentiated β-cells [95].

Although *in vitro* data on iPSC-derived β-cell insulin release are not fully satisfying, iPSC-derived β-cells transplantation in NOD-SCID mice boosts

their functional maturation, as shown by human C-peptide levels and by the successfully maintained normoglycaemia after STZ injection and until nephrectomy.

Moreover, transplanted grafts display the capacity to modulate *in vivo* insulin secretion in response to external agents, such as forskolin, diazoxide, gliclazide or high K^+. This capacity, acquired following transplantation, confirms that the *in vivo* environment has a role in promoting β-cell differentiation. It would be fundamental to understand which are the exact critical factors interacting and sustaining the functional maturation of iPSCs-derived β-cells in the *in vivo* environment. As previously mentioned, both endothelial cells and estrogen receptor signaling have been proposed to play a role in further β-cell maturation [96, 97].

Of note, transcriptomic (RNA-seq) and epigenomic (ChIP-seq for H3K27me3 and H3K4me3) characterization of β-cells derived from PSCs, *in vitro* and after *in vivo* transplantation, shows that cells exhibit more close similarity to human islets following *in vivo* engraftment (both in terms of transcriptome and chromatin structure) [286].

Overall, although further experiments are needed to optimize *in vitro* iPSC-derived β-cell function, even at the current stage of development, they can be exploited to study lipotoxicity-induced β-cell demise in diabetes. In this regards, high SCD expression in iPSC-derived β-cells has been observed, with a peculiar increase in the last stage of differentiation, suggesting they may have low susceptibility to FFA-induced lipotoxicity.

Among the advantages of iPSC-derived β-cells it should be recognize that iPSCs are a directly patient-relevant cell model, as they are reprogrammed from patient's cells.

Since it is known that T2D patients have a significantly higher prevalence of obesity than non-diabetics, but not all obese subjects eventually develop T2D, individual subject-derived iPSCs and differentiation into β-

cells may represent an interesting model to study the link between lipotoxicity and T2D susceptibility.

As regards to the generation of patient-relevant cell model, we applied it on fibroblasts reprogrammed in iPSCs from a patient affected by Friedreich ataxia (FRDA), which is an autosomal recessive neurodegenerative disease, with a high prevalence of diabetes [3]. The disease is caused by reduced frataxin protein expression that leads to oxidative stress and mitochondrial dysfunction.

The above mentioned 7-stage differentiation protocol has been applied to obtain pancreatic β-cells from the FRDA iPSC line. The differentiation has been highly efficient, resulting in 58% insulin-positive β-cells and few glucagon-positive cells and slight glucose-responsive cells. Frataxin levels in these iPSC-derived β-cells result lower than those of healthy control cell line. Then, this patient-relevant model has been exploited to evaluate the effect on β-cells of incretin analog, which was found to mildly increase frataxin expression.

Up to now, several PSCs-based diabetes-related and patient-specific cell models have been established, such as for the wolfram syndrome [287], or for neonatal form of diabetes due to mutation in the gene of STAT3 [106] or GATA6 [288], or for different form of MODY (Maturity Onset Diabetes of the Young) [289], [290], confirming the exceptional importance of having β-cells directly derived from iPSCs' patient.

However, the comparison of data from different cell lines (control- and patient-derived cell lines) can be difficult because of the quality of the iPSCs reprogramming and the variability among donors. In order to obtain more robust results, different cell lines - derived from diverse subjects - should be considered, and data should be compared with an equally large number of control individuals. In addition, when the genetic target is known, another strategy to reduce variability is the genome editing of

iPSCs to create an isogenic iPSC cell line to correct (or introduce) a specific genetic variant or mutation.

In conclusion, the present study shows that SA negatively affects both MAC function and viability, suggesting a harmful role in endothelial repair processes. Importantly, MAC lipotoxic status is ameliorated by SGLT2-I treatment, possibly via NHE-inhibition, pointing to an improvement of MAC biology as a potential mechanism underlying SGLT2-I mediated CV benefits.

Furthermore, FFA have a pivotal role also in β-cell demise, but, so far, the lack of an appropriate cell model, reduced the possibility to study β-cell lipotoxicity. This study shows promising results in β-cells differentiation, highlighting multiple advantages of using iPSCs-derived β-cell for investigating β-cell dysfunction.

Future researches are needed to unravel the effective mechanisms through which SA affects β-cells

Overall, this project points to a critical role of lipotoxicity, specifically induced by SA, in driving the development of T2D and of its major complication, i.e. CVD.

Bibliography

1 American Diabetes Association. Diagnosis and classification of diabetes mellitus. Diabetes Care. 2010 Jan;33 Suppl 1:S62-9.

2 World Health Organization. (2019). Classification of diabetes mellitus. World Health Organization. https://apps.who.int/iris/handle/10665/325182. License: CC BY-NC-SA 3.0 IGO

3 Cnop M, Mulder H, Igoillo-Esteve M. Diabetes in Friedreich ataxia. J Neurochem. 2013 Aug;126 Suppl 1:94-102

4 Farquhar JW. Early-onset diabetes in the general and the Down's syndrome population. Lancet. 1969 Aug 9;2(7615):323-4

5 Bondy CA; Turner Syndrome Study Group. Care of girls and women with Turner syndrome: a guideline of the Turner Syndrome Study Group. J Clin Endocrinol Metab. 2007 Jan;92(1):10-25. Epub 2006 Oct 17

6 Cosentino F, Grant PJ, Aboyans V, Bailey CJ, Ceriello A, Delgado V, Federici M, Filippatos G, Grobbee DE, Hansen TB, Huikuri HV, Johansson I, Jüni P, Lettino M, Marx N, Mellbin LG, Östgren CJ, Rocca B, Roffi M, Sattar N, Seferović PM, Sousa-Uva M, Valensi P, Wheeler DC; ESC Scientific Document Group. 2019 ESC Guidelines on diabetes, pre-diabetes, and cardiovascular diseases developed in collaboration with the EASD. Eur Heart J. 2019 Aug 31.

7 American Diabetes Association. 2. Classification and Diagnosis of Diabetes: Standards of Medical Care in Diabetes-2019. Diabetes Care. 2019 Jan;42(Suppl 1):S13-S28

8 https://www.who.int/news-room/fact-sheets/detail/diabetes, World Health Organization, Fact sheet, October 2018

9 GBD 2017 Risk Factor Collaborators. Global, regional, and national comparative risk assessment of 84 behavioural, environmental and occupational, and metabolic risks or clusters of risks for 195 countries and territories, 1990-2017: a systematic analysis for the Global Burden of Disease Study 2017. Lancet. 2018 Nov 10;392(10159):1923-1994.

10 NCD Risk Factor Collaboration (NCD-RisC). Worldwide trends in diabetes since 1980: a pooled analysis of 751 population-based studies with 4.4 million participants. Lancet. 2016 Apr 9;387(10027):1513-1530

11 International Diabetes Federation. IDF Diabetes Atlas, 8th edn. Brussels, Belgium: International Diabetes Federation, 2017

12 Shaw JE, Sicree RA, Zimmet PZ. Global estimates of the prevalence of diabetes for 2010 and 2030. Diabetes Res Clin Pract. 2010 Jan;87(1):4-14

[13] Zheng Y, Ley SH, Hu FB. Global aetiology and epidemiology of type 2 diabetes mellitus and its complications. Nat Rev Endocrinol. 2018 Feb;14(2):88-98

[14] Leslie RDG, ed. Molecular Pathogenesis of Diabetes Mellitus. Karger, 1997, 22: 131-156

[15] Kahn CR., Insulin resistance, insulin insensitivity, and insulin unresponsiveness: a necessary distinction. Metabolism. 1978 Dec;27

[16] Menting JG, Whittaker J, Margetts MB, Whittaker LJ, Kong GK, Smith BJ, Watson CJ, Záková L, Kletvíková E, Jiráček J, Chan SJ, Steiner DF, Dodson GG, Brzozowski AM, Weiss MA, Ward CW, Lawrence MC. How insulin engages its primary binding site on the insulin receptor. Nature. 2013 Jan 10;493(7431):241-5

[17] Scapin G, Dandey VP, Zhang Z, Prosise W, Hruza A, Kelly T, Mayhood T, Strickland C, Potter CS, Carragher B. Structure of the insulin receptor-insulin complex by single-particle cryo-EM analysis. Nature. 2018 Apr 5;556(7699):122-125

[18] White MF, Shoelson SE, Keutmann H, Kahn CR. A cascade of tyrosine autophosphorylation in the beta-subunit activates the phosphotransferase of the insulin receptor. J Biol Chem 1988; 263: 2969-2980

[19] Shepherd PR, Navé BT, Siddle K. Insulin stimulation of glycogen synthesis and glycogen synthase activity is blocked by wortmannin and rapamycin in 3T3-L1 adipocytes: evidence for the involvement of phosphoinositide 3-kinase and p70 ribosomal protein-S6 kinase. Biochem J 1995; 305 (Pt 1): 25-28

[20] Alessi DR, Cohen P. Mechanism of activation and function of protein kinase B. Curr Opin Genet Dev 1998; 8: 55-62

[21] Wolfrum C, Besser D, Luca E, Stoffel M. Insulin regulates the activity of forkhead transcription factor Hnf-3beta/Foxa-2 by Akt-mediated phosphorylation and nuclear/cytosolic localization. Proc Natl Acad Sci U S A. 2003 Sep 30;100(20):11624-9

[22] Taylor SI, Accili D, Imai Y. Insulin resistance or insulin deficiency. Which is the primary cause of NIDDM? Diabetes.

[23] Foti D, Chiefari E, Fedele M, Iuliano R, Brunetti L, Paonessa F, Manfioletti G, Barbetti F, Brunetti A, Croce CM, Fusco A, Brunetti A. Lack of the architectural factor HMGA1 causes insulin resistance and diabetes in humans and mice. Nat Med. 2005 Jul;11(7):765-73

[24] Kahn CR, Flier JS, Bar RS, Archer JA, Gorden P, Martin MM, Roth J. The syndromes of insulin resistance and acanthosis nigricans. Insulin-receptor disorders in man. N Engl J Med. 1976 Apr 1;294(14):739-45

[25] Taylor SI, Accili D, Cama A, Kadowaki H, Kadowaki T, Imano E, Sierra ML. 1991. Mutations in the insulin re- ceptor gene in patients with genetic syndromes of insulin resistance. Adv Exp Med Biol 293: 197–213

[26] Haruta T, Imamura T, Iwanishi M, Egawa K, Goji K, Koba- yashi M. 1995. Amplification and analysis of promoter region of insulin receptor gene in a patient with leprechaunism associated with severe insulin resistance. Me- tabolism 44: 430–437

[27] Morino K, Petersen KF, Dufour S, Befroy D, Frattini J, Sha- tzkes N, Neschen S, White MF, Bilz S, Sono S, Pypaert M, Shulman GI. Reduced mitochondrial density and increased IRS-1 serine phosphorylation in muscle of insulin-resistant offspring of type 2 diabetic parents. J Clin Invest 2005; 115: 3587-3593

[28] Freidenberg GR, Reichart D, Olefsky JM, Henry RR. Reversibility of defective adipocyte insulin receptor kinase activity in non- insulin dependent diabetes mellitus. Effect of weight loss. J Clin Invest 1988;82:1398-406

[29] Yu CL, Chen Y, Cline GW, Zhang DY, Zong HH, Wang YL, Bergeron R, Kim JK, Cushman SW, Cooney GJ, Atcheson B, White MF, Kraegen EW, Shulman GI: Mechanism by which fatty acids inhibit insulin activation of insulin receptor substrate-1 (IRS-1)-associated phosphatidylinositol 3-kinase activity in muscle. J Biol Chem277 :50230 – 50236,2002

[30] Cusi K, Maezono K, Osman A, et al. Insulin resistance differen- tially affects the PI 3-kinase and MAP kinase-mediated signaling in human muscle. J Clin Invest 2000;105:311-20

[31] Bonner-Weir S, In't Veld PA, Weir GC. Reanalysis of study of pancreatic effects of incretin therapy: methodological deficiencies. Diabetes Obes Metab. 2014 Jul;16(7):661-6.

[32] Rahier J, Guiot Y, Goebbels RM, Sempoux C, Henquin JC. Pancreatic beta-cell mass in European subjects with type 2 diabetes. Diabetes Obes Metab. 2008 Nov;10 Suppl 4:32-42

[33] Prasad RB, Groop L. Genetics of type 2 diabetes-pitfalls and possibilities. Genes (Basel). 2015 Mar 12;6(1):87-123

[34] Zeggini E, Scott LJ, Saxena R, Voight BF, Marchini JL, Hu T, de Bakker PI, Abecasis GR, Almgren P, Andersen G, Ardlie K, Boström KB, Bergman RN, Bonnycastle LL, Borch-Johnsen K, Burtt NP, Chen H, Chines PS, Daly MJ, Deodhar P, Ding CJ, Doney AS, Duren WL, Elliott KS, Erdos MR, Frayling TM, Freathy RM, Gianniny L, Grallert H, Grarup N, Groves CJ, Guiducci C, Hansen T, Herder C, Hitman GA, Hughes TE, Isomaa B, Jackson AU, Jørgensen T, Kong A, Kubalanza K, Kuruvilla FG, Kuusisto J, Langenberg C, Lango H, Lauritzen T, Li Y, Lindgren CM, Lyssenko V, Marvelle AF, Meisinger C, Midthjell K,

Mohlke KL, Morken MA, Morris AD, Narisu N, Nilsson P, Owen KR, Palmer CN, Payne F, Perry JR, Pettersen E, Platou C, Prokopenko I, Qi L, Qin L, Rayner NW, Rees M, Roix JJ, Sandbaek A, Shields B, Sjögren M, Steinthorsdottir V, Stringham HM, Swift AJ, Thorleifsson G, Thorsteinsdottir U, Timpson NJ, Tuomi T, Tuomilehto J, Walker M, Watanabe RM, Weedon MN, Willer CJ; Wellcome Trust Case Control Consortium, Illig T, Hveem K, Hu FB, Laakso M, Stefansson K, Pedersen O, Wareham NJ, Barroso I, Hattersley AT, Collins FS, Groop L, McCarthy MI, Boehnke M, Altshuler D. Meta-analysis of genome-wide association data and large-scale replication identifies additional susceptibility loci for type 2 diabetes. Nat Genet. 2008 May;40(5):638-45

[35] Bhandare R, Schug J, Le Lay J, Fox A, Smirnova O, Liu C, Naji A, Kaestner KH. Genome-wide analysis of histone modifications in human pancreatic islets. Genome Res. 2010 Apr;20(4):428-33. doi: 10.1101/gr.102038.109

[36] Stitzel ML, Sethupathy P, Pearson DS, Chines PS, Song L, Erdos MR, Welch R, Parker SC, Boyle AP, Scott LJ; NISC Comparative Sequencing Program, Margulies EH, Boehnke M, Furey TS, Crawford GE, Collins FS. Global epigenomic analysis of primary human pancreatic islets provides insights into type 2 diabetes susceptibility loci. Cell Metab. 2010 Nov 3;12(5):443-55

[37] Bramswig NC, Everett LJ, Schug J, Dorrell C, Liu C, Luo Y, Streeter PR, Naji A, Grompe M, Kaestner KH. Epigenomic plasticity enables human pancreatic α to β cell reprogramming. J Clin Invest. 2013 Mar;123(3):1275-84

[38] Larsen L, Tonnesen M, Ronn SG, Størling J, Jørgensen S, Mascagni P, Dinarello CA, Billestrup N, Mandrup-Poulsen T. Inhibition of histone deacetylases prevents cytokine-induced toxicity in beta cells. Diabetologia. 2007 Apr;50(4):779-89

[39] Susick L, Senanayake T, Veluthakal R, Woster PM, Kowluru A. A novel histone deacetylase inhibitor prevents IL-1beta induced metabolic dysfunction in pancreatic beta-cells. J Cell Mol Med. 2009; 13:1877–85

[40] Poy MN, Hausser J, Trajkovski M, Braun M, Collins S, Rorsman P, Zavolan M Stoffel M. miR-375 maintains normal pancreatic alpha- and beta-cell mass. Proc Natl Acad Sci U S A. 2009 Apr 7;106(14):5813-8.

[41] Li Y, Luo T, Wang L, Wu J, Guo S. MicroRNA-19a-3p enhances the proliferation and insulin secretion, while it inhibits the apoptosis of pancreatic β cells via the inhibition of SOCS3. Int J Mol Med. 2016 Nov;38(5):1515-1524

[42] Sun J, Cui J, He Q, Chen Z, Arvan P, Liu M. Proinsulin misfolding and endoplasmic reticulum stress during the development and progression of diabetes. Mol Aspects Med. 2015 Apr;42:105-18

[43] Laybutt DR, Preston AM, Akerfeldt MC, Kench JG, Busch AK, Biankin AV, Biden TJ. Endoplasmic reticulum stress contributes to beta cell apoptosis in type 2 diabetes. Diabetologia. 2007 Apr;50(4):752-63

[44] Marchetti P, Bugliani M, Lupi R, Marselli L, Masini M, Boggi U, Filipponi F, Weir GC, Eizirik DL, Cnop M. The endoplasmic reticulum in pancreatic beta cells of type 2 diabetes patients. Diabetologia. 2007 Dec;50(12):2486-94

[45] Tanaka Y, Tran PO, Harmon J, Robertson RP. A role for glutathione peroxidase in protecting pancreatic beta cells against oxidative stress in a model of glucose toxicity. Proc Natl Acad Sci U S A. 2002 Sep 17;99(19):12363-8

[46] organ D, Oliveira-Emilio HR, Keane D, Hirata AE, Santos da Rocha M, Bordin S, Curi R, Newsholme P, Carpinelli AR. Glucose, palmitate and pro-inflammatory cytokines modulate production and activity of a phagocyte-like NADPH oxidase in rat pancreatic islets and a clonal beta cell line. Diabetologia. 2007 Feb;50(2):359-69

[47] Sakai K, Matsumoto K, Nishikawa T, Suefuji M, Nakamaru K, Hirashima Y, Kawashima J, Shirotani T, Ichinose K, Brownlee M, Araki E. Mitochondrial reactive oxygen species reduce insulin secretion by pancreatic beta-cells. Biochem Biophys Res Commun. 2003 Jan 3;300(1):216-22

[48] Gurgul E, Lortz S, Tiedge M, Jörns A, Lenzen S. Mitochondrial catalase overexpression protects insulin-producing cells against toxicity of reactive oxygen species and proinflammatory cytokines. Diabetes. 2004 Sep;53(9):2271-80

[49] Fridlyand LE, Philipson LH: Does the glucose-dependent insulin secretion mechanism itself cause oxidative stress in pancreatic □-cells? Diabetes 53:1942–1948, 2004

[50] Ehses JA, Perren A, Eppler E, Ribaux P, Pospisilik JA, Maor-Cahn R, Gueripel X, Ellingsgaard H, Schneider MK, Biollaz G, Fontana A, Reinecke M, Homo-Delarche , Donath MY. Increased number of islet-associated macrophages in type 2 diabetes. Diabetes. 2007 Sep;56(9):2356-70

[51] Richardson SJ, Willcox A, Bone AJ, Foulis AK, Morgan NG. Islet-associated macrophages in type 2 diabetes. Diabetologia 2009;52:1686–1688

[52] Westwell-Roper CY, Ehses JA, Verchere CB. Resident macrophages mediate islet amyloid polypeptide-induced islet IL-1b production and b-cell dysfunction. Diabetes 2014;63:1698–1711

[53] Maedler K, Sergeev P, Ris F, Oberholzer J, Joller-Jemelka HI, Spinas GA, Kaiser N, Halban PA, Donath MY. Glucose-induced beta cell production of IL-1beta contributes to glucotoxicity in human pancreatic islets. J Clin Invest. 2002 Sep;110(6):851-60.

[54] Böni-Schnetzler M, Boller S, Debray S, Bouzakri K, Meier DT, Prazak R, Kerr-Conte J, Pattou F, Ehses JA, Schuit FC, Donath MY. Free fatty acids induce a proinflammatory

response in islets via the abundantly expressed interleukin-1 receptor I. Endocrinology. 2009 Dec;150(12):5218-29

[55] Maedler K, Sergeev P, Ehses JA, Mathe Z, Bosco D, Berney T, Dayer JM, Reinecke M, Halban PA, Donath MY. Leptin modulates beta cell expression of IL-1 receptor antagonist and release of IL-1beta in human islets. Proc Natl Acad Sci U S A. 2004 May 25;101(21):8138-43

[56] Talchai C, Xuan S, Lin HV, Sussel L, Accili D. Pancreatic β cell dedifferentiation as a mechanism of diabetic β cell failure. Cell. 2012 Sep 14;150(6):1223-34

[57] Brereton MF, Iberl M, Shimomura K, Zhang Q, Adriaenssens AE, Proks P, Spiliotis II, Dace W, Mattis KK, Ramracheya R, Gribble FM, Reimann F, Clark A, Rorsman P, Ashcroft FM. Reversible changes in pancreatic islet structure and function produced by elevated blood glucose. Nat Commun. 2014 Aug 22;5:4639

[58] Cinti, F., Bouchi, R., Kim-Muller, J. Y., Ohmura, Y., Sandoval, P. R., Masini, M., et al. (2016). Evidence of beta-cell dedifferentiation in human type 2 diabetes. J. Clin. Endocrinol. Metab. 101, 1044–1054. doi: 10.1210/jc.2015-2860

[59] Wang Z, York NW, Nichols CG, Remedi MS. Pancreatic β cell dedifferentiation in diabetes and redifferentiation following insulin therapy. Cell Metab. 2014 May 6;19(5):872-82

[60] Guo S, Dai C, Guo M, Taylor B, Harmon JS, Sander M, Robertson RP, Powers AC, Stein R. Inactivation of specific β cell transcription factors in type 2 diabetes. J Clin Invest. 2013 Aug;123(8):3305-16

[61] O'Rahilly R, Müller F. Developmental stages in human embryos: revised and new measurements. Cells Tissues Organs. 2010;192(2):73-84

[62] Jennings RE, Berry AA, Strutt JP, Gerrard DT, Hanley NA. Human pancreas development. Development. 2015 Sep 15;142(18):3126-37

[63] Jennings RE, Berry AA, Kirkwood-Wilson R, Roberts NA, Hearn T, Salisbury RJ, Blaylock J, Piper Hanley K, Hanley NA. Development of the human pancreas from foregut to endocrine commitment. Diabetes. 2013 Oct;62(10):3514-22

[64] Pan FC, Wright C. Pancreas organogenesis: from bud to plexus to gland. Dev Dyn. 2011 Mar;240(3):530-65

[65] Piper K, Brickwood S, Turnpenny LW, Cameron IT, Ball SG, Wilson DI, Hanley NA Beta cell differentiation during early human pancreas development. J Endocrinol 2004 Apr;181(1):11-23

[66] Shaw-Smith C, De Franco E, Lango Allen H, Batlle M, Flanagan SE, Borowiec M, Taplin CE, van Alfen-van der Velden J, Cruz-Rojo J, Perez de Nanclares G, Miedzybrodzka Z,

Deja G, Wlodarska I, Mlynarski W, Ferrer J, Hattersley AT, Ellard S. GATA4 mutations are a cause of neonatal and childhood-onset diabetes. Diabetes. 2014 Aug;63(8):2888-94

[67] Lyttle BM, Li J, Krishnamurthy M, Fellows F, Wheeler MB, Goodyer CG, Wang R. Transcription factor expression in the developing human fetal endocrine pancreas. Diabetologia. 2008 Jul;51(7):1169-80

[68] Gu G, Dubauskaite J, Melton DA. Direct evidence for the pancreatic lineage NGN3+ cells are islet progenitors and are distinct from duct progenitors Development. 2002 May;129(10):2447-57.

[69]Gradwohl G, Dierich A, LeMeur M, Guillemot F. neurogenin3 is required for the development of the four endocrine cell lineages of the pancreas. Proc Natl Acad Sci U S A. 2000 Feb 15;97(4):1607-11

[70] Capito C, Simon MT, Aiello V, Clark A, Aigrain Y, Ravassard P, Scharfmann R. Mouse muscle as an ectopic permissive site for human pancreatic development. Diabetes. 2013 Oct;62(10):3479-87

[71] De Los Angeles A, Ferrari F, Xi R, Fujiwara Y, Benvenisty N, Deng H, Hochedlinger K, Jaenisch R, Lee S, Leitch HG, Lensch MW, Lujan E, Pei D, Rossant J, Wernig M, Park PJ, Daley GQ. Hallmarks of pluripotency. Nature. 2015 Sep 24;525(7570):469-78

[72] Evans MJ, Kaufman MH. Establishment in culture of pluripotential cells from mouse embryos. Nature. 1981 Jul 9;292(5819):154-6

[73] Takahashi K, Yamanaka S. Induction of pluripotent stem cells from mouse embryonic and adult fibroblast cultures by defined factors. Cell. 2006 Aug 25;126(4):663-76

[74] Takahashi K, Tanabe K, Ohnuki M, Narita M, Ichisaka T, Tomoda K, Yamanaka S. Induction of pluripotent stem cells from adult human fibroblasts by defined factors. Cell. 2007 Nov 30;131(5):861-72

[75] Lowry WE, Richter L, Yachechko R, Pyle AD, Tchieu J, Sridharan R, Clark AT, Plath K. Generation of human induced pluripotent stem cells from dermal fibroblasts. Proc Natl Acad Sci U S A. 2008 Feb 26;105(8):2883-8

[76] Yu J, Vodyanik MA, Smuga-Otto K, Antosiewicz-Bourget J, Frane JL, Tian S, Nie J, Jonsdottir GA, Ruotti V, Stewart R, Slukvin II, Thomson JA. Induced pluripotent stem cell lines derived from human somatic cells. Science. 2007 Dec 21;318(5858):1917-20

[77] Sommer CA, Stadtfeld M, Murphy GJ, Hochedlinger K, Kotton DN, Mostoslavsky G. Induced pluripotent stem cell generation using a single lentiviral stem cell cassette. Stem Cells. 2009 Mar;27(3):543-9

[78] Somers A, Jean JC, Sommer CA, Omari A, Ford CC, Mills JA, Ying L, Sommer AG, Jean JM, Smith BW, Lafyatis R, Demierre MF, Weiss DJ, French DL, Gadue P, Murphy GJ, Mostoslavsky G, Kotton DN. Generation of transgene-free lung disease-specific

human induced pluripotent stem cells using a single excisable lentiviral stem cell cassette. Stem Cells. 2010 Oct;28(10):1728-40

[79] Si-Tayeb K, Noto FK, Sepac A, Sedlic F, Bosnjak ZJ, Lough JW, Duncan SA. Generation of human induced pluripotent stem cells by simple transient transfection of plasmid DNA encoding reprogramming factors. BMC Dev Biol. 2010 Aug 3;10:81

[80] Zhou W, Freed CR. Adenoviral gene delivery can reprogram human fibroblasts to induced pluripotent stem cells. Stem Cells. 2009 Nov;27(11):2667-74

[81] Fusaki N, Ban H, Nishiyama A, Saeki K, Hasegawa M. Efficient induction of transgene-free human pluripotent stem cells using a vector based on Sendai virus, an RNA virus that does not integrate into the host genome. Proc Jpn Acad Ser B Phys Biol Sci. 2009;85(8):348-62

[82] Zhou H, Wu S, Joo JY, Zhu S, Han DW, Lin T, Trauger S, Bien G, Yao S, Zhu Y, Siuzdak G, Schöler HR, Duan L, Ding S. Generation of induced pluripotent stem cells using recombinant proteins. Cell Stem Cell. 2009 May 8;4(5):381-4

[83] Warren L, Manos PD, Ahfeldt T, Loh YH, Li H, Lau F, Ebina W, Mandal PK, Smith ZD, Meissner A, Daley GQ, Brack AS, Collins JJ, Cowan C, Schlaeger TM, Rossi DJ. Highly efficient reprogramming to pluripotency and directed differentiation of human cells with synthetic modified mRNA. Cell Stem Cell. 2010 Nov 5;7(5):618-30

[84] Miyoshi N, Ishii H, Nagano H, Haraguchi N, Dewi DL, Kano Y, Nishikawa S, Tanemura M, Mimori K, Tanaka F, Saito T, Nishimura J, Takemasa I, Mizushima T, Ikeda M, Yamamoto H, Sekimoto M, Doki Y, Mori M. Reprogramming of mouse and human cells to pluripotency using mature microRNAs. Cell Stem Cell. 2011 Jun 3;8(6):633-8

[85] Stadtfeld M, Maherali N, Breault DT, Hochedlinger K. Defining molecular cornerstones during fibroblast to iPS cell reprogramming in mouse. Cell Stem Cell. 2008 Mar 6;2(3):230-40

[86] Maherali N, Sridharan R, Xie W, Utikal J, Eminli S, Arnold K, Stadtfeld M, Yachechko R, Tchieu J, Jaenisch R, Plath K, Hochedlinger K. Directly reprogrammed fibroblasts show global epigenetic remodeling and widespread tissue contribution. Cell Stem Cell. 2007 Jun 7;1(1):55-70

[87] Chan EM, Ratanasirintrawoot S, Park IH, Manos PD, Loh YH, Huo H, Miller JD, Hartung O, Rho J, Ince TA, Daley GQ, Schlaeger TM. Live cell imaging distinguishes bona fide human iPS cells from partially reprogrammed cells. Nat Biotechnol. 2009 Nov;27(11):1033-7

[88] Kubo A, Shinozaki K, Shannon JM, Kouskoff V, Kennedy M, Woo S, Fehling HJ, Keller G. Development of definitive endoderm from embryonic stem cells in culture. Development. 2004 Apr;131(7):1651-62

89 D'Amour KA, Agulnick AD, Eliazer S, Kelly OG, Kroon E, Baetge EE. Efficient differentiation of human embryonic stem cells to definitive endoderm. Nat Biotechnol. 2005 Dec;23(12):1534-41

90 D'Amour KA, Bang AG, Eliazer S, Kelly OG, Agulnick AD, Smart NG, Moorman MA, Kroon E, Carpenter MK, Baetge EE. Production of pancreatic hormone-expressing endocrine cells from human embryonic stem cells. Nat Biotechnol. 2006 Nov;24(11):1392-401

91 Nostro MC, Sarangi F, Ogawa S, Holtzinger A, Corneo B, Li X, Micallef SJ, Park IH, Basford C, Wheeler MB, Daley GQ, Elefanty AG, Stanley EG, Keller G. Stage-specific signaling through TGFβ family members and WNT regulates patterning and pancreatic specification of human pluripotent stem cells. Development. 2011 Mar;138(5):861-71

92 Kunisada Y, Tsubooka-Yamazoe N, Shoji M, Hosoya M. Small molecules induce efficient differentiation into insulin-producing cells from human induced pluripotent stem cells. Stem Cell Res. 2012 Mar;8(2):274-84

93 Rezania A, Bruin JE, Arora P, Rubin A, Batushansky I, Asadi A, O'Dwyer S, Quiskamp N, Mojibian M, Albrecht T, Yang YH, Johnson JD, Kieffer TJ. Reversal of diabetes with insulin-producing cells derived in vitro from human pluripotent stem cells. Nat Biotechnol. 2014 Nov;32(11):1121-33

94 Pagliuca FW, Millman JR, Gürtler M, Segel M, Van Dervort A, Ryu JH, Peterson QP, Greiner D, Melton DA. Generation of functional human pancreatic β cells in vitro. Cell. 2014 Oct 9;159(2):428-39

95 Velazco-Cruz L, Song J, Maxwell KG, Goedegebuure MM, Augsornworawat P, Hogrebe NJ, Millman JR. Acquisition of Dynamic Function in Human Stem Cell-Derived β Cells. Stem Cell Reports. 2019 Feb 12;12(2):351-365

96 Kao DI, Lacko LA, Ding BS, Huang C, Phung K, Gu G, Rafii S, Stuhlmann H, Chen S. Endothelial cells control pancreatic cell fate at defined stages through EGFL7 signaling. Stem Cell Reports. 2015 Feb 10;4(2):181-9

97 Saber N, Bruin JE, O'Dwyer S, Schuster H, Rezania A, Kieffer TJ. Sex Differences in Maturation of Human Embryonic Stem Cell-Derived β Cells in Mice. Endocrinology. 2018 Apr 1;159(4):1827-1841

98 https://clinicaltrials.gov/ct2/show/NCT02239354

99 Veres A, Faust AL, Bushnell HL, Engquist EN, Kenty JH, Harb G, Poh YC, Sintov E, Gürtler M, Pagliuca FW, Peterson QP, Melton DA. Charting cellular identity during human in vitro β-cell differentiation. Nature. 2019 May;569(7756):368-373

100 Segerstolpe Å, Palasantza A, Eliasson P, Andersson EM, Andréasson AC, Sun X, Picelli S, Sabirsh A, Clausen M, Bjursell MK, Smith DM, Kasper M, Ämmälä C, Sandberg

R. Single-Cell Transcriptome Profiling of Human Pancreatic Islets in Health and Type 2 Diabetes. Cell Metab. 2016 Oct 11;24(4):593-607

101 Baron M, Veres A, Wolock SL, Faust AL, Gaujoux R, Vetere A, Ryu JH, Wagner BK, Shen-Orr SS, Klein AM, Melton DA, Yanai I. A Single-Cell Transcriptomic Map of the Human and Mouse Pancreas Reveals Inter- and Intra-cell Population Structure. Cell Syst. 2016 Oct 26;3(4):346-360.e4

102 Ravassard P, Hazhouz Y, Pechberty S, Bricout-Neveu E, Armanet M, Czernichow P, Scharfmann R. A genetically engineered human pancreatic β cell line exhibiting glucose-inducible insulin secretion. J Clin Invest. 2011 Sep;121(9):3589-97

103 Tsonkova VG, Sand FW, Wolf XA, Grunnet LG, Kirstine Ringgaard A, Ingvorsen C, Winkel L, Kalisz M, Dalgaard K, Bruun C, Fels JJ, Helgstrand C, Hastrup S, Öberg FK, Vernet E, Sandrini MPB, Shaw AC, Jessen C, Grønborg M, Hald J, Willenbrock H, Madsen D, Wernersson R, Hansson L, Jensen JN, Plesner A, Alanentalo T, Petersen MBK, Grapin-Botton A, Honoré C, Ahnfelt-Rønne J, Hecksher-Sørensen J, Ravassard P, Madsen OD, Rescan C, Frogne T. The EndoC-βH1 cell line is a valid model of human beta cells and applicable for screenings to identify novel drug target candidates. Mol Metab. 2018 Feb;8:144-157

104 Scharfmann R, Pechberty S, Hazhouz Y, von Bülow M, Bricout-Neveu E, Grenier-Godard M, Guez F, Rachdi L, Lohmann M, Czernichow P, Ravassard P. Development of a conditionally immortalized human pancreatic β cell line. J Clin Invest. 2014 May;124(5):2087-98

105 Benazra M, Lecomte MJ, Colace C, Müller A, Machado C, Pechberty S, Bricout-Neveu E, Grenier-Godard M, Solimena M, Scharfmann R, Czernichow P, Ravassard P. A human beta cell line with drug inducible excision of immortalizing transgenes. Mol Metab. 2015 Oct 20;4(12):916-25

106 Saarimäki-Vire J, Balboa D, Russell MA, Saarikettu J, Kinnunen M, Keskitalo S,Malhi A, Valensisi C, Andrus C, Eurola S, Grym H, Ustinov J, Wartiovaara K, Hawkins RD, Silvennoinen O, Varjosalo M, Morgan NG, Otonkoski T. An Activating STAT3 Mutation Causes Neonatal Diabetes through Premature Induction of Pancreatic Differentiation. Cell Rep. 2017 Apr 11;19(2):281-294

107 Balboa D, Saarimäki-Vire J, Borshagovski D, Survila M, Lindholm P, Galli E, Eurola S, Ustinov J, Grym H, Huopio H, Partanen J, Wartiovaara K, Otonkoski T. Insulin mutations impair beta-cell development in a patient-derived iPSC model of neonatal diabetes. Elife. 2018 Nov 9;7. pii: e38519

108 Zeng H, Guo M, Zhou T, Tan L, Chong CN, Zhang T, Dong X, Xiang JZ, Yu AS, Yue L, Qi Q, Evans T, Graumann J, Chen S. An Isogenic Human ESC Platform for Functional

Evaluation of Genome-wide-Association-Study-Identified Diabetes Genes and Drug Discovery. Cell Stem Cell. 2016 Sep 1;19(3):326-40.

109 Booth GL, Kapral MK, Fung K, Tu JV. Relation between age and cardiovascular disease in men and women with diabetes compared with non-diabetic people: a population-based retrospective cohort study. Lancet. 2006 Jul 1;368(9529):29-36

110 Emerging Risk Factors Collaboration, Sarwar N, Gao P, Seshasai SR, Gobin R, Kaptoge S, Di Angelantonio E, Ingelsson E, Lawlor DA, Selvin E, Stampfer M, Stehouwer CD, Lewington S, Pennells L, Thompson A, Sattar N, White IR, Ray KK, Danesh J. Diabetes mellitus, fasting blood glucose concentration, and risk of vascular disease: a collaborative meta-analysis of 102 prospective studies. Lancet. 2010 Jun 26;375(9733):2215-22

111 Beckman JA, Paneni F, Cosentino F, Creager MA. Diabetes and vascular disease: pathophysiology, clinical consequences, and medical therapy: part II. Eur Heart J. 2013 Aug;34(31):2444-52

112 Einarson TR, Acs A, Ludwig C, Panton UH. Prevalence of cardiovascular disease in type 2 diabetes: a systematic literature review of scientific evidence from across the world in 2007-2017. Cardiovasc Diabetol. 2018 Jun 8;17(1):83

113 Piepoli MF, Hoes AW, Agewall S, Albus C, Brotons C, Catapano AL, Cooney MT, Corrà U, Cosyns B, Deaton C, Graham I, Hall MS, Hobbs FDR, Løchen ML, Löllgen H, Marques-Vidal P, Perk J, Prescott E, Redon J, Richter DJ, Sattar N, Smulders Y, Tiberi M, van der Worp HB, van Dis I, Verschuren WMM, Binno S; ESC Scientific Document Group. 2016 European Guidelines on cardiovascular disease prevention in clinical practice: The Sixth Joint Task Force of the European Society of Cardiology and Other Societies on Cardiovascular Disease Prevention in Clinical Practice (constituted by representatives of 10 societies and by invited experts) Developed with the special contribution of the European Association for Cardiovascular Prevention & Rehabilitation (EACPR). Eur Heart J. 2016 Aug 1;37(29):2315-2381

114 Mentzer SJ, Burakoff SJ, Faller DV. Adhesion of T lymphocytes to human endothelial cells is regulated by the LFA-1 membrane molecule. J Cell Physiol. 1986 Feb;126(2):285-90

115 Swirski FK, Libby P, Aikawa E, Alcaide P, Luscinskas FW, Weissleder R, Pittet MJ. Ly-6Chi monocytes dominate hypercholesterolemia-associated monocytosis and give rise to macrophages in atheromata. J Clin Invest. 2007 Jan;117(1):195-205

116 Ross R. Atherosclerosis--an inflammatory disease. N Engl J Med. 1999 Jan 14;340(2):115-26

117 Guidance for industry diabetes mellitus—evaluating cardiovascular risk in new antidiabetic therapies to treat type 2 diabetes, FDA, Editor. 2008.

118 Scirica BM, Bhatt DL, Braunwald E, Steg PG, Davidson J, Hirshberg B, Ohman P, Frederich R, Wiviott SD, Hoffman EB, Cavender MA, Udell JA, Desai NR, Mosenzon O, McGuire DK, Ray KK, Leiter LA, Raz I; SAVOR-TIMI 53 Steering Committee and Investigators. Saxagliptin and cardiovascular outcomes in patients with type 2 diabetes mellitus. N Engl J Med. 2013 Oct 3;369(14):1317-26

119 White WB, Bakris GL, Bergenstal RM, Cannon CP, Cushman WC, Fleck P, Heller S, Mehta C, Nissen SE, Perez A, Wilson C, Zannad F. EXamination of cArdiovascular outcoMes with alogliptIN versus standard of carE in patients with type 2 diabetes mellitus and acute coronary syndrome (EXAMINE): a cardiovascular safety study of the dipeptidyl peptidase 4 inhibitor alogliptin in patients with type 2 diabetes with acute coronary syndrome. Am Heart J. 2011 Oct;162(4):620-626.e1

120 Green JB, Bethel MA, Armstrong PW, Buse JB, Engel SS, Garg J, Josse R, Kaufman KD, Koglin J, Korn S, Lachin JM, McGuire DK, Pencina MJ, Standl E, Stein PP, Suryawanshi S, Van de Werf F, Peterson ED, Holman RR; TECOS Study Group. Effect of Sitagliptin on Cardiovascular Outcomes in Type 2 Diabetes. N Engl J Med. 2015 Jul 16;373(3):232-42

121 Pfeffer MA, Claggett B, Diaz R, Dickstein K, Gerstein HC, Køber LV, Lawson FC, Ping L, Wei X, Lewis EF, Maggioni AP, McMurray JJ, Probstfield JL, Riddle MC, Solomon SD, Tardif JC; ELIXA Investigators. Lixisenatide in Patients with Type 2 Diabetes and Acute Coronary Syndrome. N Engl J Med. 2015 Dec 3;373(23):2247-57

122 Marso SP, Daniels GH, Brown-Frandsen K, Kristensen P, Mann JF, Nauck MA, Nissen SE, Pocock S, Poulter NR, Ravn LS, Steinberg WM, Stockner M, Zinman B, Bergenstal RM, Buse JB; LEADER Steering Committee; LEADER Trial Investigators. Liraglutide and Cardiovascular Outcomes in Type 2 Diabetes. N Engl J Med. 2016 Jul 28;375(4):311-22

123 Marso SP, Bain SC, Consoli A, Eliaschewitz FG, Jódar E, Leiter LA, Lingvay I, Rosenstock J, Seufert J, Warren ML, Woo V, Hansen O, Holst AG, Pettersson J, Vilsbøll T; SUSTAIN-6 Investigators. Semaglutide and Cardiovascular Outcomes in Patients with Type 2 Diabetes. N Engl J Med. 2016 Nov 10;375(19):1834-1844

124 Holman RR, Bethel MA, Mentz RJ, Thompson VP, Lokhnygina Y, Buse JB, Chan JC, Choi J, Gustavson SM, Iqbal N, Maggioni AP, Marso SP, Öhman P, Pagidipati NJ, Poulter N, Ramachandran A, Zinman B, Hernandez AF; EXSCEL Study Group. Effects of Once-Weekly Exenatide on Cardiovascular Outcomes in Type 2 Diabetes. N Engl J Med. 2017 Sep 28;377(13):1228-1239

125 Hernandez AF, Green JB, Janmohamed S, D'Agostino RB Sr, Granger CB, Jones NP, Leiter LA, Rosenberg AE, Sigmon KN, Somerville MC, Thorpe KM, McMurray JJV, Del Prato S; Harmony Outcomes committees and investigators. Albiglutide and cardiovascular outcomes in patients with type 2 diabetes and cardiovascular disease (Harmony Outcomes): a double-blind, randomised placebo-controlled trial. Lancet. 2018 Oct 27;392(10157):1519-1529

126 Gerstein HC, Colhoun HM, Dagenais GR, Diaz R, Lakshmanan M, Pais P, Probstfield J, Riesmeyer JS, Riddle MC, Rydén L, Xavier D, Atisso CM, Dyal L, Hall S, Rao-Melacini P, Wong G, Avezum A, Basile J, Chung N, Conget I, Cushman WC, Franek E, Hancu N, Hanefeld M, Holt S, Jansky P, Keltai M, Lanas F, Leiter LA, Lopez-Jaramillo P, Cardona Munoz EG, Pirags V, Pogosova N, Raubenheimer PJ, Shaw JE, Sheu WH, Temelkova-Kurktschiev T; REWIND Investigators. Dulaglutide and cardiovascular outcomes in type 2 diabetes (REWIND): a double-blind, randomized placebo-controlled trial. Lancet. 2019 Jul 13;394(10193):121-130

127 Husain M, Birkenfeld AL, Donsmark M, Dungan K, Eliaschewitz FG, Franco DR, Jeppesen OK, Lingvay I, Mosenzon O, Pedersen SD, Tack CJ, Thomsen M, Vilsbøll T, Warren ML, Bain SC; PIONEER 6 Investigators. Oral Semaglutide and Cardiovascular Outcomes in Patients with Type 2 Diabetes. N Engl J Med. 2019 Aug 29;381(9):841-851

128 Zinman B, Wanner C, Lachin JM, Fitchett D, Bluhmki E, Hantel S, Mattheus M, Devins T, Johansen OE, Woerle HJ, Broedl UC, Inzucchi SE; EMPA-REG OUTCOME Investigators. Empagliflozin, Cardiovascular Outcomes, and Mortality in Type 2 Diabetes. N Engl J Med. 2015 Nov 26;373(22):2117-28

129 Neal B, Perkovic V, Mahaffey KW, de Zeeuw D, Fulcher G, Erondu N, Shaw W, Law G, Desai M, Matthews DR; CANVAS Program Collaborative Group. Canagliflozin and Cardiovascular and Renal Events in Type 2 Diabetes. N Engl J Med. 2017 Aug 17;377(7):644-657

130 Wiviott SD, Raz I, Bonaca MP, Mosenzon O, Kato ET, Cahn A, Silverman MG, Zelniker TA, Kuder JF, Murphy SA, Bhatt DL, Leiter LA, McGuire DK, Wilding JPH, Ruff CT, Gause-Nilsson IAM, Fredriksson M, Johansson PA, Langkilde AM, Sabatine MS; DECLARE–TIMI 58 Investigators. Dapagliflozin and Cardiovascular Outcomes in Type 2 Diabetes. N Engl J Med. 2019 Jan 24;380(4):347-357

131 ORIGIN Trial Investigators, Gerstein HC, Bosch J, Dagenais GR, Díaz R, Jung H, Maggioni AP, Pogue J, Probstfield J, Ramachandran A, Riddle MC, Rydén LE, Yusuf S. Basal insulin and cardiovascular and other outcomes in dysglycemia. N Engl J Med. 2012 Jul 26;367(4):319-28

132 Marso SP, McGuire DK, Zinman B, Poulter NR, Emerson SS, Pieber TR, Pratley RE, Haahr PM, Lange M, Brown-Frandsen K, Moses A, Skibsted S, Kvist K, Buse JB; DEVOTE Study Group. Efficacy and Safety of Degludec versus Glargine in Type 2 Diabetes. N Engl J Med. 2017 Aug 24;377(8):723-732

133 Sabatine MS, Giugliano RP, Keech AC, Honarpour N, Wiviott SD, Murphy SA, Kuder JF, Wang H, Liu T, Wasserman SM, Sever PS, Pedersen TR; FOURIER Steering Committee and Investigators. Evolocumab and Clinical Outcomes in Patients with Cardiovascular Disease. N Engl J Med. 2017 May 4;376(18):1713-1722

134 Schwartz GG, Steg PG, Szarek M, Bhatt DL, Bittner VA, Diaz R, Edelberg JM, Goodman SG, Hanotin C, Harrington RA, Jukema JW, Lecorps G, Mahaffey KW, Moryusef A, Pordy R, Quintero K, Roe MT, Sasiela WJ, Tamby JF, Tricoci P, White HD, Zeiher AM; ODYSSEY OUTCOMES Committees and Investigators. Alirocumab and Cardiovascular Outcomes after Acute Coronary Syndrome. N Engl J Med. 2018 Nov 29;379(22):2097-2107

135 Deacon CF, Pridal L, Klarskov L, Olesen M, Holst JJ. Glucagon-like peptide 1 undergoes differential tissue-specific metabolism in the anesthetized pig. Am J Physiol. 1996 Sep;271(3 Pt 1):E458-64

136 Deacon CF, Nauck MA, Meier J, Hücking K, Holst JJ. Degradation of endogenous and exogenous gastric inhibitory polypeptide in healthy and in type 2 diabetic subjects as revealed using a new assay for the intact peptide. J Clin Endocrinol Metab. 2000 Oct;85(10):3575-81

137 Drucker DJ, Philippe J, Mojsov S, Chick WL, Habener JF. Glucagon-like peptide I stimulates insulin gene expression and increases cyclic AMP levels in a rat islet cell line. Proc Natl Acad Sci U S A. 1987 May;84(10):3434-8

138 Widenmaier SB, Kim SJ, Yang GK, De Los Reyes T, Nian C, Asadi A, Seino Y, Kieffer TJ, Kwok YN, McIntosh CH. A GIP receptor agonist exhibits beta-cell anti-apoptotic actions in rat models of diabetes resulting in improved beta-cell function and glycemic control. PLoS One. 2010 Mar 9;5(3):e9590

139 Yusta B, Baggio LL, Estall JL, Koehler JA, Holland DP, Li H, Pipeleers D, Ling Z, Drucker DJ. GLP-1 receptor activation improves beta cell function and survival following induction of endoplasmic reticulum stress. Cell Metab. 2006 Nov;4(5):391-40

140 Marre M, Shaw J, Brändle M, Bebakar WM, Kamaruddin NA, Strand J, Zdravkovic M, Le Thi TD, Colagiuri S; LEAD-1 SU study group. Liraglutide, a once-daily human GLP-1 analogue, added to a sulphonylurea over 26 weeks produces greater improvements in glycaemic and weight control compared with adding rosiglitazone or placebo in subjects with Type 2 diabetes (LEAD-1 SU). Diabet Med. 2009 Mar;26(3):268-78

141 Baggio LL, Drucker DJ. Biology of incretins: GLP-1 and GIP. Gastroenterology. 2007 May;132(6):2131-57

142 Vilsbøll T, Krarup T, Deacon CF, Madsbad S, Holst JJ. Reduced postprandial concentrations of intact biologically active glucagon-like peptide 1 in type 2 diabetic patients. Diabetes. 2001 Mar;50(3):609-13

143 Lund A, Knop FK, Vilsbøll T. Glucagon-like peptide-1 receptor agonists for the treatment of type 2 diabetes: differences and similarities. Eur J Intern Med. 2014 Jun;25(5):407-14

144 Kristensen SL, Rørth R, Jhund PS, Docherty KF, Sattar N, Preiss D, Køber L, Petrie MC, McMurray JJV. Cardiovascular, mortality, and kidney outcomes with GLP-1 receptor agonists in patients with type 2 diabetes: a systematic review and meta-analysis of cardiovascular outcome trials. Lancet Diabetes Endocrinol. 2019 Oct;7(10):776-785

145 Ban K, Noyan-Ashraf MH, Hoefer J, Bolz SS, Drucker DJ, Husain M. Cardioprotective and vasodilatory actions of glucagon-like peptide 1 receptor are mediated through both glucagon-like peptide 1 receptor-dependent and -independent pathways. Circulation. 2008 May 6;117(18):2340-50

146 Krasner NM, Ido Y, Ruderman NB, Cacicedo JM. Glucagon-like peptide-1 (GLP-1) analog liraglutide inhibits endothelial cell inflammation through a calcium and AMPK dependent mechanism. PLoS One. 2014 May 16;9(5):e97554

147 Burgmaier M, Liberman A, Möllmann J, Kahles F, Reith S, Lebherz C, Marx N, Lehrke M. Glucagon-like peptide-1 (GLP-1) and its split products GLP-1(9-37) and GLP-1(28-37) stabilize atherosclerotic lesions in apoe$^{-/-}$ mice. Atherosclerosis. 2013 Dec;231(2):427-35

148 Zelniker TA, Wiviott SD, Raz I, Im K, Goodrich EL, Bonaca MP, Mosenzon O, Kato ET, Cahn A, Furtado RHM, Bhatt DL, Leiter LA, McGuire DK, Wilding JPH, Sabatine MS. SGLT2 inhibitors for primary and secondary prevention of cardiovascular and renal outcomes in type 2 diabetes: a systematic review and meta-analysis of cardiovascular outcome trials. Lancet. 2019 Jan 5;393(10166):31-39

149 Chilton R, Tikkanen I, Cannon CP, Crowe S, Woerle HJ, Broedl UC, Johansen OE. Effects of empagliflozin on blood pressure and markers of arterial stiffness and vascular resistance in patients with type 2 diabetes. Diabetes Obes Metab. 2015 Dec;17(12):1180-93

150 Striepe K, Jumar A, Ott C, Karg MV, Schneider MP, Kannenkeril D, Schmieder RE. Effects of the Selective Sodium-Glucose Cotransporter 2 Inhibitor Empagliflozin on Vascular Function and Central Hemodynamics in Patients With Type 2 Diabetes Mellitus. Circulation. 2017 Sep 19;136(12):1167-1169

151 Solini A, Giannini L, Seghieri M, Vitolo E, Taddei S, Ghiadoni L, Bruno RM. Dapagliflozin acutely improves endothelial dysfunction, reduces aortic stiffness and renal resistive index in type 2 diabetic patients: a pilot study. Cardiovasc Diabetol. 2017 Oct 23;16(1):138

152 Ferrannini E, Mark M, Mayoux E. CV Protection in the EMPA-REG OUTCOME Trial: A "Thrifty Substrate" Hypothesis. Diabetes Care. 2016 Jul;39(7):1108-14

153 Devenny JJ, Godonis HE, Harvey SJ, Rooney S, Cullen MJ, Pelleymounter MA. Weight loss induced by chronic dapagliflozin treatment is attenuated by compensatory hyperphagia in diet-induced obese (DIO) rats. Obesity (Silver Spring). 2012 Aug;20(8):1645-52

154 Mudaliar S, Alloju S, Henry RR. Can a Shift in Fuel Energetics Explain the Beneficial Cardiorenal Outcomes in the EMPA-REG OUTCOME Study? A Unifying Hypothesis. Diabetes Care. 2016 Jul;39(7):1115-22

155 Shimazu T, Hirschey MD, Newman J, He W, Shirakawa K, Le Moan N, Grueter CA, Lim H, Saunders LR, Stevens RD, Newgard CB, Farese RV Jr, de Cabo R, Ulrich S, Akassoglou K, Verdin E. Suppression of oxidative stress by β-hydroxybutyrate, an endogenous histone deacetylase inhibitor. Science. 2013 Jan 11;339(6116):211-4

156 Kappel BA, Lehrke M, Schütt K, Artati A, Adamski J, Lebherz C, Marx N. Effect of Empagliflozin on the Metabolic Signature of Patients With Type 2 Diabetes Mellitus and Cardiovascular Disease. Circulation. 2017 Sep 5;136(10):969-972

157 Lee TM, Chang NC, Lin SZ. Dapagliflozin, a selective SGLT2 Inhibitor, attenuated cardiac fibrosis by regulating the macrophage polarization via STAT3 signaling in infarcted rat hearts. Free Radic Biol Med. 2017 Mar;104:298-310

158 Januzzi JL Jr, Butler J, Jarolim P, Sattar N, Vijapurkar U, Desai M, Davies MJ. Effects of Canagliflozin on Cardiovascular Biomarkers in Older Adults With Type 2 Diabetes. J Am Coll Cardiol. 2017 Aug 8;70(6):704-712

159 Garvey WT, Van Gaal L, Leiter LA, Vijapurkar U, List J, Cuddihy R, Ren J, Davies MJ. Effects of canagliflozin versus glimepiride on adipokines and inflammatory biomarkers in type 2 diabetes. Metabolism. 2018 Aug;85:32-37

160 Packer M. Do sodium-glucose co-transporter-2 inhibitors prevent heart failure with a preserved ejection fraction by counterbalancing the effects of leptin? A novel hypothesis. Diabetes Obes Metab. 2018 Jun;20(6):1361-1366

161 Uthman L, Baartscheer A, Bleijlevens B, Schumacher CA, Fiolet JWT, Koeman A, Jancev M, Hollmann MW, Weber NC, Coronel R, Zuurbier CJ. Class effects of SGLT2 inhibitors in mouse cardiomyocytes and hearts: inhibition of Na(+)/H(+) exchanger, lowering of cytosolic Na(+) and vasodilation. Diabetologia. 2018 Mar;61(3):722-726

[162] Baartscheer A, Schumacher CA, Wüst RC, Fiolet JW, Stienen GJ, Coronel R, Zuurbier CJ. Empagliflozin decreases myocardial cytoplasmic Na(+) through inhibition of the cardiac Na(+)/H(+) exchanger in rats and rabbits. Diabetologia. 2017 Mar;60(3):568-573

[163] Asahara T, Murohara T, Sullivan A, Silver M, van der Zee R, Li T, Witzenbichler B, Schatteman G, Isner JM. Isolation of putative progenitor endothelial cells for angiogenesis. Science. 1997 Feb 14;275(5302):964-7

[164] Gill M, Dias S, Hattori K, Rivera ML, Hicklin D, Witte L, Girardi L, Yurt R, Himel H, Rafii S. Vascular trauma induces rapid but transient mobilization of VEGFR2(+)AC133(+) endothelial precursor cells. Circ Res. 2001 Feb 2;88(2):167-74

[165] Odent Grigorescu G, Rosca AM, Preda MB, Tutuianu R, Simionescu M, Burlacu A. Synergic effects of VEGF-A and SDF-1 on the angiogenic properties of endothelial progenitor cells. J Tissue Eng Regen Med. 2017 Nov;11(11):3241-3252

[166] Ceradini DJ, Kulkarni AR, Callaghan MJ, Tepper OM, Bastidas N, Kleinman ME, Capla JM, Galiano RD, Levine JP, Gurtner GC. Progenitor cell trafficking is regulated by hypoxic gradients through HIF-1 induction of SDF-1. Nat Med. 2004 Aug;10(8):858-6

[167] Urbich C, Dimmeler S. Endothelial progenitor cells: characterization and role in vascular biology. Circ Res. 2004 Aug 20;95(4):343-53

[168] Medina RJ, Barber CL, Sabatier F, Dignat-George F, Melero-Martin JM, Khosrotehrani K, Ohneda O, Randi AM, Chan JKY, Yamaguchi T, Van Hinsbergh VWM, Yoder MC, Stitt AW. Endothelial Progenitors: A Consensus Statement on Nomenclature. Stem Cells Transl Med. 2017 May;6(5):1316-1320

[169] Critser PJ, Yoder MC. Endothelial colony-forming cell role in neoangiogenesis and tissue repair. Curr Opin Organ Transplant. 2010 Feb;15(1):68-72

[170] Medina RJ, O'Neill CL, Sweeney M, Guduric-Fuchs J, Gardiner TA, Simpson DA, Stitt AW. Molecular analysis of endothelial progenitor cell (EPC) subtypes reveals two distinct cell populations with different identities. BMC Med Genomics. 2010 May 13;3:18

[171] Tasev D, Koolwijk P, van Hinsbergh VW. Therapeutic Potential of Human-Derived Endothelial Colony-Forming Cells in Animal Models. Tissue Eng Part B Rev. 2016 Oct;22(5):371-382

[172] Prater DN, Case J, Ingram DA, Yoder MC. Working hypothesis to redefine endothelial progenitor cells. Leukemia. 2007 Jun;21(6):1141-9

[173] Spigoni V, Picconi A, Cito M, Ridolfi V, Bonomini S, Casali C, Zavaroni I, Gnudi L, Metra M, Dei Cas A. Pioglitazone improves in vitro viability and function of endothelial progenitor cells from individuals with impaired glucose tolerance. PLoS One. 2012;7(11):e48283

174 Medina RJ, O'Neill CL, O'Doherty TM, Knott H, Guduric-Fuchs J, Gardiner TA, Stitt AW. Myeloid angiogenic cells act as alternative M2 macrophages and modulate angiogenesis through interleukin-8. Mol Med. 2011 Sep-Oct;17(9-10):1045-55

175 Aragona CO, Imbalzano E, Mamone F, Cairo V, Lo Gullo A, D'Ascola A, Sardo MA, Scuruchi M, Basile G1, Saitta A, Mandraffino G. Endothelial Progenitor Cells for Diagnosis and Prognosis in Cardiovascular Disease. Stem Cells Int. 2016; 2016:8043792.

176 Zeoli A, Dentelli P, Brizzi MF. Endothelial progenitor cells and their potential clinical implication in cardiovascular disorders. J Endocrinol Invest. 2009; 32(4):370-82.

177 Schmidt-Lucke C, Rössig L, Fichtlscherer S, Vasa M, Britten M, Kämper U, Dimmeler S, Zeiher AM. Reduced number of circulating endothelial progenitor cells predicts future cardiovascular events: proof of concept for the clinical importance of endogenous vascular repair. Circulation. 2005 Jun 7;111(22):2981-7. Epub 2005 May 31.

178 Rigato M, Avogaro A, Fadini GP. Levels of Circulating Progenitor Cells, Cardiovascular Outcomes and Death: A Meta-Analysis of Prospective Observational Studies. Circ Res. 2016 Jun 10;118(12):1930-9.

179 Di Stefano R, Barsotti MC, Felice F, Magera A, Lekakis J, Leone A, Balbarini A. Smoking and endothelial progenitor cells: a revision of literature. Current Pharmaceutical Design. 2010;16:2559 –2566

180 Ludwig A, Jochmann N, Kertesz A, Kuhn C, Mueller S, Gericke C, Baumann G, Stangl K, Stangl V. Smoking decreases the level of circulating CD34+ progenitor cells in young healthy women–a pilot study. BMC Womens Health. 2010;10:200

181 Pirro M, Schillaci G, Menecali C, Bagaglia F, Paltriccia R, Vaudo G, Mannarino MR, Mannarino E. Reduced number of circulating endothelial progenitors and hoxa9 expression in CD34+ cells of hypertensive patients. Journal of Hypertension. 2007;25:2093–2099

182 Chen JZ, Zhang FR, Tao QM, Wang XX, Zhu JH. Number and activity of endothelial progenitor cells from peripheral blood in patients with hypercholesterolaemia. Clinical Science (London). 2004;107:273–280.

183 Tobler K, Freudenthaler A, Baumgartner-Parzer SM, Wolzt M, Ludvik B, Nansalmaa E, Nowotny PJ, Seidinger D, Steiner S, Luger A, Artwohl M. Reduction of both number and proliferative activity of human endothelial progenitor cells in obesity. International Journal of Obesity (London). 2010;34:687–700

184 Egan CG, Lavery R, Caporali F, Fondelli C, Laghi-Pasini F, Dotta F, Sorrentino V. Generalised reduction of putative endothelial progenitors and CXCR4-positive peripheral blood cells in type 2 diabetes. Diabetologia. 2008; 51:1296– 1305.

185 Fadini GP, Agostini C, Boscaro E, Avogaro A. Mechanisms and significance of progenitor cell reduction in the metabolic syndrome. Metabolic Syndrome and Related Disorders. 2009;7:5–10

186 Yiu KH, Tse HF. Specific role of impaired glucose metabolism and diabetes mellitus in endothelial progenitor cell characteristics and function. Arterioscler Thromb Vasc Biol. 2014 Jun;34(6):1136-43

187 Hamed S, Brenner B, Abassi Z, Aharon A, Daoud D, Roguin A. Hyperglycemia and oxidized-LDL exert a deleterious effect on endothelial progenitor cell migration in type 2 diabetes mellitus. Thromb Res. 2010 Sep;126(3):166-74

188 Chambers SEJ, O'Neill CL, Guduric-Fuchs J, McLoughlin KJ, Liew A, Egan AM, O'Brien T, Stitt AW, Medina RJ. The Vasoreparative Function of Myeloid Angiogenic Cells Is Impaired in Diabetes Through the Induction of IL1β. Stem Cells. 2018 Jun;36(6):834-843

189 Wei H, Yang M, Yu K, Dong W, Liang W, Wang Z, Jiang R, Zhang J. Atorvastatin Protects Against Cerebral Aneurysmal Degenerative Pathology by Promoting Endothelial Progenitor Cells (EPC) Mobilization and Attenuating Vascular Deterioration in a Rat Model. Med Sci Monit. 2019 Feb 2;25:928-936

190 Chen J, Xiao X, Chen S, Zhang C, Chen J, Yi D, Shenoy V, Raizada MK, Zhao B, Chen Y. Angiotensin-converting enzyme 2 priming enhances the function of endothelial progenitor cells and their therapeutic efficacy. Hypertension. 2013 Mar;61(3):681-9

191 Zhuge Y, Regueiro MM, Tian R, Li Y, Xia X, Vazquez-Padron R, Elliot S, Thaller SR, Liu ZJ, Velazquez OC. The effect of estrogen on diabetic wound healing is mediated through increasing the function of various bone marrow-derived progenitor cells. J Vasc Surg. 2018 Dec;68(6S):127S-135S

192 Asadian S, Alibabrdel M, Daei N, Cheraghi H, Maedeh Jafari S, Noshadirad E, Jabarpour M, Siavashi V, Nassiri SM. Improved angiogenic activity of endothelial progenitor cell in diabetic patients treated with insulin plus metformin. J Cell Biochem. 2018 Oct 30. doi: 10.1002/jcb.27985

193 Dei Cas A, Spigoni V, Cito M, Aldigeri R, Ridolfi V, Marchesi E, Marina M, Derlindati E, Aloe R, Bonadonna RC, Zavaroni I. Vildagliptin, but not glibenclamide, increases circulating endothelial progenitor cell number: a 12-month randomized controlled trial in patients with type 2 diabetes. Cardiovasc Diabetol. 2017 Feb 23;16(1):27

194 Bonora BM, Cappellari R, Albiero M, Avogaro A, Fadini GP. Effects of SGLT2 Inhibitors on Circulating Stem and Progenitor Cells in Patients with Type 2 Diabetes. J Clin Endocrinol Metab. 2018 Oct 1;103(10):3773-3782

195 DeFronzo RA. Insulin resistance, lipotoxicity, type 2 diabetes and atherosclerosis: the missing links. The Claude Bernard Lecture 2009. Diabetologia. 2010 Jul;53(7):1270-87. doi: 10.1007/s00125-010-1684-1

196 Virtue S, Vidal-Puig A. Adipose tissue expandability, lipotoxicity and the Metabolic Syndrome--an allostatic perspective. Biochim Biophys Acta. 2010 Mar;1801(3):338-49

197 Wellen KE, Hotamisligil GS. Obesity-induced inflammatory changes in adipose tissue. J Clin Invest. 2003 Dec;112(12):1785-8

198 Uysal KT, Wiesbrock SM, Marino MW, Hotamisligil GS. Protection from obesity-induced insulin resistance in mice lacking TNF-alpha function. Nature. 1997 Oct 9;389(6651):610-4

199 Burnett MS, Lee CW, Kinnaird TD, Stabile E, Durrani S, Dullum MK, Devaney JM, Fishman C, Stamou S, Canos D, Zbinden S, Clavijo LC, Jang GJ, Andrews JA, Zhu J, Epstein SE. The potential role of resistin in atherogenesis. Atherosclerosis. 2005 Oct;182(2):241-8

200 Mauer J, Chaurasia B, Goldau J, Vogt MC, Ruud J, Nguyen KD, Theurich S, Hausen AC, Schmitz J, Brönneke HS, Estevez E, Allen TL, Mesaros A, Partridge L, Febbraio MA, Chawla A, Wunderlich FT, Brüning JC. Signaling by IL-6 promotes alternative activation of macrophages to limit endotoxemia and obesity-associated resistance to insulin. Nat Immunol. 2014 May;15(5):423-30

201 Kawahito H, Yamada H, Irie D, Kato T, Akakabe Y, Kishida S, Takata H, Wakana N, Ogata T, Ikeda K, Ueyama T, Matoba S, Mori Y, Matsubara H. Periaortic adipose tissue-specific activation of the renin-angiotensin system contributes to atherosclerosis development in uninephrectomized apoE-/- mice. Am J Physiol Heart Circ Physiol. 2013 Sep 1;305(5):H667-75

202 Van de Voorde J, Pauwels B, Boydens C, Decaluwé K. Adipocytokines in relation to cardiovascular disease. Metabolism. 2013 Nov;62(11):1513-21

203 Torre-Villalvazo I, Bunt AE, Alemán G, Marquez-Mota CC, Diaz-Villaseñor A, Noriega LG, Estrada I, Figueroa-Juárez E, Tovar-Palacio C, Rodriguez-López LA, López-Romero P, Torres N, Tovar AR. Adiponectin synthesis and secretion by subcutaneous adipose tissue is impaired during obesity by endoplasmic reticulum stress. J Cell Biochem. 2018 Jul;119(7):5970-5984

204 Hotamisligil GS. Inflammation, metaflammation and immunometabolic disorders. Nature. 2017 Feb 8;542(7640):177-185

205 Koves TR, Ussher JR, Noland RC, Slentz D, Mosedale M, Ilkayeva O, Bain J, Stevens R, Dyck JR, Newgard CB, Lopaschuk GD, Muoio DM. Mitochondrial overload and

incomplete fatty acid oxidation contribute to skeletal muscle insulin resistance. Cell Metab. 2008 Jan;7(1):45-56

206 Donnelly KL, Smith CI, Schwarzenberg SJ, Jessurun J, Boldt MD, Parks EJ. Sources of fatty acids stored in liver and secreted via lipoproteins in patients with nonalcoholic fatty liver disease. J Clin Invest. 2005 May;115(5):1343-51

207 Drosatos K, Schulze PC. Cardiac lipotoxicity: molecular pathways and therapeutic implications. Curr Heart Fail Rep. 2013 Jun;10(2):109-21

208 Pilz S, Scharnagl H, Tiran B, Seelhorst U, Wellnitz B, Boehm BO, Schaefer R, Marz W. Free fatty acids are independently associated with all-cause and cardiovascular mortality in subjects with coronary artery disease. J Clin Endocrinol Metab. 2006; 91: 2542-2547

209 Choy JC, Granville DJ, Hunt DWC, Manus BM. Endothelial cell apoptosis: biochemical characteristics and potential implications for atherosclerosis. J Mol Cell Cardiol. 2001; 33: 1673-1690

210 Forouhi NG, Koulman A, Sharp SJ, Imamura F, Kröger J, Schulze MB, Crowe FL, Huerta JM, Guevara M, Beulens JW, van Woudenbergh GJ, Wang L, Summerhill K, Griffin JL, Feskens EJ, Amiano P, Boeing H, Clavel-Chapelon F, Dartois L, Fagherazzi G, Franks PW, Gonzalez C, Jakobsen MU, Kaaks R, Key TJ, Khaw KT, Kühn T, Mattiello A, Nilsson PM, Overvad K, Pala V, Palli D, Quirós JR, Rolandsson O, Roswall N, Sacerdote C, Sánchez MJ, Slimani N, Spijkerman AM, Tjonneland A, Tormo MJ, Tumino R, van der A DL, van der Schouw YT, Langenberg C, Riboli E, Wareham NJ. Differences in the prospective association between individual plasma phospholipid saturated fatty acids and incident type 2 diabetes: the EPIC-InterAct case-cohort study. Lancet Diabetes Endocrinol. 2014 Oct;2(10):810-8

211 Hudgins LC, Hellerstein M, Seidman C, Neese R, Diakun J, Hirsch J. Human fatty acid synthesis is stimulated by a eucaloric low fat, high carbohydrate diet. J Clin Invest. 1996 May 1;97(9):2081-91

212 Siler SQ, Neese RA, Hellerstein MK. De novo lipogenesis, lipid kinetics, and whole-body lipid balances in humans after acute alcohol consumption. Am J Clin Nutr. 1999 Nov;70(5):928-36

213 Kahn SE, Hull RL, Utzschneider KM. Mechanisms linking obesity to insulin resistance and type 2 diabetes. Nature. 2006 Dec 14;444(7121):840-6

214 Wong SW, Kwon MJ, Choi AM, Kim HP, Nakahira K, Hwang DH. Fatty acids modulate Toll-like receptor 4 activation through regulation of receptor dimerization andrecruitment into lipid rafts in a reactive oxygen species-dependent manner. J Biol Chem. 2009 Oct 2;284(40):27384-92

215 Wen H, Gris D, Lei Y, Jha S, Zhang L, Huang MT, Brickey WJ, Ting JP. Fatty acid-induced NLRP3-ASC inflammasome activation interferes with insulin signaling. Nat Immunol. 2011 May;12(5):408-15

216 Jager J, Grémeaux T, Cormont M, Le Marchand-Brustel Y, Tanti JF. Interleukin-1beta-induced insulin resistance in adipocytes through down-regulation of insulin receptor substrate-1 expression. Endocrinology. 2007 Jan;148(1):241-51

217 Gao D, Madi M, Ding C, Fok M, Steele T, Ford C, Hunter L, Bing C. Interleukin-1β mediates macrophage-induced impairment of insulin signaling in human primary adipocytes. Am J Physiol Endocrinol Metab. 2014 Aug 1;307(3):E289-304

218 Li Y, Soos TJ, Li X, Wu J, Degennaro M, Sun X, Littman DR, Birnbaum MJ, Polakiewicz RD. Protein kinase C Theta inhibits insulin signaling by phosphorylating IRS1 at Ser(1101). J Biol Chem. 2004 Oct 29;279(44):45304-7

219 Kumashiro N, Erion DM, Zhang D, Kahn M, Beddow SA, Chu X, Still CD, Gerhard GS, Han X, Dziura J, Petersen KF, Samuel VT, Shulman GI. Cellular mechanism of insulin resistance in nonalcoholic fatty liver disease. Proc Natl Acad Sci U S A. 2011 Sep 27;108(39):16381-5

220 Samuel VT, Petersen KF, Shulman GI. Lipid-induced insulin resistance: unravelling the mechanism. Lancet. 2010 Jun 26;375(9733):2267-77.

221 Holland WL, Bikman BT, Wang LP, Yuguang G, Sargent KM, Bulchand S, Knotts TA, Shui G, Clegg DJ, Wenk MR, Pagliassotti MJ, Scherer PE, Summers SA. Lipid-induced insulin resistance mediated by the proinflammatory receptor TLR4 requires saturated fatty acid-induced ceramide biosynthesis in mice. J Clin Invest. 2011 May;121(5):1858-70

222 Stratford S, Hoehn KL, Liu F, Summers SA. Regulation of insulin action by ceramide: dual mechanisms linking ceramide accumulation to the inhibition of Akt/protein kinase B. J Biol Chem. 2004 Aug 27;279(35):36608-15

223 Kawasaki N, Asada R, Saito A, Kanemoto S, Imaizumi K. Obesity-induced endoplasmic reticulum stress causes chronic inflammation in adipose tissue. Sci Rep. 2012;2:799

224 Jiao P, Ma J, Feng B, Zhang H, Diehl JA, Chin YE, Yan W, Xu H. FFA-induced adipocyte inflammation and insulin resistance: involvement of ER stress and IKKβ pathways. Obesity (Silver Spring). 2011 Mar;19(3):483-91

225 Panzhinskiy E, Hua Y, Culver B, Ren J, Nair S. Endoplasmic reticulum stress upregulates protein tyrosine phosphatase 1B and impairs glucose uptake in cultured myotubes. Diabetologia. 2013 Mar;56(3):598-607

226 Ly LD, Xu S, Choi SK, Ha CM, Thoudam T, Cha SK, Wiederkehr A, Wollheim CB, Lee IK, Park KS. Oxidative stress and calcium dysregulation by palmitate in type 2 diabetes. Exp Mol Med. 2017 Feb 3;49(2):e291

227 Vincent HK, Taylor AG. Biomarkers and potential mechanisms of obesity-induced oxidant stress in humans. Int J Obes (Lond). 2006 Mar;30(3):400-18

228 Houstis N, Rosen ED, Lander ES. Reactive oxygen species have a causal role in multiple forms of insulin resistance. Nature. 2006 Apr 13;440(7086):944-8

229 Inoguchi T, Li P, Umeda F, Yu HY, Kakimoto M, Imamura M, Aoki T, Etoh T, Hashimoto T, Naruse M, Sano H, Utsumi H, Nawata H. High glucose level and free fatty acid stimulate reactive oxygen species production through protein kinase C--dependent activation of NAD(P)H oxidase in cultured vascular cells. Diabetes. 2000 Nov;49(11):1939-45

230 Maloney E, Sweet IR, Hockenbery DM, Pham M, Rizzo NO, Tateya S, Handa P, Schwartz MW, Kim F. Activation of NF-kappaB by palmitate in endothelial cells: a key role for NADPH oxidase-derived superoxide in response to TLR4 activation. Arterioscler Thromb Vasc Biol. 2009 Sep;29(9):1370-5

231 Prentki M, Nolan CJ. Islet beta cell failure in type 2 diabetes. J Clin Invest. 2006 Jul;116(7):1802-12

232 Prentki M, Matschinsky FM, Madiraju SR. Metabolic signaling in fuel-induced insulin secretion. Cell Metab. 2013 Aug 6;18(2):162-85

233 Poitout V, Amyot J, Semache M, Zarrouki B, Hagman D, Fontés G. Glucolipotoxicity of the pancreatic beta cell. Biochim Biophys Acta. 2010 Mar;1801(3):289-98

234 Cnop M, Abdulkarim B, Bottu G, Cunha DA, Igoillo-Esteve M, Masini M,Turatsinze JV, Griebel T, Villate O, Santin I, Bugliani M, Ladriere L, Marselli L, McCarthy MI, Marchetti P, Sammeth M, Eizirik DL. RNA sequencing identifies dysregulation of the human pancreatic islet transcriptome by the saturated fatty acid palmitate. Diabetes. 2014 Jun;63(6):1978-93

235 Lupi R, Dotta F, Marselli L, Del Guerra S, Masini M, Santangelo C, Patané G, Boggi U, Piro S, Anello M, Bergamini E, Mosca F, Di Mario U, Del Prato S, Marchetti P. Prolonged exposure to free fatty acids has cytostatic and pro-apoptotic effects on human pancreatic islets: evidence that beta-cell death is caspase mediated, partially dependent on ceramide pathway, and Bcl-2 regulated. Diabetes. 2002 May;51(5):1437-42

236 Carlsson C, Borg LA, Welsh N. Sodium palmitate induces partial mitochondrial uncoupling and reactive oxygen species in rat pancreatic islets in vitro. Endocrinology. 1999 Aug;140(8):3422-8

237 Listenberger LL, Ory DS, Schaffer JE. Palmitate-induced apoptosis can occur through a ceramide-independent pathway. J Biol Chem. 2001 May 4;276(18):14890-5

238 Cnop M, Ladriere L, Hekerman P, Ortis F, Cardozo AK, Dogusan Z, Flamez D, Boyce M, Yuan J, Eizirik DL. Selective inhibition of eukaryotic translation initiation factor 2 a

dephosphorylation potentiates fatty acid-induced endoplasmic reticulum stress and causes pancreatic b-cell dysfunction and apoptosis. J Biol Chem. 2007;282(6):3989–3997.

239 Kharroubi I, Ladrie`re L, Cardozo AK, Dogusan Z, Cnop M, Eizirik DL. Free fatty acids and cytokines induce pancreatic b-cell apoptosis by different mechanisms: role of nuclear factor-kappaB and en- doplasmic reticulum stress. Endocrinology. 2004;145(11):5087–5096.

240 Preston AM, Gurisik E, Bartley C, Laybutt DR, Biden TJ. Reduced endoplasmic reticulum (ER)-to- Golgi protein trafficking contributes to ER stress in lipotoxic mouse beta cells by promoting protein overload. Diabetologia. 2009;52(11):2369–2373.

241 Rharass T, Lemcke H, Lantow M, Kuznetsov SA, Weiss DG, Panáková D. Ca2+-mediated mitochondrial reactive oxygen species metabolism augments Wnt/β-catenin pathway activation to facilitate cell differentiation. J Biol Chem. 2014 Oct 3;289(40):27937-51

242 Oliveira HR, Verlengia R, Carvalho CR, Britto LR, Curi R, Carpinelli AR. Pancreatic beta-cells express phagocyte-like NAD(P)H oxidase. Diabetes. 2003 Jun;52(6):1457-63

243 ewsholme P, Morgan D, Rebelato E, Oliveira-Emilio HC, Procopio J, Curi R, Carpinelli A. Insights into the critical role of NADPH oxidase(s) in the normal and dysregulated pancreatic beta cell. Diabetologia. 2009 Dec;52(12):2489-98

244 Maechler P, Jornot L, Wollheim CB. Hydrogen peroxide alters mitochondrial activation and insulin secretion in pancreatic beta cells. J Biol Chem. 1999 Sep 24;274(39):27905-13

245 Park HS, Jung HY, Park EY, Kim J, Lee WJ, Bae YS. Cutting edge: direct interaction of TLR4 with NAD(P)H oxidase 4 isozyme is essential for lipopolysaccharide-induced production of reactive oxygen species and activation of NF-kappa B. J Immunol. 2004 Sep 15;173(6):3589-93

246 Nordmann TM, Dror E, Schulze F, Traub S, Berishvili E, Barbieux C, Böni-Schnetzler M, Donath MY. The Role of Inflammation in β-cell Dedifferentiation. Sci Rep. 2017 Jul 24;7(1):6285

247 Beeharry N, Chambers JA, Green IC. Fatty acid protection from palmitic acid-induced apoptosis is lost following PI3-kinase inhibition. Apoptosis. 2004 Sep;9(5):599-607

248 Lupi R, Dotta F, Marselli L, Del Guerra S, Masini M, Santangelo C, Patané G, Boggi U, Piro S, Anello M, Bergamini E, Mosca F, Di Mario U, Del Prato S, Marchetti P. Prolonged exposure to free fatty acids has cytostatic and

pro-apoptotic effects on human pancreatic islets: evidence that beta-cell death is caspase mediated, partially dependent on ceramide pathway, and Bcl-2 regulated. Diabetes. 2002 May;51(5):1437-42

[249] Boslem E, Weir JM, MacIntosh G, Sue N, Cantley J, Meikle PJ, Biden TJ. Alteration of endoplasmic reticulum lipid rafts contributes to lipotoxicity in pancreatic β-cells. J Biol Chem. 2013 Sep 13;288(37):26569-82

[250] Kelpe CL, Moore PC, Parazzoli SD, Wicksteed B, Rhodes CJ, Poitout V. Palmitate inhibition of insulin gene expression is mediated at the transcriptional level via ceramide synthesis. J Biol Chem. 2003 Aug 8;278(32):30015-21

[251] Wang, X., Li, H., De Leo, D., Guo, W., Koshkin, V., Fantus, I.G., et al., 2004. Gene and protein kinase expression profiling of reactive oxygen species-associated lipotoxicity in the pancreatic beta-cell line MIN6. Diabetes 53(1): 129–40.

[252] Boslem E, MacIntosh G, Preston AM, Bartley C, Busch AK, Fuller M, Laybutt DR, Meikle PJ, Biden TJ. A lipidomic screen of palmitate-treated MIN6 β-cells links sphingolipid metabolites with endoplasmic reticulum (ER) stress and impaired protein trafficking. Biochem J. 2011 Apr 1;435(1):267-76

[253] Brozzi F, Nardelli TR, Lopes M, Millard I, Barthson J, Igoillo-Esteve M, Grieco FA, Villate O, Oliveira JM, Casimir M, Bugliani M, Engin F, Hotamisligil GS, Marchetti P, Eizirik DL. Cytokines induce endoplasmic reticulum stress in human, rat and mouse beta cells via different mechanisms. Diabetologia. 2015 Oct;58(10):2307-16

[254] Marselli L, Suleiman M, Masini M, Campani D, Bugliani M, Syed F, Martino L, Focosi D, Scatena F, Olimpico F, Filipponi F, Masiello P, Boggi U, Marchetti P. Are we overestimating the loss of beta cells in type 2 diabetes? Diabetologia. 2014 Feb;57(2):362-5

[255] Trokovic R, Weltner J, Nishimura K, Ohtaka M, Nakanishi M, Salomaa V, Jalanko A, Otonkoski T, Kyttälä A. Advanced feeder-free generation of induced pluripotent stem cells directly from blood cells. Stem Cells Transl Med. 2014 Dec;3(12):1402-9

[256] Cosentino C, Toivonen S, Diaz Villamil E, Atta M, Ravanat JL, Demine S, Schiavo AA, Pachera N, Deglasse JP, Jonas JC, Balboa D, Otonkoski T, Pearson ER, Marchetti P, Eizirik DL, Cnop M, Igoillo-Esteve M. Pancreatic β-cell tRNA hypomethylation and fragmentation link TRMT10A deficiency with diabetes. Nucleic Acids Res. 2018 Nov 2;46(19):10302-10318

[257] Cousin SP, Hügl SR, Wrede CE, Kajio H, Myers MG Jr, Rhodes CJ. Free fatty acid-induced inhibition of glucose and insulin-like growth factor I-induced deoxyribonucleic acid synthesis in the pancreatic beta-cell line INS-1. Endocrinology. 2001 Jan;142(1):229-40

[258] Overbergh L, Valckx D, Waer M, Mathieu C. Quantification of murine cytokine mRNAs using real time quantitative reverse transcriptase PCR. Cytokine. 1999 Apr;11(4):305-12

[259] Nair GG, Liu JS, Russ HA, Tran S, Saxton MS, Chen R, Juang C, Li ML, Nguyen VQ, Giacometti S, Puri S, Xing Y, Wang Y, Szot GL, Oberholzer J, Bhushan A, Hebrok M.

Recapitulating endocrine cell clustering in culture promotes maturation of human stem-cell-derived β cells. Nat Cell Biol. 2019 Feb;21(2):263-274.

260 Melo RC, Morgan E, Monahan-Earley R, Dvorak AM, Weller PF. Pre-embedding immunogold labeling to optimize protein localization at subcellular compartments and membrane microdomains of leukocytes. Nat Protoc. 2014 Oct;9(10):2382-94

261 Cunha DA, Igoillo-Esteve M, Gurzov EN, Germano CM, Naamane N, Marhfour I, Fukaya M, Vanderwinden JM, Gysemans C, Mathieu C, Marselli L, Marchetti P, Harding HP, Ron D, Eizirik DL, Cnop M. Death protein 5 and p53-upregulated
modulator of apoptosis mediate the endoplasmic reticulum stress-mitochondrial dialog triggering lipotoxic rodent and human β-cell apoptosis. Diabetes. 2012 Nov;61(11):2763-75

262 Khaldi MZ, Guiot Y, Gilon P, Henquin JC, Jonas JC. Increased glucose sensitivity of both triggering and amplifying pathways of insulin secretion in rat islets cultured for 1 wk in high glucose. Am J Physiol Endocrinol Metab. 2004 Aug;287(2):E207-17

263 rapov D, Adams SH, Pedersen TL, Garvey WT, Newman JW. Type 2 diabetes associated changes in the plasma non-esterified fatty acids, oxylipins and endocannabinoids. PLoS One. 2012;7(11):e48852

264 Artwohl M, Lindenmair A, Sexl V, Maier C, Rainer G, Freudenthaler A, Huttary N, Wolzt M, Nowotny P, Luger A, Baumgartner-Parzer SM. Different mechanisms of saturated versus polyunsaturated FFA-induced apoptosis in human endothelial cells. J Lipid Res. 2008 Dec;49(12):2627-40

265 van den Berg SA, Guigas B, Bijland S, Ouwens M, Voshol PJ, Frants RR, Havekes LM, Romijn JA, van Dijk KW. High levels of dietary stearate promote adiposity and deteriorate hepatic insulin sensitivity. Nutr Metab (Lond). 2010 Mar 27;7:24

266 Janssens S, Heemskerk MM, van den Berg SA, van Riel NA, Nicolay K, Willems van Dijk K, Prompers JJ. Effects of low-stearate palm oil and high-stearate lard high-fat diets on rat liver lipid metabolism and glucose tolerance. Nutr Metab (Lond). 2015 Dec 18;12:57

267 Esposito K, Nappo F, Giugliano F, Di Palo C, Ciotola M, Barbieri M, Paolisso G, Giugliano D. Cytokine milieu tends toward inflammation in type 2 diabetes. Diabetes Care. 2003 May;26(5):1647

268 Cimini FA, Barchetta I, Porzia A, Mainiero F, Costantino C, Bertoccini L, Ceccarelli V, Morini S, Baroni MG, Lenzi A, Cavallo MG. Circulating IL-8 levels are increased in patients with type 2 diabetes and associated with worse inflammatory and cardiometabolic profile. Acta Diabetol. 2017 Oct;54(10):961-967

269 Cavusoglu E, Marmur JD, Yanamadala S, Chopra V, Hegde S, Nazli A, Singh KP, Zhang M, Eng C. Elevated baseline plasma IL-8 levels are an independent predictor of

long-term all-cause mortality in patients with acute coronary syndrome. Atherosclerosis. 2015 Oct;242(2):589-94

270 Nguyen MT, Satoh H, Favelyukis S, Babendure JL, Imamura T, Sbodio JI, Zalevsky J, Dahiyat BI, Chi NW, Olefsky JM. JNK and tumor necrosis factor-alpha mediate free fatty acid-induced insulin resistance in 3T3-L1 adipocytes. J Biol Chem. 2005 Oct 21;280(42):35361-71

271 Krogmann A, Staiger K, Haas C, Gommer N, Peter A, Heni M, Machicao F, Häring HU, Staiger H. Inflammatory response of human coronary artery endothelial cells to saturated long-chain fatty acids. Microvasc Res. 2011 Jan;81(1):52-9

272 Nguyen MT, Favelyukis S, Nguyen AK, Reichart D, Scott PA, Jenn A, Liu-Bryan R, Glass CK, Neels JG, Olefsky JM. A subpopulation of macrophages infiltrates hypertrophic adipose tissue and is activated by free fatty acids via Toll-like receptors 2 and 4 and JNK-dependent pathways. J Biol Chem. 2007 Nov
30;282(48):35279-92

273 Anderson EK, Hill AA, Hasty AH. Stearic acid accumulation in macrophages induces toll-like receptor 4/2-independent inflammation leading to endoplasmic reticulum stress-mediated apoptosis. Arterioscler Thromb Vasc Biol. 2012 Jul;32(7):1687-95

274 Lu Y, Qian L, Zhang Q, Chen B, Gui L, Huang D, Chen G, Chen L. Palmitate induces apoptosis in mouse aortic endothelial cells and endothelial dysfunction in mice fed high-calorie and high-cholesterol diets. Life Sci. 2013 Jul 10;92(24-26):1165-73

275 Jaikumkao K, Pongchaidecha A, Chueakula N, Thongnak LO, Wanchai K, Chatsudthipong V, Chattipakorn N, Lungkaphin A. Dapagliflozin, a sodium-glucose co-transporter-2 inhibitor, slows the progression of renal complications through the suppression of renal inflammation, endoplasmic reticulum stress and apoptosis in prediabetic rats. Diabetes Obes Metab. 2018 Nov;20(11):2617-2626

276 Tahara A, Kurosaki E, Yokono M, Yamajuku D, Kihara R, Hayashizaki Y, Takasu T, Imamura M, Li Q, Tomiyama H, Kobayashi Y, Noda A, Sasamata M, Shibasaki M. Effects of sodium-glucose cotransporter 2 selective inhibitor ipragliflozin on hyperglycaemia, oxidative stress, inflammation and liver injury in
streptozotocin-induced type 1 diabetic rats. J Pharm Pharmacol. 2014 Jul;66(7):975-87

277 Ishibashi Y, Matsui T, Yamagishi S. Tofogliflozin, A Highly Selective Inhibitor of SGLT2 Blocks Proinflammatory and Proapoptotic Effects of Glucose Overload on Proximal Tubular Cells Partly by Suppressing Oxidative Stress Generation. Horm Metab Res. 2016 Mar;48(3):191-5

278 Ye Y, Bajaj M, Yang HC, Perez-Polo JR, Birnbaum Y. SGLT-2 Inhibition with

Dapagliflozin Reduces the Activation of the Nlrp3/ASC Inflammasome and Attenuates the Development of Diabetic Cardiomyopathy in Mice with Type 2 Diabetes. Further Augmentation of the Effects with Saxagliptin, a DPP4 Inhibitor. Cardiovasc Drugs Ther. 2017 Apr;31(2):119-132

279 Németh ZH, Deitch EA, Lu Q, Szabó C, Haskó G. NHE blockade inhibits chemokine production and NF-kappaB activation in immunostimulated endothelial cells. Am J Physiol Cell Physiol. 2002 Aug;283(2):C396-403

280 Rolfe MW, Kunkel SL, Rowens B, Standiford TJ, Cragoe EJ Jr, Strieter RM. Suppression of human alveolar macrophage-derived cytokines by amiloride. Am J Respir Cell Mol Biol. 1992 Jun;6(6):576-82

281 Hall E, Volkov P, Dayeh T, Bacos K, Rönn T, Nitert MD, Ling C. Effects of palmitate on genome-wide mRNA expression and DNA methylation patterns in human pancreatic islets. BMC Med. 2014 Jun 23;12:103

282 Igoillo-Esteve M, Marselli L, Cunha DA, Ladrière L, Ortis F, Grieco FA, Dotta F, Weir GC, Marchetti P, Eizirik DL, Cnop M. Palmitate induces a pro-inflammatory response in human pancreatic islets that mimics CCL2 expression by beta cells in type 2 diabetes. Diabetologia. 2010 Jul;53(7):1395-405

283 Plötz T, von Hanstein AS, Krümmel B, Laporte A, Mehmeti I, Lenzen S. Structure-toxicity relationships of saturated and unsaturated free fatty acids for elucidating the lipotoxic effects in human EndoC-βH1 beta-cells. Biochim Biophys Acta Mol Basis Dis. 2019 Nov 1;1865(11):165525

284 Krizhanovskii C, Kristinsson H, Elksnis A, Wang X, Gavali H, Bergsten P, Scharfmann R, Welsh N. EndoC-βH1 cells display increased sensitivity to sodium palmitate when cultured in DMEM/F12 medium. Islets. 2017 May 4;9(3):e1296995

285 Jaafar R, Tran S, Shah AN, Sun G, Valdearcos M, Marchetti P, Masini M, Swisa A, Giacometti S, Bernal-Mizrachi E, Matveyenko A, Hebrok M, Dor Y, Rutter GA, Koliwad SK, Bhushan A. mTORC1 to AMPK switching underlies β-cell metabolic plasticity during maturation and diabetes. J Clin Invest. 2019 Jul 2;130:4124-4137

286 Xie R, Everett LJ, Lim HW, Patel NA, Schug J, Kroon E, Kelly OG, Wang A, D'Amour KA, Robins AJ, Won KJ, Kaestner KH, Sander M. Dynamic chromatin remodeling mediated by polycomb proteins orchestrates pancreatic differentiation of human embryonic stem cells. Cell Stem Cell. 2013 Feb 7;12(2):224-37

287 Shang L, Hua H, Foo K, Martinez H, Watanabe K, Zimmer M, Kahler DJ, Freeby M, Chung W, LeDuc C, Goland R, Leibel RL, Egli D. β-cell dysfunction due to increased ER stress in a stem cell model of Wolfram syndrome. Diabetes. 2014 Mar;63(3):923-33

[288] Tiyaboonchai A, Cardenas-Diaz FL, Ying L, Maguire JA, Sim X, Jobaliya C, Gagne AL, Kishore S, Stanescu DE, Hughes N, De Leon DD, French DL, Gadue P. GATA6 Plays an Important Role in the Induction of Human Definitive Endoderm, Development of the Pancreas, and Functionality of Pancreatic β Cells. Stem Cell Reports. 2017 Mar 14;8(3):589-604

[289] Teo AK, Lau HH, Valdez IA, Dirice E, Tjora E, Raeder H, Kulkarni RN. Early Developmental Perturbations in a Human Stem Cell Model of MODY5/HNF1B Pancreatic Hypoplasia. Stem Cell Reports. 2016 Mar 8;6(3):357-67

[290] Vethe H, Bjørlykke Y, Ghila LM, Paulo JA, Scholz H, Gygi SP, Chera S, Ræder H. Probing the missing mature β-cell proteomic landscape in differentiating patient iPSC-derived cells. Sci Rep. 2017 Jul 6;7(1):4780

ACKNOWLEDGEMENTS

During my PhD, I have had several mentors and I would like to sincerely thank all of them for their priceless support and for teaching me so much. Prof. Alessandra Dei Cas, my tutor, showed me by example that hard work, patience and care for details lead to the achievement of your own goals. She is extremely altruist and she always made time for my needs and those of others.

Prof. Riccardo Bonadonna, to whom I would like to address my deepest gratitude and respect, has always been an inspirational professional figure. I admire his passion for research, his broad knowledge and his constant questioning.

Prof. Miriam Cnop, who introduced me into a new working reality and kindly welcomed me to the ULB Center for Diabetes Research, always offered me numerous advices and continuous support. I would like to thank her for the great opportunity she provided me and the trust she placed on me.

Last, but not least, Dr. Valentina Spigoni, who is a true, great friend and a wise mentor. She contributed to both my personal and professional growth more than anyone else, offering me support, constructive criticism and an example to follow day by day. Our friendship is very precious to me.

Additional special thanks go to my friends and collogues in Parma as well as the “new” ones in Brussels. They made me feel at home and beloved, supporting me in every possible way. I hope they know how much I appreciate it and how much I love them back.

Finally, I have been blessed with a lovely family and caring friends and I would like to thank each of them: my mum, who is the strongest woman I know and I wish to resemble her; my dad, who I hope would be proud of his little girl; my sister, the person I admire and care the most; and the best friends I had the luck to grow up with. They are the reason why coming back home is always beautiful.